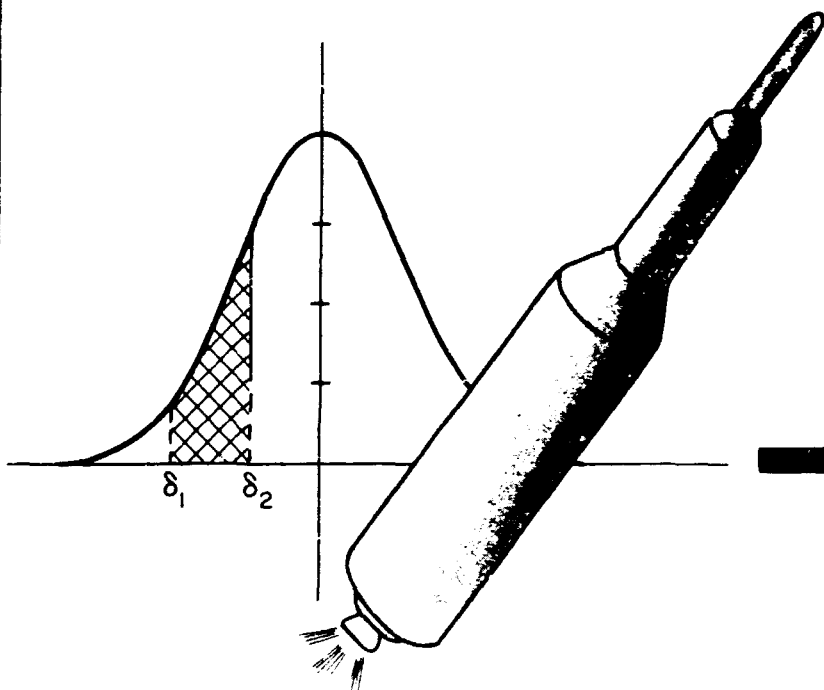


NASA CR 65677

MOTION OF A SPACECRAFT NEAR A
TRIANGULAR LIBRATION POINT
OF THE EARTH-MOON SYSTEM



LIBRARY COPY

AUG 4 1967

TEXAS CENTER FOR RESEARCH
P. O. BOX 8472, UNIVERSITY STATION, MANITEX, TEXAS
MANNED SPACECRAFT CENTER
HOUSTON, TEXAS

FACILITY FORM 802

N67-34670
(ACCESSION NUMBER)

194
(PAGES)

CR-65677
(NASA CR OR TMX OR AD NUMBER)

(THRU)

(CODE)

(CATEGORY)

1
30

**MOTION OF A SPACECRAFT NEAR A
TRIANGULAR LIBRATION POINT
OF THE EARTH-MOON SYSTEM**

By

BOB EWALD SCHUTZ

TCR - 6

JANUARY 1966

3 MOTION OF A SPACECRAFT NEAR A TRIANGULAR LIBRATION
POINT OF THE EARTH-MOON SYSTEM 6

by

6 BOB EWALD SCHUTZ⁷, B. S. A. S. E. .

THESIS

Presented to the Faculty of the Graduate School of
The University of Texas in Partial Fulfillment
of the Requirements

For the Degree of

MASTER OF SCIENCE IN AEROSPACE ENGINEERING

THE UNIVERSITY OF TEXAS, AUSTIN 3
9. January, 1966 100V

**This report was prepared under
NASA MANNED SPACE FLIGHT CENTER**

25 Contract 9-2619 2920
/ NESC
under the direction of

Dr. Byron D. Tapley

**Associate Professor of Aerospace Engineering
and Engineering Mechanics**

Page 132

Ordinate should read h_S

Page 143

Ordinate should read h_S

Page 159

Line 5 - Quantity in brackets should be

$$Y, \dot{z}_y - z_y \dot{Y}_y$$

Page 167

The $\bar{\epsilon}_\theta$ component of \bar{V}_S should read

$$r_{BL} \dot{\theta}^* - \dot{x}_S \sin \phi + \dot{y}_S \cos \phi$$

Page 167

Eq. (C-10), the second row of the matrix on the right side should read

$$r_{BL} \dot{\theta}^* - \dot{x}_S \sin \phi + \dot{y}_S \cos \phi$$

Page 171

Eq. (D-6) should read

$$\dot{\xi}_y = \text{etc.}$$

ABSTRACT

The motion of a spacecraft near the triangular earth-moon libration points is studied to determine the nature of the long term motion. Two different mathematical models are used. In one model, it is assumed that the earth and the moon move in circular orbits around their barycenter, the barycenter moves in a circular orbit around the sun, and the earth-moon plane regresses with a constant rate of one revolution in 18.6 years. Two initial orientations of the earth-moon-sun system are used. In the other mathematical model, ephemeris information is used to represent the physical world to a much greater extent than the model with circular orbits. The sun and all planets except Uranus, Neptune, and Pluto, are included in this "real world" model. Two initial dates are used, viz., January 10, 1967, 12^h GMT, and November 2, 1967, 5.^h64 GMT. The equations of motion for each of the two models are numerically integrated and the results of the models for approximately the same initial orientation are compared. The results of the study lead to the conclusions that 1.) the modified four-body model with circular orbits and nodal regression does not simulate very well the "real world" model which uses ephemeris information; 2.) the initial date and the initial velocity specification have an important effect on the subsequent motion; 3.) long-term stability of greater than five years is found to exist in the "real world" model.

PREFACE

With the realization of the age old dream of journies to other celestial bodies, researchers have begun to investigate many facets of celestial mechanics as applied to man-made bodies. Many of the problems under investigation today would not only have been formidable to the researcher only a score of years past, but it is doubtful that such research would have been undertaken because of either lack of funds or lack of application. Today, however, it is not uncommon to seriously discuss flights to other members of the solar system and even beyond the solar system. Man is now technologically capable of making journies to nearby celestial bodies. However, such undertakings require vast financial support, hence, it is necessary to investigate every possible scheme for some practical application which may produce results similar to another scheme, but with either less expenditure of resources or with more effective results.

The so-called "libration points" of the Restricted Three Body Problem may have practical applications in space flight. The investigation reported herein is a study of the triangular libration points of the earth-moon system. If the motion of an artificial body is such that the vehicle remains in the vicinity of an earth-moon triangular libration point for a reasonable length of time, then these points may have many uses in space flight operations. The possible uses of the region and a more detailed statement regarding the

investigation are discussed in Chapter I in the sections entitled "Application" and "Statement of the Problem."

The author wishes to express his gratitude to Dr. B. D. Tapley for serving as supervising professor for this investigation. He has offered not only enthusiasm for the investigation, but also time and effort to enable the project to reach fruition. The author is also indebted to Dr. P. H. Miller for serving on the supervising committee. Thanks is due Gilbert Rivera for his aid in preparing the many plots for publication. The author wishes to acknowledge and express his appreciation to the National Aeronautics and Space Administration for support given in the final stages of this investigation. In addition, a study of this nature could not have been undertaken without the aid of the digital computer and the author is deeply indebted to The University of Texas Computation Center for providing computer time. The author also wishes to thank those individuals who have given him invaluable advice. Thanks is also due Dr. M. J. Thompson and the Department of Aerospace Engineering for providing support to the author in his graduate study. Finally, the author wishes to thank his parents for their help in innumerable ways.

Bob Ewald Schutz

The University of Texas
Austin, Texas
January, 1966

TABLE OF CONTENTS

	Page
ABSTRACT	iii
PREFACE	iv
LIST OF FIGURES.	ix
LIST OF TABLES	xii
NOMENCLATURE	xiii
 Chapter	
I. INTRODUCTION.	1
Classical Three-Body Problem	1
Statement of the Problem.	3
Application	8
Procedure	12
II. MATHEMATICAL MODEL	14
Motion of the Planets and the Solar System.	15
Physical Characteristics of the Natural Bodies	19
Assumptions	20
III. A MODIFIED RESTRICTED FOUR-BODY PROBLEM.	25
Mathematical Model	25
Case I: Rotating Coordinate System at L_4	27
Equations of motion.	27
Constants in the mathematical model	37
Evaluation of equations of motion for $\Omega = 0$	40
Case I results and comparison with Reference 5	42
Case II: Nonrotating Coordinate System	59
Equations of motion.	59
Initial conditions	60

Chapter	Page
Case II results and Comparison with Case I	62
Case III: Earth-Moon Orbital Plane Defined by Angular Momentum.	66
Equations of motion and initial conditions	66
Case III results and comparison with Case I	72
Case IV: Orientation Corresponding to JD 2, 439, 501.0	74
IV. MATHEMATICAL MODEL UTILIZING EPHEMERIS INFORMATION	76
Mathematical Model	76
Equations of Motion	79
Jet Propulsion Laboratory Ephemeris Tapes.	86
Constants	89
Transformation to Libration-Point-Centered Rotating System	91
Case I: Initial Date JD 2, 439, 501.0 (January 10, 1967; 12 ^h GMT)	92
Orientation of the solar system and the earth-moon system	92
Initial conditions and results with inclusion of \dot{r}_{BL}	94
Initial conditions and results with $\dot{r}_{BL} = 0$	109
Case II: Initial Date JD 2, 439, 796.735 (November 2, 1967; 5 ^h .64 GMT)	110
Method of determining initial date	110
Orientation of the solar system and the earth-moon system	121
Initial conditions and results in nonrotating and rotating coordinate systems for spacecraft placement at L_4	123
Initial conditions and results in nonrotating and rotating coordinate systems for spacecraft placement at L_5	133
Accuracy	134
V. CONCLUSIONS AND RECOMMENDATIONS	145

APPENDIX A	ORDER OF MAGNITUDE OF GRAVITATIONAL FORCES.	150
APPENDIX B	DERIVATION OF EQUATIONS FOR DETERMINING THE ORIENTATION OF THE EARTH-MOON SYSTEM . . .	154
APPENDIX C	DETERMINATION OF INITIAL CONDITIONS USING THE EARTH-MOON ORBITAL PLANE	162
APPENDIX D	PROOF OF $\dot{\zeta}_y = 0$	170
REFERENCES	172
VITA	175

LIST OF FIGURES

Figure		Page
1	Restricted Three-Body Problem Libration Points.	4
2	L_4 and L_5 of the Sun-Jupiter System	4
3	Use of L_4 and L_5 in Lunar Communications.	10
4	Solar System Center of Mass Location for Period from JD 2439500.5 to JD 2442200.5	18
5	$f(\phi, R)$ vs. Latitude (or Declination) for $R = 240,000$ Miles . .	22
6	Coordinate Systems and Geometry of the Mathematical Model .	29
7	Vector Representation of Position.	29
8	Acceleration of the Barycenter	34
9	L_4 Rotating (x, y) -Results for $\psi_0 = 180^\circ$	44
10	L_4 Rotating (x, y) -Results for $\psi_0 = 225^\circ$	51
11	Spacecraft Motion Subsequent to Lunar Encounter at 1334 to 1335 Days with $\psi_0 = 225^\circ$	54
12	Magnitude of Displacement Vector vs. Time for $\psi_0 = 180^\circ$, $\Omega = 0$	55
13	Magnitude of Displacement Vector vs. Time for $\psi_0 = 225^\circ$, $\Omega = 0$	56
14	Magnitude of Displacement Vector vs. Time for $\psi_0 = 180^\circ$, $\Omega \neq 0$	57
15	Magnitude of Displacement Vector vs. Time for $\psi_0 = 225^\circ$, $\Omega \neq 0$	58
16	Initial Orientation of the Earth-Moon System with L_4 Assumed to Exist in the Earth-Moon Plane	69

Figure	Page
17	Orientation of the Earth-Moon Orbit Plane Defined by the Angular Momentum 69
18	L_4 Rotating (x, y)-Results for $\psi_0 = 225^\circ$ from 1250 Days to 1500 Days Using the Earth-Moon ⁰ Orbital Plane 73
19	Magnitude of Spacecraft Displacement Vector vs. Time for Orientation Corresponding to JD 2439501.0 75
20	Vector Representation of Positions 80
21	Orientation of Coordinate System Used in the Ephemeris Tapes 88
22	Relation between Equatorial and Ecliptic Coordinate Systems. 88
23	Solar System Orientation at JD 2439501.0 (Jan. 10, 1967; 12 ^h GMT) 93
24	Orientation of the Earth-Moon System on Julian Date 2439501.0 (Jan. 10, 1967; 12 ^h GMT). 93
25	Ω^* of the Earth-Moon Orbital Plane for 750 Day Period Beginning JD 2439501.0 95
26	i^* of the Earth-Moon Orbital Plane for 750 Day Period Beginning JD 2439501.0 96
27	ξ_p for 750 Day Period Beginning JD 2439501.0 97
28	η_p for 750 Day Period Beginning JD 2439501.0 98
29	L_4 Nonrotating (X, Y)-Results for Initial JD 2439501.0 101
30	L_4 Rotating (x, y)-Results for Initial JD 2439501.0 105
31	Magnitude of Displacement Vector from L_4 vs. Time for Initial JD 2439501.0 107
32	Magnitude of Spacecraft Angular Momentum Vector Relative to the Barycenter vs. Time for Initial JD 2439501.0 108
33	L_4 Nonrotating (X, Y)-Results for Initial JD 2439501.0 and $\dot{r}_{BL} = 0$ 111
34	L_4 Rotating (x, y)-Results for Initial JD 2439501.0 and $\dot{r}_{BL} = 0$ 116

Figure		Page
35	Magnitude of Spacecraft Angular Momentum Vector Relative to the Barycenter vs. Time for Initial JD 2439501.0 and $\dot{r}_{BL} = 0$	118
36	Determination of d	122
37	d vs. Time for JD 2439796.68 to JD 2439796.78	122
38	Solar System Orientation at JD 2439796.735 (Nov. 2, 1967; 5 ^h .64 GMT)	124
39	L_4 Nonrotating (X, Y)-Results for Initial JD 2439796.735	126
40	L_4 Rotating (x, y)-Results for Initial JD 2439796.735	130
41	Magnitude of Spacecraft Angular Momentum Vector Relative to the Barycenter vs. Time for Initial JD 2439796.735	132
42	L_5 Nonrotating (X, Y)-Results for Initial JD 2439796.735	135
43	L_5 Rotating (x, y)-Results for Initial JD 2439796.735	139
44	Magnitude of Displacement Vector from L_5 vs. Time for Initial JD 2439796.735	141
45	Magnitude of Spacecraft Angular Momentum Vector Relative to the Barycenter vs. Time for Initial JD 2439796.735	143
A-1	Aspects of the Inferior and the Superior Planets	152
B-1	Definition of Angles	156
B-2	Determination of i^* and Ω^*	156
C-1	Locations of Coordinate Systems	163
C-2	Distances and Velocities in the Earth-Moon Orbital Plane	163
C-3	In-Plane Orientation of the L_4 and L_5 Coordinate Systems.	169

LIST OF TABLES

Table		Page
1	Comparison of Rotating and Nonrotating Data (Miles) for $\psi_0 = 180^\circ$	63
2	Comparison of Rotating and Nonrotating Data (Miles) for $\psi_0 = 225^\circ$	64
3	Gravitation Parameters of the Major Bodies in the Solar System	90
A-1	Order of Magnitude of Gravitational Attraction on Spacecraft 1 A. U. from the Sun.	153

NOMENCLATURE

Coordinate Systems

X_C, Y_C, Z_C	Inertial system centered at the solar system center of mass, oriented with respect to the Ecliptic of Epoch 1950
X, Y, Z	Sun-centered nonrotating system oriented with respect to the Ecliptic of Epoch 1950
X_e, Y_e, Z_e	Sun-centered nonrotating system oriented with respect to the earth's equatorial plane of Epoch 1950
X, Y, Z	Barycenter nonrotating system oriented with respect to the Ecliptic of Epoch 1950 with unit vectors $\bar{i}, \bar{j}, \bar{k}$
ξ, η, ζ	Barycenter rotating system oriented with respect to the earth-moon orbital plane or earth-moon plane with unit vectors $\bar{\epsilon}_\xi, \bar{\epsilon}_\eta, \bar{\epsilon}_\zeta$
x, y, z	L_4 or L_5 centered rotating system with unit vectors $\bar{\epsilon}_x, \bar{\epsilon}_y, \bar{\epsilon}_z$

Subscripts

B	Barycenter
C	Solar system center of mass
L	Libration point L_4 or L_5
S	Spacecraft
$()_0$	Initial value of ()

NOMENCLATURE (Cont.)

\odot	Sun
♁	Mercury
♀	Venus
\oplus	Earth
☾	Moon
♂	Mars
♃	Jupiter
♄	Saturn
♅	Uranus
♆	Neptune
♇	Pluto

Superscripts

d	Days
h	Hours
m	Minutes
s	Seconds
$()^T$	Matrix transpose
$()^{-1}$	Matrix inverse
$(\bar{\quad})$	Vector quantity
$(\dot{\quad})$	First derivative with respect to time
$(\ddot{\quad})$	Second derivative with respect to time

NOMENCLATURE (Cont.)

Symbols

Coordinates of () in the coordinate system (D, E, F) are $D_{()}$, $E_{()}$, $F_{()}$

A Transformation Matrix

A. U. Astronomical Unit

F Force

G Universal gravitational constant

GMT Greenwich Mean Time

$\bar{H}_{()}$ Total angular momentum vector of ()

$H_{()}$ Magnitude of angular momentum of ()

$\bar{h}_{()}$ Angular momentum per unit mass vector of ()

$h_{X_{()}}$, $h_{Y_{()}}$, $h_{Z_{()}}$ Components of $\bar{h}_{()}$

i Inclination of the earth-moon plane to the ecliptic

i^* Inclination of the earth-moon orbital plane to the ecliptic

JD Julian Date

km Kilometers

$m_{()}$ Mass of ()

mi or s. mi Statute miles

\bar{r}_{AB} Radius vector from point A to point B

r_{AB} Magnitude of radius vector \bar{r}_{AB}

t Time elapsed from reference

\bar{V} Velocity vector

η_p distance to L_4 or L_5

θ Angle measured in the earth-moon plane from the line of nodes to the earth-moon line

NOMENCLATURE (Cont.)

θ^*	Same as θ , except that the angle is measured in the earth-moon orbital plane
ξ_p	ξ distance to L_4 or L_5
ϕ	Angle measured in the earth-moon orbital plane from the line of nodes to the barycenter -L line
Φ	Potential function
ψ	Angle measured in the ecliptic from the X -axis to the sun-barycenter line
Ω	Angle measured in the ecliptic from the X -axis to the earth-moon plane line of nodes
Ω^*	Same as Ω , except that the angle is measured to the earth-moon orbital plane line of nodes
$\bar{\omega}$	Angular velocity
Υ_{1950}	Vernal Equinox of Epoch 1950
$ \bar{r} $	Magnitude of the vector (\bar{r})

Definitions

Earth-Moon Plane	Plane in which the circular motion of the earth and moon is assumed to occur (used in the Modified Restricted Four-Body Problem).
Earth-Moon Orbital Plane	Plane defined by the angular momentum vector of the earth-moon system.
Julian Date	The number of mean solar days elapsed from January 1, 4713 B. C. to the date of interest.
Epoch 1950	A Julian Date chosen as reference, viz., JD 2,433,282.423 .

CHAPTER I

INTRODUCTION

Classical Three-Body Problem

The system of n-bodies, in which each body attracts every other body in accordance with Newton's Law of Gravitation, has been used as the basic mathematical model for bodies in the solar system for over two centuries. Unfortunately, a closed-form solution (i. e., an analytical solution for which the position of each body is specified for all epochs of time) has been found only for the two-body case and for a special case of the three-body problem. The only means available for solving the differential equations of motion for the general n-body case is through the numerical integration of the equations of motion with the digital computer or by using the analog computer.

The solution of a special case in the three-body problem is of considerable interest. In the year 1772, J. L. Lagrange, a mathematician, presented to the Paris Academy a memoir entitled Essai sur le Problème des Trois Corps (Essay on the Problem of Three Bodies). Lagrange had studied a three-body problem in which each body attracted the others in accordance with Newton's Law of Gravitation, the mass of one body was infinitesimally small, and the two large masses moved in circular orbits around their mutual center of mass. This special case of the three-body problem has become known as the "Restricted Three-Body Problem." Lagrange mentioned as a

curiosity the prediction of five equilibrium points in the vicinity of the two large bodies which possessed the property that the infinitesimally small body, when placed at one of these points with zero velocity relative to the point, would remain indefinitely at that point. These equilibrium points will subsequently be referred to as libration points (they are also known as Lagrangian Points and Trojan Points). The general location of the libration points is illustrated in Fig. 1. The libration points L_1 , L_2 , and L_3 occur on a line joining the two bodies of finite mass. The actual location of the points is dependent on the mass ratio of the two bodies. Libration points L_4 and L_5 occur at the vertices of two equilateral triangles which have as a common base the line joining the two bodies of finite mass (Refs. 1 and 2).

Further studies of the restricted three-body problem have been carried out since Lagrange's initial investigation. Among the individuals associated with these investigations are Liouville, Laplace, Jacobi, and Poincaré. One of the most important results obtained during these investigations has been the demonstration of the stability of the triangular libration points for certain mass ratios and of the instability of the straight-line libration points for all mass ratios. That is, if the infinitesimal third body is placed at one of the straight-line libration points and displaced slightly from the exact point, it will depart from the vicinity of that point. However, in the case of a triangular libration point, if the ratio of the mass of the smaller body to the mass of the larger body is less than 0.0385, then the infinitesimal mass when displaced slightly from the libration point will oscillate about that point indefinitely.

It is of some interest to note that Lagrange's analysis was made at the time when only six of the planets (including earth) were known and none of

the minor planets had as yet been discovered. Therefore, it was not then known that the triangular configuration actually exists in the solar system. More than a century after Lagrange's prediction, an astronomer named Wolf at the Königstuhl Observatory in Heidelberg, Germany, discovered a minor planet located at approximately the L_4 position of the sun-Jupiter system (see Fig. 2). It was named 588 Achilles. In October of the same year, 1906, a minor planet was discovered near the L_5 location and was named 617 Patroclus. During the next two years, two additional minor planets were discovered and named Hector and Nestor. Subsequent investigations have revealed a total of 15 bodies (known at this writing) located at the two libration points. It was decided to name the L_4 asteroids after the Greek heroes of the Trojan War; therefore, they have become known as the Greek planets. Among those occupying the L_4 position are Agamemnon, Ulysses, Nestor, Ajax, and Diomedes. One might note that the first asteroid found at L_4 , viz., Achilles, is a member of the Trojan camp and not the Greek. The asteroids which occupy the L_5 position are named after the Trojan heroes. Consequently, they are called the Trojan Planets and among their members are Priam, Anchises, Aeneas, and Troilus (Ref. 3).

Statement of the Problem

The ratio of the lunar mass to the earth's mass is 0.0123. Hence, the stability criteria of the triangular libration points is satisfied and if all the assumptions of the restricted three-body problem were satisfied also, then the motion of a spacecraft (a body with mass very much less than either the earth or the moon) near either the L_4 or the L_5 point would be stable in the sense previously stated. Obviously, the earth-moon-spacecraft system

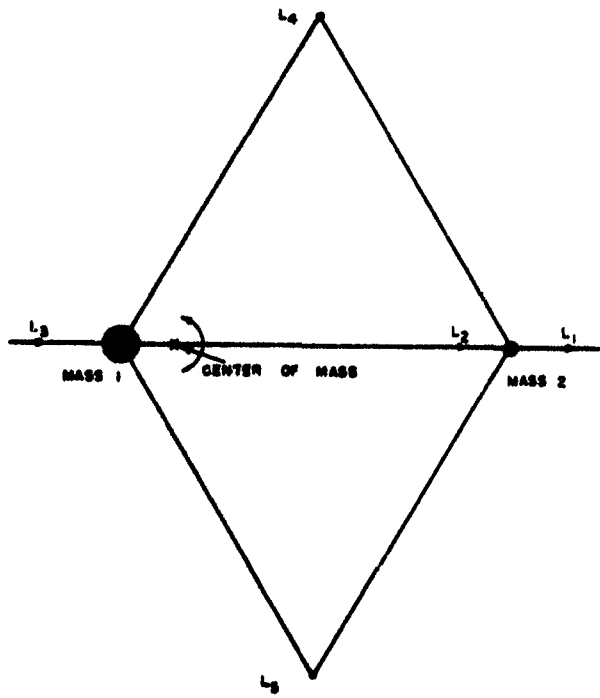


FIGURE 1. RESTRICTED THREE-BODY PROBLEM LIBRATION POINTS

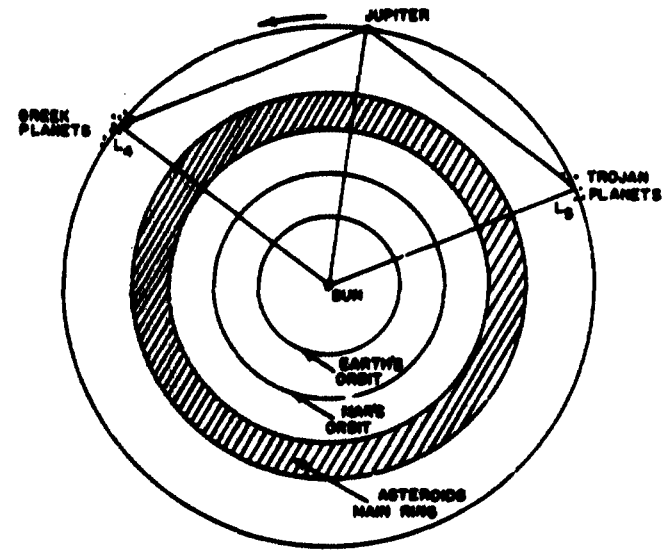


FIGURE 2. L_4 AND L_5 OF THE SUN-JUPITER SYSTEM

cannot be treated as a three-body problem in the physical world. There are external forces on the system due to the gravitational attraction of the sun, planets, and other bodies. With the inclusion of these external forces on the system, the restricted three-body assumption is no longer valid and it is unknown whether or not the spacecraft would have a stable motion near the triangular points. A "stable" motion is defined as one in which the spacecraft remains within some prescribed distance of the libration point during the time of interest. In this investigation the word "stable" is used in the same sense as "libration-point-centered motion."

The Trojan and the Greek Planets in the sun-Jupiter system have external forces on them due to the gravitational attraction of the other planets and yet they oscillate about their respective libration point in an apparently stable motion. One might be tempted to conclude that this would also be the case in the earth-moon system; however, this has not been shown to be true. The perturbing forces on a spacecraft in the earth-moon system would be much greater than those acting on the Trojan or the Greek Planets in the sun-Jupiter system. The sun and Jupiter would have a much stronger influence on the motion of a spacecraft in the earth-moon system than Saturn and the other planets would have on the aforementioned asteroid groups.

Therefore, the primary purpose of the study presented in the subsequent discussion is to investigate the stability of spacecraft motion in the vicinity of the earth-moon triangular libration points. The definition of a libration point is a consequence of the restricted three-body problem. Furthermore, a true equilibrium point in the actual earth-moon system would not, in general, correspond to the L_4 or L_5 position. However, in the subsequent study, the libration points defined in the restricted three-body problem

will be used as reference points and the effects of the remaining bodies will be included as perturbing forces on the spacecraft. The resultant motion will represent the deviation from the restricted three-body case.

The straight-line libration points will not be considered since, as stated previously, these points are unstable in the restricted three-body problem. Furthermore, it has been shown that the sun produces a disturbance which forces the infinitesimal body to move away from the straight-line libration point and an unstable motion results (Ref. 7).

Previous investigations into the stability of motion at the triangular libration points are given by Refs. 4 to 16. References 4 and 5 assume a mathematical model in which the earth and the moon move in circular orbits around their mutual center of mass (barycenter), the barycenter moves in a circular orbit around the sun, and the earth-moon orbital plane maintains a fixed orientation in space. Reference 6 reports an investigation which includes both the effects of the time rate of change of the inclination of the earth-moon orbital plane and the regression of the orbital plane. The equations of motion are linearized by expanding all the forces on the spacecraft in a Taylor Series about the libration point. A solution is then obtained to these equations; however, the results presented must be viewed with a degree of caution because of the linearization. Results of the evaluation of the linearized equations up to 1500 days are presented for position coordinates, and one finds that the particle does not exceed 50,000 to 60,000 miles displacement from the libration point. It appears that this small displacement over such a long period may be the result of the linearization. With allowance for the difference in models, other results are presented in Ref. 6 which agree with those of Ref. 5. References 7 and 8 discuss motion near the triangular points and

the straight-line points. The problem of launching from the earth and injecting into a libration-point-centered orbit is considered also. Numerical integration of the differential equations is employed; however, the integrations are carried out for a period of only 180 days in one model and 475 days in another model. It is interesting to note that in Ref. 7, the results of numerical computations with a mathematical model which includes the ephemeris positions of the sun, moon, and earth are given. This will be discussed further in Chapter IV under the heading "Mathematical Model." Results of other investigations are reported in Refs. 9 to 16. All of these references, with the exceptions of Ref. 9 and Ref. 14, are concerned with some aspect of an analytical solution of a simplified mathematical model. Both of these references report numerical results obtained with a general n-body model which uses ephemeris input for the planetary positions. The results of Ref. 14 are particularly interesting in that they treat the initial condition effects for the general n-body problem.

The investigation presented in the subsequent discussion considers two different mathematical models. One is a mathematical model which extends the work of Refs. 4 and 5 by the inclusion of the effects of the nodal regression. The other is a mathematical model which assumes a general n-body problem formulation and utilizes the Jet Propulsion Laboratory Ephemeris Tapes to obtain the positions of the sun, the moon and the appropriate planets. This latter model is, therefore, a much more realistic model than the former and will be referred to as the "real world" model. Furthermore, this entire investigation approaches the problem from the standpoint of deriving the differential equations of motion of the spacecraft and numerically integrating them with specified initial conditions. It is realized that this may not be the

"best" approach for investigating the question of long term stability. There are, of course, an extremely large number of initial conditions available, and to try a representative sample would require prodigious amounts of computer time. Therefore, only certain cases are investigated and implications advanced to other cases.

Obviously, closed form solutions for studying stability are preferred to numerical solutions. But closed form solutions are extremely difficult to obtain, even for the restricted four-body problem. For a model including the sun and the planets, one requires a solution to a twelve-body problem. Obtaining such a solution would be a formidable task.

The problem of stabilizing the motion by applying thrust to the spacecraft at intervals in such a manner that the spacecraft would remain very close to the libration point is not considered in the investigation reported herein. Instead, the primary interest of this investigation is to determine the natural motion of the spacecraft subsequent to its placement at or near the libration point of interest.

Application

Although the problem may at first appear to be of academic interest only, it appears that the earth-moon triangular libration points could be utilized in several ways. Sometime in the near future, lunar exploration bases will be established on the side of the moon which cannot be seen from the earth, i. e., the "far side of the moon." Undoubtedly, communications between the earth and these lunar bases will be desirable; however, communication could not be achieved directly from the earth since the moon itself would block reception and transmission of radio signals. If, however, a

communications spacecraft were placed at the L_4 and L_5 points of the earth-moon system, communication with a large portion of the far side of the moon could be maintained over a considerable period of time provided the spacecraft stayed in the vicinity of the libration point. Figure 3 illustrates an approximation of the possible communication coverage. Obviously, communication is possible with a larger area via the libration spacecraft than with straight-line earth-moon communications. Another alternative would be to use a lunar satellite. However, a near lunar satellite could provide communication for only a short period of time and this method would require a network of such satellites to provide direct communication at all times. In Ref. 17, a system of five equally spaced lunar satellites at a circular orbit radius of 3500 miles is suggested. However, the libration point satellites of which there would be only two, may provide sufficient coverage at a more favorable cost. In addition, a synchronous satellite similar to that of the earth is not possible. In fact, the five libration points of the restricted three-body problem are the lunar equivalent of a terrestrial synchronous orbit.

Another possible use for the triangular libration points would be the establishment of an astronomical observatory, either manned or unmanned. A major advantage would be the accessibility for observation of any portion of the universe except the very small sectors blocked by the earth, the moon, and the sun. The observational accessibility would be much greater than that available to a terrestrial observatory or even a lunar observatory. Both the lunar and terrestrial-based observatories are limited in their observations by the body on which they are located. Earth-based observations can occur only during hours of darkness (except solar observations) and then these observations are sometimes hampered by moonlight. Therefore, the period available

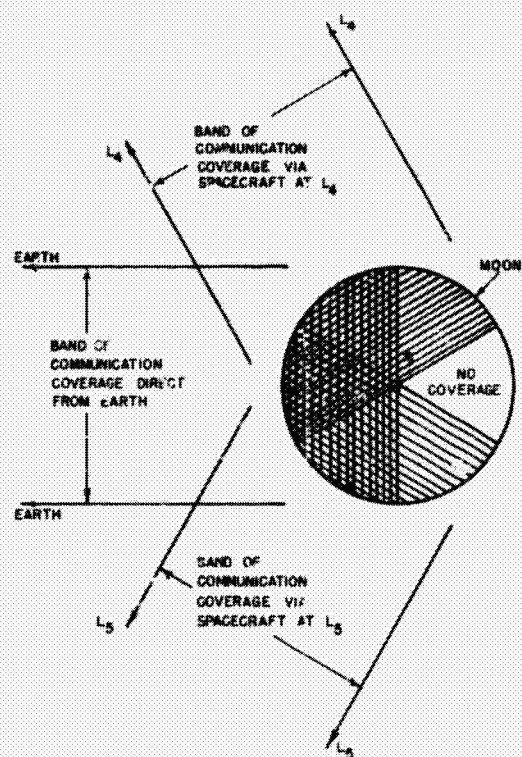


FIGURE 3. USE OF L_4 AND L_5 IN LUNAR COMMUNICATIONS

for observation is about 12 hours per day. The possible observation period is greater on the moon; the entire universe can be observed in a four-week period and observations can be made even when the sun is overhead. However, the section of the sky observable is constrained by the rotation of the moon, and it could be as much as two weeks before the moon rotated sufficiently for a certain portion of the universe to be visible. At the libration points L_4 and L_5 , any portion of the sky could be observed at any time by merely rotating the observatory. An astronomical observatory in a near-earth orbit could also be just as useful. However, photographic plates must be exposed for extended periods of time in stellar photography. Therefore, the telescope must maintain a fixed orientation in space, at least within certain limits to avoid "smudging" of the plate. It may be somewhat simpler to maintain an orientation at the libration points, since it would take about four weeks to complete one revolution around the barycenter. One possible hazard to the use of the libration points for this purpose lies in the possibility of cosmic debris collecting at the libration points, either hampering observations or damaging delicate optical equipment. Optical sightings of such dust clouds at both the L_4 and L_5 points have been reported in Refs. 18 and 19. Such debris could be of lunar origin having been ejected from the moon by a meteor impact on the lunar surface (Ref. 20) or it could be virgin galactic material trapped during an encounter with the libration point.

Additional possible applications are noted in Ref. 16. These include the use of the triangular libration points for long term solar-flare observations. By its very location, the libration point would be essentially free from perturbations on charged particles due to the geomagnetic field. Information

obtained by observing the motion of a vehicle at the triangular points could be used to refine the value of the earth-moon mass ratio.

Still other possibilities of application would be the establishment of facilities to assemble, check out, and launch interplanetary spacecraft. In addition, it may be useful to establish navigation buoys at these locations as an aid in earth-moon and interplanetary flight operations.

Procedure

In the subsequent study, the equations of motion for the spacecraft were derived for each of the mathematical models examined. These equations, viz., three second-order nonlinear differential equations expressing the rectangular components of the spacecraft acceleration were numerically integrated utilizing a standard computer program available at The University of Texas Computation Center Library (Ref. 21). This program is capable of numerically integrating up to 100 simultaneous, first-order, nonlinear differential equations. Therefore, the equations of motion are rewritten as a system of six first-order differential equations. The program is written in FORTRAN 63 language and uses the Runge-Kutta method for obtaining three starting values in addition to the initial conditions which must be provided. After the three values for each variable have been obtained, control is switched to an Adams-Moulton procedure. The Adams-Moulton procedure requires four values to predict the next value; this value is then corrected using all five values, i. e., including the predicted value. While most computations in the program are carried out with single precision arithmetic (approximately 12 digits), certain additions in Runge-Kutta and Adams-Moulton are carried out in double precision (approximately 24 digits). It was found during the course of this research that if all

computations were carried out in double precision, the computer time was in some cases tripled with no appreciable change in the results. In some cases, the initial conditions were computed in double precision. If they are computed in single precision, there will be some round-off error introduced. Since the subsequent trajectory is extremely sensitive to the initial conditions, it is important to supply initial conditions which are accurate. In addition, the program computes the so-called "single-step error," i. e., the error existing at the point of interest using the Adams-Moulton Predictor-Corrector as if all the previous values had been exact solutions to the differential equations. Although this does not give a "true error," it does allow some control of the inherent error in the numerical integration procedure. If the single-step error is outside a range specified by the program user, the step size can be halved to reduce the error. If the single-step error is lower than the minimum error specified, the step size can be doubled to reduce the computation time. Additional information on the numerical integration procedure will be provided in the discussion of results of the numerical studies.

Although the integration was carried out numerically on the Control Data Corporation (CDC) 1604 digital computer at The University of Texas Computation Center, it is feasible to carry out the integration on an analog computer. Because of the complexity of the equations and the limited capability of the analog facilities at The University of Texas, the project of performing the integration on the analog computer was abandoned. In addition, it would not be feasible to use the present analog computer at The University of Texas for the mathematical model utilizing ephemeris information. Planetary position and velocity information is stored on magnetic tapes in eight-day records and in order to use these tapes on the analog, a hybrid digital-analog computer system would be required.

CHAPTER II

MATHEMATICAL MODEL

In order to predict the motion of a spacecraft near the libration point of interest, it is necessary to define a mathematical model. It seems reasonable to suppose that if the mathematical model represents very accurately the actual physical system, viz., the motions of the members of the solar system and their noncentral gravitation fields, then the prediction of the acceleration of the spacecraft will be accurate also. Unfortunately, if all the features of the actual physical system are incorporated into the model to a high degree of accuracy, the problem can become exceedingly complex and may require prodigious amounts of computer time. On the other hand, if the model has too many simplifying assumptions, it may not accurately predict the motion of the vehicle. As Richard Bellman stated (Ref. 22): ". . . the Scientist [or Engineer] like the Pilgrim, must wend a straight and narrow path between the Pitfalls of Oversimplification and the Morass of Overcomplication." To prove that he understands the physical phenomenon he observes, the scientist must be able to predict the recurrence of that phenomenon. To predict it, he defines a mathematical model to represent the phenomenon under consideration and then proceeds to study the mathematical model in an effort to understand the phenomenon. The objective of the investigation reported here is to determine the nature of the motion of a spacecraft near the triangular libration points.

In order to predict this motion, it is necessary to define a mathematical model. Furthermore, the accuracy of the prediction will depend on how well the model represents the physical world. Unfortunately, as more effects of the physical world are included in the mathematical model, the more complex the mathematical model becomes, and the more extensive the calculations for the numerical solution become. Some of the physical world effects can be neglected in certain cases and still have a fairly accurate prediction of the spacecraft motion. In order to establish a mathematical model for the motion of a spacecraft at the L_4 - or L_5 - points of the earth-moon system, it is necessary to understand the motions and effects of the natural bodies of the solar system so that certain simplifying assumptions can be justified. The motion of the individual members of the solar system, particularly the earth-moon system, is the subject of the following section. Another section will state the physical characteristics of the natural bodies which have an effect on the motion of the spacecraft. Finally, the simplifying assumptions incorporated in the specific mathematical models will be stated.

Motion of the Planets and the Solar System

The motion of the earth-moon system, and for that matter, all of the members of the solar system, is very complex. As an aid to understanding the total motion, the motion can be divided into several different components. In effect, a model of the physical system which is comprised of several separate motions is defined.

Probably the most noticeable motion to an observer on the earth is the daily motion, i. e., the motion of the earth which creates the day-night cycle. It is convenient to define an axis of rotation for the earth, calling the

intersections of this axis with the surface of the earth the North Pole and the South Pole. For most purposes, the axis of rotation (defined by the angular velocity vector) can be assumed to have a fixed direction in space. The direction of the angular velocity vector is very nearly toward Polaris, the North Star, i. e., toward the North Celestial Pole. However, this vector does not actually have a fixed direction. There is a long-term motion, called precession, in which a point on the axis describes a conical path. This path is not quite circular; furthermore, about 26,000 years are required for this vector to make one revolution. In addition to precession, there is a short-term motion, called nutation or nodding of the poles. To complicate this motion even further, the poles of the earth are not at fixed points on the earth, i. e., the earth shifts about the axis of rotation. There also are variations in the rate of the earth's rotation. All of these effects (some of which cannot be predicted) will affect the motion of a spacecraft at the libration point only by changing the earth's noncentral gravitational field components (see Physical Characteristics of the Natural Bodies).

A second motion is the revolution of the earth-moon mass center around the sun, the nearest star to the earth. Because of the size of the moon in comparison to the size of the primary body, viz., the earth, the system has the characteristics of a double planet. The center of mass of the earth-moon system, or barycenter, describes a near elliptical path around the sun. Astronomers generally define the ecliptic as the apparent annual path of the sun's center on the celestial sphere. An accurate definition would be that the ecliptic is a plane perpendicular to the barycenter's angular momentum vector which includes the barycenter. The orientation of this plane in space is not fixed, and for most purposes some reference ecliptic must be selected. The motion

of the ecliptic with respect to some reference ecliptic fixed in space is less than one degree. It should be pointed out that in two-body motion this plane would remain fixed in space. This is not the case for the physical world because of the gravitational attractions of other bodies both in and external to the solar system.

Another motion is that of the earth and moon around the barycenter. These orbits deviate somewhat from an elliptical path. The earth-moon orbit plane, defined as a plane which is perpendicular to the angular momentum vector of the earth-moon system and which contains the earth, moon, and their barycenter, does not maintain a fixed direction in space. First of all, the inclination between some reference ecliptic and the earth-moon orbital plane varies. Secondly, the line of nodes between the ecliptic and the earth-moon orbital plane does not remain fixed, but moves in a westerly, or retrograde, direction along the ecliptic.

In addition, the other planets (both minor and major) and their satellites move in near elliptical orbits around the mass center of the solar system. The sun, of course, also moves around the center of mass of the entire solar system. In Fig. 4, the center of mass location relative to the center of the sun is shown for the period from January 10, 1967, 0^hGMT to June 2, 1974, 0^hGMT. It is of interest to note that the center of mass is over 400,000 miles from the center of the sun for several months during this period. The information shown in Fig. 4 was computed from information stored on the Jet Propulsion Laboratory Ephemeris Tapes.

The center of mass of the solar system is also in motion. It is revolving about the center of the Milky Way Galaxy at a distance of perhaps 30,000 light-years. It takes 230 million years to complete one revolution. The solar

system center of mass is also moving toward the constellation of Hercules with a relative velocity of about 12 miles per second. Finally, the entire Milky Way Galaxy is in motion with respect to the external galaxies.

Physical Characteristics of the Natural Bodies

None of the natural bodies are homogeneous spheres. The earth, in fact, is somewhat flattened at the poles and bulged near the equator. In some mathematical models it has been treated as an oblate spheroid. This bulge causes artificial satellites to deviate from the two-body conic predictions even if the effects of the other bodies are not included. Due to this bulge, the earth's gravitational field is not a central force field. In a central field there is no angular component of force; hence, the force has only a radial component. However, in the noncentral force field, there is an angular component of force in addition to a radial component. The potential function Φ of the oblate spheroid which is used to represent the earth, is expressed as

$$\Phi(R, \phi) = \frac{Gm_{\oplus}}{R} \left[1 + \frac{J_2}{2} \frac{R_{\oplus}^2}{R^2} (1 - 3 \sin^2 \phi) + \frac{J_3}{3} \frac{R_{\oplus}^3}{R^3} (3 - 5 \sin^2 \phi) \sin \phi - \frac{J_4}{8} \frac{R_{\oplus}^4}{R^4} (3 - 30 \sin^2 \phi + 35 \sin^4 \phi) \right] \quad (1)$$

or

$$\Phi(R, \phi) = \frac{Gm_{\oplus}}{R} [1 + f(\phi, R)] \quad (2)$$

where ϕ is the latitude, J_2 , J_3 , and J_4 are constants, R is the radial distance to some mass, and R_{\oplus} is the mean radius of the earth (Ref. 23).

The moon also deviates from a homogeneous sphere. In some mathematical models the moon is represented by a triaxial ellipsoid; again, as in

the case of the earth, the gravitational field is noncentral. For the triaxial ellipsoid representing the moon, the potential function is

$$\Phi(R, \mu, \lambda) = \frac{Gm_m}{R} \left[1 + J \frac{R_m^2}{R^2} \left(\frac{1}{3} - \sin^2 \mu \right) + L \frac{R_m^2}{R^2} \cos^2 \mu \cos 2\lambda \right] \quad (3)$$

or

$$\Phi(R, \mu, \lambda) = \frac{Gm_m}{R} [1 + f^*(\mu, \lambda, R)] \quad (4)$$

where μ is the selenographic latitude, λ is the selenographic longitude, J and L are constants, and R_m is the mean radius of the moon (Ref. 23).

In addition, the other planets and the sun are not true spheres. Because of the noncentral force fields of these bodies, they produce forces on a spacecraft in addition to the Newtonian gravitational attraction for a point mass. However, at planetary distances the noncentral force components are negligible and the planetary bodies can be treated as mass points.

Assumptions

In the subsequent analysis, Newton's Laws of Motion and Newton's Law of Gravitation will be accepted as postulates. The latter law expresses the force of attraction between two point masses as

$$\bar{F}_{12} = \frac{Gm_1 m_2 \bar{r}_{12}}{r_{12}^3} \quad (5)$$

where \bar{F}_{12} is the force exerted on m_1 by m_2 , G is the universal gravitational constant, and \bar{r}_{12} is the radius vector between the two masses m_1 and m_2 . As can be seen from Eq. (5), the direction of the gravitational force \bar{F} is along the vector \bar{r}_{12} . The differential equations of motion of a spacecraft in the earth-moon system are expressed by Newton's Second Law, viz.,

$$\mathbf{F} = m_S \ddot{\mathbf{r}}_S \quad (6)$$

where m_S is the mass of the spacecraft and $\ddot{\mathbf{r}}_S$ is the acceleration of the spacecraft with respect to an inertial coordinate system. Obviously, the magnitude and direction of the acceleration is dependent on the magnitude and direction of the resultant force on the spacecraft. The forces on the spacecraft which can be predicted are the gravitational forces and those forces due to solar radiation pressure. In an actual flight, of course, these would not be the only forces acting on the spacecraft; there would also be forces due to propulsion systems, reaction controls, and impact forces due to meteor strikes. However, the occurrence of the latter force cannot be predicted. With the aforementioned set of postulates, the assumptions common to both mathematical models studied are stated as follows:

1. All the bodies under consideration will be treated as point masses. Since the libration points of interest are approximately 240,000 miles from the earth and moon, the effect of the noncentral force fields of these two bodies will be small, however, they would probably have a noticeable effect on the long-term motion, i. e., motion over many years. Figure 5 shows the magnitude of the noncentral component of the earth's gravitational force, i. e., $f(\phi, R)$, as defined in Eq. (2), for a body at a distance of 240,000 miles from the earth, i. e., $R = 240,000$ miles. The moon's declination varies from about 28.5° to -28.5° . A spacecraft in the earth-moon orbital plane will have the same range in declination or latitude. The $f(\phi, R)$ term of Eq. (2) varies from 1.48×10^{-7} to 3.69×10^{-8} for this range in latitude. The term $f^*(\mu, \lambda, R)$ of Eq. (4) is 10^{-1} or

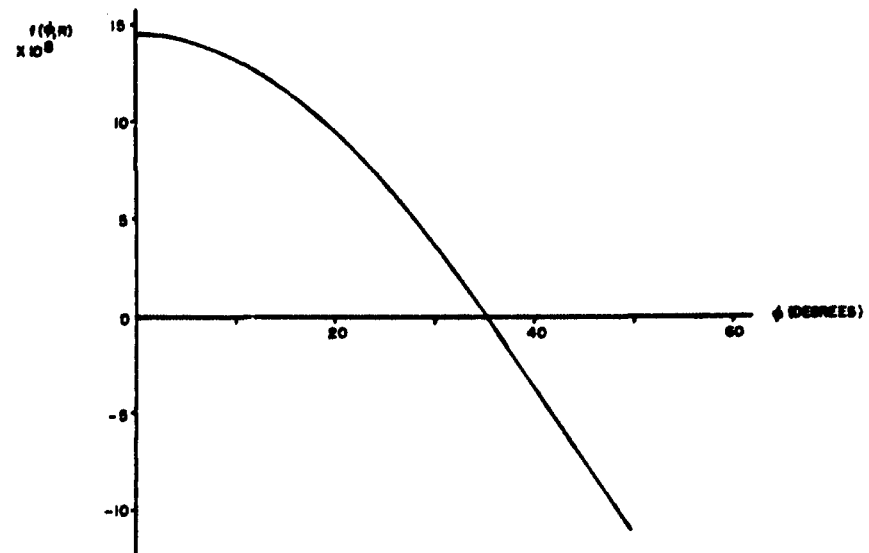


FIGURE 5 . $f(\phi, R)$ VS. LATITUDE (OR DECLINATION)
FOR $R = 240,000$ MILES

smaller than $f(\phi, R)$. This indicates that the effect of the terrestrial and lunar noncentral gravitational fields is on the same order of magnitude as the point mass gravitational attraction of Uranus, Neptune, and Pluto as can be seen from Table A-1 in Appendix A. In addition, the noncentral force fields of bodies other than the earth and moon have a negligible effect on a spacecraft in the earth-moon system.

2. The spacecraft will be assumed to be a particle of very small mass, i. e., it produces no effect on the motions of the earth, moon, etc.

3. External forces on the solar system will be neglected. Even the nearest stars to the solar system are more than four light-years away and their gravitational attractions will certainly be very small. By this assumption, the center of mass of the solar system will move on a straight line with constant velocity relative to a true inertial coordinate system. This assumption allows use of the center of mass of the solar system as the location of an inertial coordinate system.

4. Relativistic effects will be excluded.

5. Solar radiation pressure on the spacecraft will be neglected, i. e., the area to mass ratio of the spacecraft is assumed to be very small.

These assumptions form the basis for the derivation of the differential equations of motion. Further assumptions will be stated as they are necessary in defining a particular mathematical model. There will be two different mathematical models considered here. In one model, a modified restricted

four-body model, certain assumptions will be made regarding the orbits of the earth, moon, and sun in order to express the positions of these bodies algebraically. The other model will utilize the Jet Propulsion Laboratory Ephemeris Tapes for the positions of the natural bodies. These tapes provide ephemeris information to the highest degree of accuracy available at this time.

In the modified restricted four-body mathematical model, only the libration point L_4 is considered. Preliminary studies found that the motion near L_5 is very similar to the motion near L_4 for some initial orientations of the earth-moon-sun system. However, consideration of motion near the L_5 point has not been thorough. Hence, additional consideration of the motion at L_5 using ephemeris information is warranted. Such a study is included here.

CHAPTER III

A MODIFIED RESTRICTED FOUR-BODY PROBLEM

Mathematical Model

Since computations with the general n-body model are quite time consuming, efforts to define a model which is more realistic than the restricted four-body problem, but less complicated than the general n-body model seems warranted. In the model discussed in the present chapter, the restricted four-body model is modified to the effects of the regression of the earth-moon plane. The assumptions made in this model (in addition to those already stated in the section entitled "Assumptions" of the previous chapter) are as follows:

1. Since the sun is the largest mass in the solar system, and has several thousand times greater effect on a spacecraft at a triangular libration point in the earth-moon system than any of the planets (see Table A-1, Appendix A) with the exception, of course, of the earth and the moon, the gravitational attractions of the planets are neglected. Therefore the problem reduces to a four-body problem, viz., sun, moon, earth, and spacecraft.

2. Since forces due to bodies external to the solar system are neglected, the center of mass of the four-body system will move with constant velocity relative to an absolute coordinate system. The

center of mass of this four-body system is approximately 50 miles from the center of the sun; however, this is a small fraction of the total distance from the solar center to the earth-moon barycenter, and it will be assumed that the four-body center of mass is at the center of the sun.

3. The barycenter moves in a circular orbit around the sun; the earth and moon move in circular orbits around the barycenter. As stated previously, these bodies actually move in near elliptical orbits. In effect, the earth and the moon are being constrained to move in circular orbits around the barycenter. The indirect action of the sun on the earth and the moon would actually cause these bodies to move in non-circular orbits.

4. The ecliptic plane is assumed to have a fixed orientation in space.

5. The earth-moon plane, a plane in which the circular motion of the earth and moon occurs, is inclined to the ecliptic at a constant angle of $5^{\circ}9$ minutes.

6. The line of nodes of the earth-moon plane and the ecliptic regresses at the constant rate of one revolution in about 18.6 years. In effect, part of the sun's indirect action on the motion of the moon is being included.

The first five assumptions are incorporated in Refs. 4 and 5. Therefore, this investigation differs from the investigation reported in these references only by the inclusion of the nodal regression. One important point to note here is that the earth-moon plane as defined in the fifth assumption is not the earth-moon orbital plane as defined by the angular momentum. Instead, it is simply

a plane in which the circular motion occurs. If there were no nodal regression, the orbital plane defined by the angular momentum would coincide with the earth-moon plane.

Utilizing these assumptions, four cases will be investigated. The first of these will present the equations of motion in a libration-point-centered rotating coordinate system. This was done in order to permit a comparison with the studies reported in Refs. 4 and 5. In the second case, the equations of motion are derived in the barycentered nonrotating coordinate system and the integration is carried out. The results are compared with the case in which the libration-point-centered rotating coordinate system was used. In both of these cases, it was assumed that the triangular libration points lie in the earth-moon plane. In the third case, it is assumed that the libration point exists in the earth-moon orbital plane as defined by the angular momentum vector. The same initial conditions are used in the first three cases and the results are compared. In the last case, an initial earth-moon-sun configuration is used which corresponds to the configuration existing on Julian Date 2,439,501.0 (January 10, 1967; 12^h GMT). This latter case will be used as a comparison to the "real world" model with the same initial date.

Case I: Rotating Coordinate System at L_4

Equations of motion. With the assumptions stated in the previous section, the coordinate systems and geometry of the mathematical model can be illustrated as shown in Fig. 6. The (X , Y , Z)-coordinate system is located at the center of the sun. The X -axis points in a fixed direction and was chosen for convenience to be the vernal equinox, the Y -axis lies in the ecliptic, and the Z -axis is perpendicular to the ecliptic. At the barycenter, the

axes of the nonrotating (X, Y, Z)-coordinate system are parallel to their counterparts in the sun-centered coordinate system. The (ξ, η, ζ)-coordinate system is oriented such that the origin is at the barycenter, the ξ -axis lies along the earth-moon line, the η -axis lies in the earth-moon plane, and the ζ -axis is perpendicular to that plane. The (x, y, z)-coordinate system is centered at the L_4 point (assumed to be in the earth-moon plane) and the (x, y, z)-axes are parallel to the (ξ, η, ζ)-axes, respectively.

The differential equations of motion for a spacecraft referred to the sun-centered inertial coordinate system are expressed by application of Eqs. (5) and (6), i. e.,

$$m_S \ddot{\bar{r}}_{\odot S} = - \frac{Gm_{\odot} m_S \bar{r}_{\odot S}}{r_{\odot S}^3} - \frac{Gm_{\oplus} m_S \bar{r}_{\oplus S}}{r_{\oplus S}^3} - \frac{Gm_{\text{J}} m_S \bar{r}_{\text{J}S}}{r_{\text{J}S}^3} \quad (7)$$

Equation (7) is valid for the mathematical model under consideration with the assumptions stated previously. In this particular study, the acceleration with respect to a coordinate system located at one of the triangular libration points, viz., L_4 , is desired. It is therefore necessary to relate the motions in a sun-centered inertial coordinate system to the motions in a rotating libration-point-centered coordinate system.

The position of the spacecraft with respect to the inertial coordinate system is, as shown in Fig. 7,

$$\bar{r}_{\odot S} = \bar{r}_{\odot B} + \bar{r}_{BS} \quad (8)$$

where $\bar{r}_{\odot B}$ is measured in the (X, Y, Z)-inertial coordinate system and \bar{r}_{BS} is measured in the (X, Y, Z)-nonrotating coordinate system located at the barycenter. The inertial velocity and acceleration of the spacecraft is then

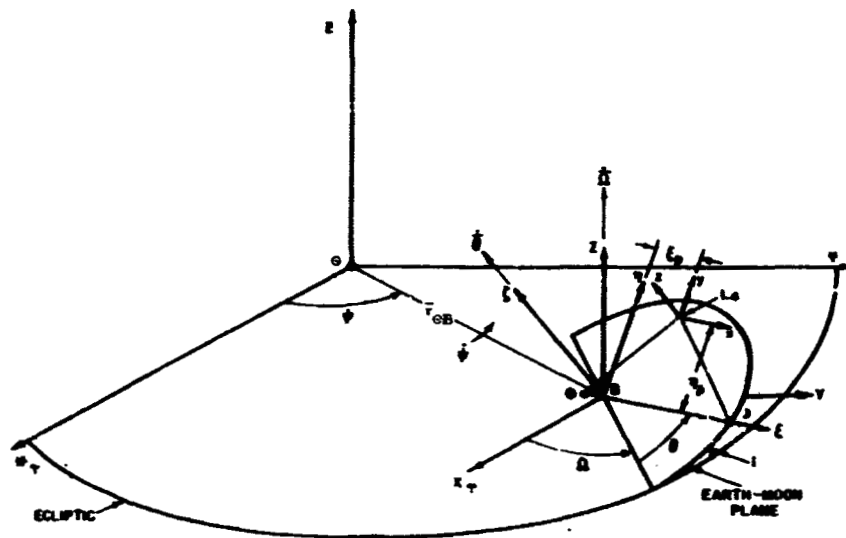


FIGURE 6. COORDINATE SYSTEMS AND GEOMETRY OF THE MATHEMATICAL MODEL

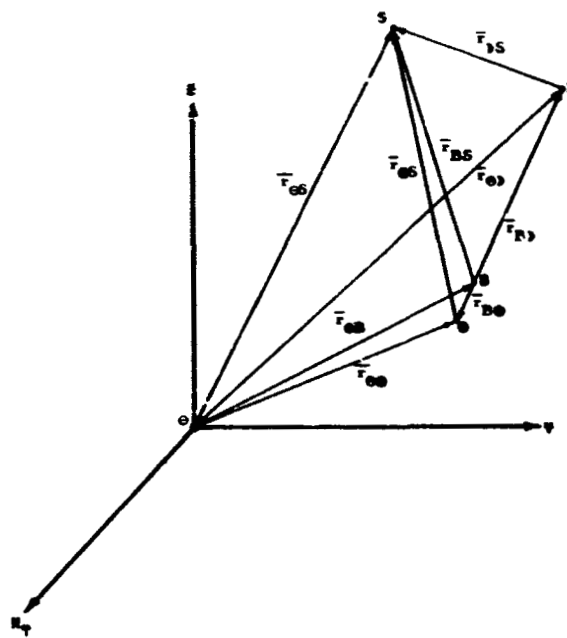


FIGURE 7. VECTOR REPRESENTATION OF POSITION

$$\dot{\mathbf{r}}_{\odot S} = \dot{\mathbf{r}}_{\odot B} + \dot{\mathbf{r}}_{BS} \quad (9)$$

$$\ddot{\mathbf{r}}_{\odot S} = \ddot{\mathbf{r}}_{\odot B} + \ddot{\mathbf{r}}_{BS} \quad (10)$$

The term $\ddot{\mathbf{r}}_{BS}$ is the acceleration of the spacecraft as observed in the (X, Y, Z)-nonrotating system. The term $\ddot{\mathbf{r}}_{BS}$ expressed in the rotating (ξ, η, ζ)-coordinate system is given by the following expression (Ref. 24):

$$\ddot{\mathbf{r}}_{BS} = \bar{\omega} \times (\bar{\omega} \times \bar{\mathbf{r}}_{BS}) + \dot{\bar{\omega}} \times \bar{\mathbf{r}}_{BS} + \bar{\mathbf{r}}_{BS}'' + 2\bar{\omega} \times \bar{\mathbf{r}}_{BS}' \quad (11)$$

where all quantities on the right are expressed in the (ξ, η, ζ)-coordinate system; $\bar{\mathbf{r}}'$ and $\bar{\mathbf{r}}''$ are the velocity and acceleration observed in the rotating (ξ, η, ζ)-system. The relation between positions measured in the (ξ, η, ζ)-coordinate system and the (X, Y, Z)-system is derived in Ref. 25. Expressed in matrix notation, the relation is

$$\begin{bmatrix} X \\ Y \\ Z \end{bmatrix} = A \begin{bmatrix} \xi \\ \eta \\ \zeta \end{bmatrix} \quad (12)$$

where

$$A = \begin{bmatrix} (\cos\Omega\cos\theta - \sin\Omega\sin\theta\cos i) & (-\cos\Omega\sin\theta - \sin\Omega\cos\theta\cos i) & (\sin\Omega\sin i) \\ (\sin\Omega\cos\theta + \cos\Omega\sin\theta\cos i) & (-\sin\Omega\sin\theta + \cos\Omega\cos\theta\cos i) & (-\cos\Omega\sin i) \\ (\sin\theta\sin i) & (\cos\theta\sin i) & (\cos i) \end{bmatrix} \quad (13)$$

Then,

$$\begin{bmatrix} \xi \\ \eta \\ \zeta \end{bmatrix} = A^{-1} \begin{bmatrix} X \\ Y \\ Z \end{bmatrix} \quad (14)$$

Note that A is an orthogonal matrix and hence (Ref. 25)

$$A^{-1} = A^T \quad . \quad (15)$$

The total angular velocity vector, $\bar{\omega}$, can be expressed as

$$\bar{\omega} = \omega_{\xi} \bar{\epsilon}_{\xi} + \omega_{\eta} \bar{\epsilon}_{\eta} + \omega_{\zeta} \bar{\epsilon}_{\zeta} \quad (16)$$

where

$$\begin{aligned} \omega_{\xi} &= \dot{\Omega} \sin \theta \sin i \\ \omega_{\eta} &= \dot{\Omega} \cos \theta \sin i \\ \omega_{\zeta} &= \dot{\Omega} \cos i + \dot{\theta} \quad . \end{aligned} \quad (17)$$

Furthermore, by differentiating Eq. (16) it follows that

$$\dot{\bar{\omega}} = \dot{\omega}_{\xi} \bar{\epsilon}_{\xi} + \dot{\omega}_{\eta} \bar{\epsilon}_{\eta} + \dot{\omega}_{\zeta} \bar{\epsilon}_{\zeta} \quad (18)$$

where

$$\begin{aligned} \dot{\omega}_{\xi} &= \ddot{\Omega} \sin \theta \sin i + \dot{\Omega} \dot{\theta} \cos \theta \sin i \\ \dot{\omega}_{\eta} &= \ddot{\Omega} \cos \theta \sin i - \dot{\Omega} \dot{\theta} \sin \theta \sin i \\ \dot{\omega}_{\zeta} &= \ddot{\Omega} \cos i + \ddot{\theta} \end{aligned} \quad (19)$$

Since the motion is assumed to be circular, $\ddot{\theta} = 0$. Also, by assumption, $\dot{\Omega}$ is constant, therefore, $\ddot{\Omega} = 0$. Hence, Eqs. (19) reduce to the following expressions.

$$\begin{aligned} \dot{\omega}_{\xi} &= \dot{\Omega} \dot{\theta} \cos \theta \sin i \\ \dot{\omega}_{\eta} &= - \dot{\Omega} \dot{\theta} \sin \theta \sin i \\ \dot{\omega}_{\zeta} &= 0 \quad . \end{aligned} \quad (20)$$

In the (ξ, η, ζ) -rotating coordinate system,

$$\begin{aligned}\bar{r}_{BS} &= \xi_S \bar{\epsilon}_\xi + \eta_S \bar{\epsilon}_\eta + \zeta_S \bar{\epsilon}_\zeta \\ \dot{\bar{r}}_{BS} &= \dot{\xi}_S \bar{\epsilon}_\xi + \dot{\eta}_S \bar{\epsilon}_\eta + \dot{\zeta}_S \bar{\epsilon}_\zeta \\ \ddot{\bar{r}}_{BS} &= \ddot{\xi}_S \bar{\epsilon}_\xi + \ddot{\eta}_S \bar{\epsilon}_\eta + \ddot{\zeta}_S \bar{\epsilon}_\zeta\end{aligned}\quad (21)$$

Substituting Eqs. (16), (18), and (21) into Eq. (11) and carrying out the indicated operation leads to the following expression:

$$\begin{aligned}\ddot{\bar{r}}_{BS} &= [\ddot{\xi}_S + 2(\omega_\eta \dot{\xi}_S - \omega_\zeta \dot{\eta}_S) - \xi_S(\omega_\eta^2 + \omega_\zeta^2) + \eta_S(\omega_\xi \omega_\eta - \dot{\omega}_\zeta) \\ &\quad + \zeta_S(\omega_\xi \omega_\zeta + \dot{\omega}_\eta)] \bar{\epsilon}_\xi + [\ddot{\eta}_S + 2(\omega_\zeta \dot{\xi}_S - \omega_\xi \dot{\zeta}_S) \\ &\quad + \xi_S(\omega_\xi \omega_\eta + \dot{\omega}_\zeta) - \eta_S(\omega_\xi^2 + \omega_\zeta^2) + \zeta_S(\omega_\eta \omega_\zeta - \dot{\omega}_\xi)] \bar{\epsilon}_\eta \\ &\quad + [\ddot{\zeta}_S + 2(\omega_\xi \dot{\eta}_S - \omega_\eta \dot{\zeta}_S) + \xi_S(\omega_\xi \omega_\zeta - \dot{\omega}_\eta) \\ &\quad + \eta_S(\omega_\eta \omega_\zeta + \dot{\omega}_\xi) - \zeta_S(\omega_\xi^2 + \omega_\eta^2)] \bar{\epsilon}_\zeta\end{aligned}\quad (22)$$

The acceleration expressed in the rotating (ξ, η, ζ) -coordinate system can be expressed in the (x, y, z) -coordinate system by noting that

$$\begin{aligned}\xi_S &= x_S + \xi_p \\ \eta_S &= y_S + \eta_p \\ \zeta_S &= z_S\end{aligned}\quad (23)$$

It should be pointed out that the origin of the (x, y, z) -coordinate system lies in the earth-moon plane. Furthermore, by differentiating Eqs. (23) with respect to time yields

$$\begin{aligned}\dot{\xi}_S &= \dot{x}_S + \dot{\xi}_p, & \ddot{\xi}_S &= \ddot{x}_S + \ddot{\xi}_p \\ \dot{\eta}_S &= \dot{y}_S + \dot{\eta}_p, & \ddot{\eta}_S &= \ddot{y}_S + \ddot{\eta}_p \\ \dot{\zeta}_S &= \dot{z}_S, & \ddot{\zeta}_S &= \ddot{z}_S.\end{aligned}$$

Since the locations of the triangular libration points are defined by the earth-moon distance which is constant because of the circular orbit assumption, it follows that

$$\dot{\xi}_p = \ddot{\xi}_p = 0, \quad \dot{\eta}_p = \ddot{\eta}_p = 0$$

and

$$\begin{aligned}\dot{\xi}_S &= \dot{x}_S, & \dot{\eta}_S &= \dot{y}_S, & \dot{\zeta}_S &= \dot{z}_S \\ \ddot{\xi}_S &= \ddot{x}_S, & \ddot{\eta}_S &= \ddot{y}_S, & \ddot{\zeta}_S &= \ddot{z}_S.\end{aligned}\tag{24}$$

Since the barycenter moves in a circular orbit around the sun, the acceleration of the barycenter with respect to the sun is

$$\ddot{\bar{r}}_{\odot B} = (-R_{\odot B} \dot{\psi}^2 \cos \psi) \bar{i} + (-R_{\odot B} \dot{\psi}^2 \sin \psi) \bar{j}\tag{25}$$

as shown in Fig. 8, where $R_{\odot B} = |\bar{r}_{\odot B}|$. The coordinates of the sun, expressed in the barycentered (X, Y, Z)-system are

$$\begin{aligned}X_{\odot} &= -R_{\odot B} \cos \psi \\ Y_{\odot} &= -R_{\odot B} \sin \psi \\ Z_{\odot} &= 0.\end{aligned}\tag{26}$$

Therefore Eq. (25) reduces to the following:

$$\ddot{\bar{r}}_{\odot B} = (X_{\odot} \dot{\psi}^2) \bar{i} + (Y_{\odot} \dot{\psi}^2) \bar{j}\tag{27}$$

The acceleration vector expressed by Eq. (27) can be rewritten in the (x, y, z)-coordinate system as

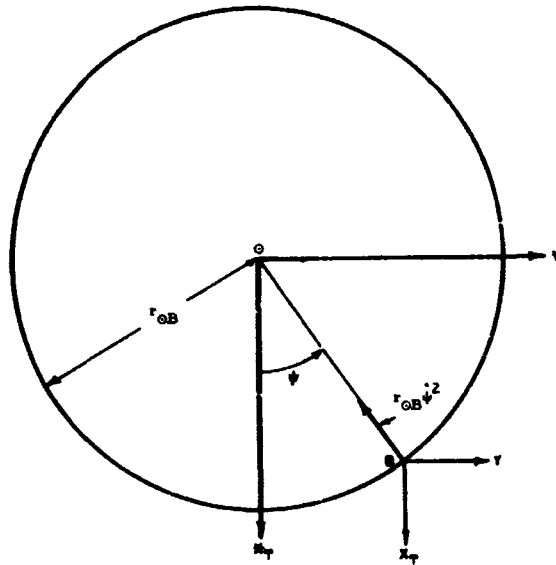


FIGURE 8 . ACCELERATION OF THE BAR CENTER

$$\begin{bmatrix} \ddot{x}_{\odot B} \\ \ddot{y}_{\odot B} \\ \ddot{z}_{\odot B} \end{bmatrix} = \dot{\psi}^2 A^T \begin{bmatrix} X_{\odot} \\ Y_{\odot} \\ 0 \end{bmatrix} \quad (28)$$

where $\ddot{x}_{\odot B}$, $\ddot{y}_{\odot B}$, $\ddot{z}_{\odot B}$ are the components of the absolute acceleration, $\ddot{\vec{r}}_{\odot B}$, expressed in the rotating (x, y, z)-coordinate system. The coordinates of the sun expressed in the (x, y, z)-system are

$$\begin{bmatrix} x_{\odot} \\ y_{\odot} \\ z_{\odot} \end{bmatrix} = A^T \begin{bmatrix} X_{\odot} \\ Y_{\odot} \\ 0 \end{bmatrix} - \begin{bmatrix} \xi_p \\ \eta_p \\ 0 \end{bmatrix} \quad (29)$$

Now combining Eq. (29) with Eq. (28), the following expression can be obtained

$$\begin{bmatrix} x_{\odot B} \\ y_{\odot B} \\ z_{\odot B} \end{bmatrix} = \dot{\psi}^2 \begin{bmatrix} x_{\odot} + \xi_p \\ y_{\odot} + \eta_p \\ z_{\odot} \end{bmatrix} \quad (30)$$

Furthermore, Eq. (27) can now be expressed as

$$\ddot{\vec{r}}_{\odot B} = \ddot{x}_{\odot B} \bar{\epsilon}_x + \ddot{y}_{\odot B} \bar{\epsilon}_y + \ddot{z}_{\odot B} \bar{\epsilon}_z \quad (31)$$

Substituting Eqs. (22), (23), (24), (30), and (31) into the right hand side of Eq. (10) and Eq. (7) into the left hand side of Eq. (10) and collecting components in the respective (x, y, z)-directions will lead to the three following scalar equations:

$$\begin{aligned}
\ddot{x}_S = & -2[\omega_\eta \dot{z}_S - \omega_\zeta \dot{y}_S] + (x_S + \xi_p)(\omega_\eta^2 + \omega_\zeta^2) \\
& - (y_S + \eta_p)(\omega_\xi \omega_\eta - \dot{\omega}_\zeta) - z_S(\omega_\xi \omega_\zeta + \dot{\omega}_\eta) \\
& - \dot{\psi}^2(x_\odot + \xi_p) - \frac{Gm_\odot}{r_{\odot S}^3}(x_S - x_\odot) - \frac{Gm_\oplus}{r_{\oplus S}^3}(x_S - x_\oplus) \\
& - \frac{Gm_J}{r_{J S}^3}(x_S - x_J)
\end{aligned}$$

$$\begin{aligned}
\ddot{y}_S = & -2[\omega_\zeta \dot{x}_S - \omega_\xi \dot{z}_S] - (x_S + \xi_p)(\omega_\xi \omega_\eta + \dot{\omega}_\zeta) \\
& + (y_S + \eta_p)(\omega_\xi^2 + \omega_\zeta^2) - z_S(\omega_\eta \omega_\zeta - \dot{\omega}_\xi) \\
& - \dot{\psi}^2(y_\odot + \eta_p) - \frac{Gm_\odot}{r_{\odot S}^3}(y_S - y_\odot) - \frac{Gm_\oplus}{r_{\oplus S}^3}(y_S - y_\oplus) \\
& - \frac{Gm_J}{r_{J S}^3}(y_S - y_J)
\end{aligned}$$

$$\begin{aligned}
\ddot{z}_S = & -2[\omega_\xi \dot{y}_S - \omega_\eta \dot{x}_S] - (x_S + \xi_p)(\omega_\xi \omega_\zeta - \dot{\omega}_\eta) \\
& - (y_S + \eta_p)(\omega_\eta \omega_\zeta + \dot{\omega}_\xi) + z_S(\omega_\xi^2 + \omega_\eta^2) \\
& - \dot{\psi}^2(z_\odot) - \frac{Gm_\odot}{r_{\odot S}^3}(z_S - z_\odot) - \frac{Gm_\oplus}{r_{\oplus S}^3}(z_S - z_\oplus) \\
& - \frac{Gm_J}{r_{J S}^3}(z_S - z_J) \quad ,
\end{aligned}$$

(32)

where

$$\begin{aligned}
 r_{\odot S} &= [(x_S - x_{\odot})^2 + (y_S - y_{\odot})^2 + (z_S - z_{\odot})^2]^{1/2} \\
 r_{\oplus S} &= [(x_S - x_{\oplus})^2 + (y_S - y_{\oplus})^2 + (z_S - z_{\oplus})^2]^{1/2} \quad (33) \\
 r_{\text{J}S} &= [(x_S - x_{\text{J}})^2 + (y_S - y_{\text{J}})^2 + (z_S - z_{\text{J}})^2]^{1/2} .
 \end{aligned}$$

Equations (32) are the differential equations of motion referred to the (x, y, z) -rotating coordinate system whose origin is located at the libration point L_4 . They are a system of simultaneous, second order, nonlinear, differential equations. As stated previously, this system of equations was integrated numerically using the Adams-Moulton method with a Runge-Kutta starter. To use these computation techniques, it is necessary to have a system of first-order differential equations. Equations (32) can be rewritten as a system of six first-order equations by noting that

$$\begin{aligned}
 \dot{u}_S &= \ddot{x}_S \quad , \quad \dot{v}_S = \ddot{y}_S \quad , \quad \dot{w}_S = \ddot{z}_S \\
 \dot{x}_S &= u_S \quad , \quad \dot{y}_S = v_S \quad , \quad \dot{z}_S = w_S
 \end{aligned} \quad (34)$$

Constants in the mathematical model. Constants such as the planetary masses are not known exactly, and revisions of these constants take place with the acquisition of additional data. The mass constants used in the mathematical model of this chapter are those generally accepted by and used in the Jet Propulsion Laboratory trajectory programs (Ref. 23). They are as follows:

$$\begin{aligned}
 \frac{m_{\oplus}}{m_{\text{J}}} &= 81.3015 \\
 Gm_{\oplus} &= 3.986032 \times 10^5 \frac{\text{km}^3}{\text{sec}^2} \\
 Gm_{\odot} &= 1.32715445 \times 10^{11} \frac{\text{km}^3}{\text{sec}^2} .
 \end{aligned} \quad (35)$$

Because of the circular orbit assumptions, it is necessary to obtain from the actual physical model "constants" for the mathematical model which are representative of the range of values in the physical model. This task is more difficult than it may at first appear to be. For example, if the moon moved in an elliptical orbit around the barycenter, then the semimajor axis of that orbit could be used as the radius of the circular orbit in the mathematical model under discussion. Since the moon does not move in an elliptical orbit (in fact, neither its perigee radius nor apogee radius is the same from month to month), the choice of representative values becomes more difficult. In addition, the lunar sidereal period varies from month to month. These variations are, of course, the result of solar and planetary perturbations on the two-body motion. A possible choice of "constants" would be to use the osculating elements at some epoch, e. g., 1900 or 1950. In fact, it is these elements that are commonly quoted in tables of constants. Another choice is to use the sidereal period at an epoch for the purpose of calculating an average angular velocity. This latter method was selected since the sidereal periods are essentially constant. It should be noted that the value selected for the average angular velocity will depend on the method selected.

The period of the barycenter's revolution around the sun was taken to be 365.256 days and the period of the earth-moon revolution around the barycenter was taken to be 27.322 days (Ref. 2). For circular motion, the angular velocity is constant and can be computed by dividing the period by 2π . Therefore, the following values were adopted for the angular velocities:

$$\begin{aligned}\dot{\psi} &= 1.9909866 \times 10^{-7} \text{ rad/sec} \\ \dot{\theta} &= 2.6616995 \times 10^{-6} \text{ rad/sec.}\end{aligned}\tag{36}$$

Because of the circular orbit assumption, the radius of each of the circular orbits can be computed from the two-body expression for velocity V , viz.,

$$V = \left(\frac{Gm}{r} \right)^{1/2} = \omega r$$

Therefore,

$$r = \left(\frac{Gm}{\omega^2} \right)^{1/3} \quad (37)$$

Using Eq. (37), the circular orbit radii are computed to be

$$\begin{aligned} |\bar{r}_{\odot B}| &= R_{\odot B} = 1.4959885 \times 10^8 \text{ km} \\ &= 9.29607 \times 10^7 \text{ mi} \end{aligned} \quad (38)$$

$$\begin{aligned} |\bar{r}_{\oplus})| &= 3.847488 \times 10^8 \text{ km} \\ &= 2.39083 \times 10^5 \text{ mi.} \end{aligned}$$

From the distance between the earth and moon, the barycenter is computed to be 4674.87 km or 2907.45 mi from the center of the earth. Also, the ξ_p and η_p distances are calculated to be

$$\begin{aligned} \xi_p &= 1.876995 \times 10^5 \text{ km} \\ &= 1.16631 \times 10^5 \text{ mi} \\ \eta_p &= 3.33202 \times 10^5 \text{ km} \\ &= 2.07052 \times 10^5 \text{ mi.} \end{aligned} \quad (39)$$

The value of the inclination of the earth-moon plane to the Ecliptic of the Epoch 1900 is given in Ref. 2 as

$$i = 5^{\circ}9'$$

In Ref. 26, the longitude of the ascending node is given as

$$\Omega = 259^{\circ}10'59''.79 - 5^r134^{\circ}08'31''.23T + 7''.48T^2 + 0''.008T^3 \quad (40)$$

where the superscript r represents revolutions and T is the time expressed as a fraction of Julian Centuries since the Epoch 1900, viz. ,

$$T = \frac{\text{Julian Day No.} - 2415020}{36525} \quad (41)$$

This expression is an approximate relation for the location of the ascending node. Differentiating once with respect to time yields

$$\dot{\Omega} = -5^r134^{\circ}08'31''.23 + 2(7''.48)T + 3(0''.008)T^2 \quad (42)$$

Neglecting the last two terms, since the first term will be affected only slightly and also because of the sixth assumption , it follows that

$$\begin{aligned} \dot{\Omega} &= -5^r134^{\circ}08'31''.23/\text{century} \\ &= -19.341420 \text{ degrees/year} \\ &= -1.0696994 \times 10^{-8} \text{ rad/sec.} \end{aligned} \quad (43)$$

The minus sign simply indicates that the node moves in a retrograde direction, i. e. , regresses westward along the ecliptic.

Evaluation of equations of motion for $\dot{\Omega} = 0$. Equations (32) differ from the equations of motion in Refs. 4 and 5 only by the inclusion of the nodal regression, $\dot{\Omega}$, in the present analysis. Therefore, if $\dot{\Omega}$ is placed equal to zero in Eqs. (32), these equations should reduce to the equations of Ref. 4. Setting $\dot{\Omega}$ equal to zero in Eqs. (17) and Eqs. (20) yields the following expressions.

$$\begin{aligned} \omega_{\xi} &= 0 \quad , \quad \omega_{\eta} = 0 \quad , \quad \omega_{\zeta} = \dot{\theta} \\ \dot{\omega}_{\xi} &= 0 \quad , \quad \dot{\omega}_{\eta} = 0 \quad , \quad \dot{\omega}_{\zeta} = 0 \end{aligned}$$

Therefore, Eqs. (32) will reduce to the following

$$\begin{aligned} \ddot{x}_S = & + 2\dot{\theta} \dot{y}_S + (x_S + \xi_p) \dot{\theta}^2 - (x_\odot + \xi_p) \dot{\psi}^2 \\ & - \frac{Gm_\odot}{r_{\odot S}^3} (x_S - x_\odot) - \frac{Gm_\oplus}{r_{\oplus S}^3} (x_S - x_\oplus) \\ & - \frac{Gm_J}{r_{J S}^3} (x_S - x_J) \end{aligned}$$

$$\begin{aligned} \ddot{y}_S = & - 2\dot{\theta} \dot{x}_S + (y_S + \eta_p) \dot{\theta}^2 - (y_\odot + \eta_p) \dot{\psi}^2 \\ & - \frac{Gm_\odot}{r_{\odot S}^3} (y_S - y_\odot) - \frac{Gm_\oplus}{r_{\oplus S}^3} (y_S - y_\oplus) \\ & - \frac{Gm_J}{r_{J S}^3} (y_S - y_J) \end{aligned}$$

$$\begin{aligned} \ddot{z}_S = & - z_\odot \dot{\psi}^2 - \frac{Gm_\odot}{r_{\odot S}^3} (z_S - z_\odot) - \frac{Gm_\oplus}{r_{\oplus S}^3} (z_S - z_\oplus) \\ & - \frac{Gm_J}{r_{J S}^3} (z_S - z_J) \quad . \end{aligned}$$

The above equations are the same as those given in Refs. 4 and 5.

It is also important to note some differences in the initial orientation of the mathematical model of Ref. 4 and the model of this chapter. If all variable angles, viz., θ and ψ , are set equal to zero in Ref. 4, one will observe that the initial orientation of the earth, moon, and sun for that model corresponds to an orientation of

$$\Omega = 180^\circ, \quad \theta = 180^\circ, \quad \psi = 180^\circ$$

in the model discussed in this chapter. If the angles $\hat{\theta}$ and $\hat{\psi}$ are measured from the orientation which corresponds to that of Ref 4, the position of the sun measured in the (x, y, z) -rotating coordinate system, as given by Eq. (29), becomes

$$\begin{bmatrix} x_\odot \\ y_\odot \\ z_\odot \end{bmatrix} = A^T \begin{bmatrix} R_{\odot B} \cos \hat{\psi} \\ R_{\odot B} \sin \hat{\psi} \\ 0 \end{bmatrix} - \begin{bmatrix} \xi_p \\ \eta_p \\ 0 \end{bmatrix}$$

where

$$A^T = \begin{bmatrix} \cos \hat{\theta} \sin \hat{\theta} \cos i - \sin \hat{\theta} \sin i \\ -\sin \hat{\theta} \cos \hat{\theta} \cos i - \cos \hat{\theta} \sin i \\ 0 \quad \sin i \quad \cos i \end{bmatrix}$$

or

$$\begin{aligned} x_\odot &= R_{\odot B} (\cos \hat{\theta} \cos \hat{\psi} + \sin \hat{\theta} \sin \hat{\psi} \cos i) - \xi_p \\ y_\odot &= -R_{\odot B} (\sin \hat{\theta} \cos \hat{\psi} - \cos \hat{\theta} \sin \hat{\psi} \cos i) - \eta_p \\ z_\odot &= R_{\odot B} \sin \hat{\psi} \sin i, \end{aligned}$$

and again these are the same equations as those given in Ref. 4.

Case I results and comparison with Ref. 5. Equations (32) were numerically integrated using the Adams-Moulton method with the Runge-Kutta starter. The integration was carried out with a maximum step size of 6000 seconds. In some instances, it was necessary for the program to reduce the step size to 3000 seconds or 1500 seconds. The maximum single step error was set at 1×10^{-5} and the minimum single-step error was set at 5×10^{-11} .

In order to make a comparison with the results of Ref. 5, initial conditions were used in this study which yield the same initial orientation of the earth-moon-sun system. These initial conditions are $\theta_0 = 180^\circ$, $\Omega_0 = 180^\circ$, and $\psi_0 = 180^\circ$ or $\psi_0 = 225^\circ$. In Ref. 5, the spacecraft was assumed to be placed at the libration point with zero velocity relative to the rotating (x, y, z)-system. These initial positions and velocities are also used in this study and are $x_S = y_S = z_S = 0$ and $\dot{x}_S = \dot{y}_S = \dot{z}_S = 0$. The results of the integration giving the projection of the motion on the (x, y)-plane are shown in Figs. 9 to 10. The case in which the initial solar position is along the earth-moon line, i. e., $\psi_0 = 180^\circ$, is represented by Figs. 9. The case in which $\psi_0 = 225^\circ$ is represented by Figs. 10.

For the case in which $\psi_0 = 180^\circ$, the spacecraft maintains a libration point centered motion for the 2500 days studied. As shown in Figs. 9e and 9f, the envelope of motion for the spacecraft increases to a maximum distance of about 220,000 miles in the period from 1000 days to 1250 days after insertion. After this time, the envelope of motion steadily decreases until it reaches a value of about 26,000 miles (Fig. 9k). This "pulsating behavior" was observed in Ref. 5 in which the model excluded the nodal regression. It should be noted that the motion in this case is considerably different than that of Ref. 5 for the same initial orientation of the earth-moon-sun system and the same initial displacement and velocity of the spacecraft.

The motion for $\psi_0 = 225^\circ$ is somewhat different than $\psi_0 = 180^\circ$. The spacecraft continues on a libration-point centered motion for approximately 1200 days. As can be seen from Fig. 10e, the spacecraft appears to be leaving this libration-point centered motion. In Fig. 10f, it is obvious that the spacecraft has taken up an entirely different type of motion than heretofore

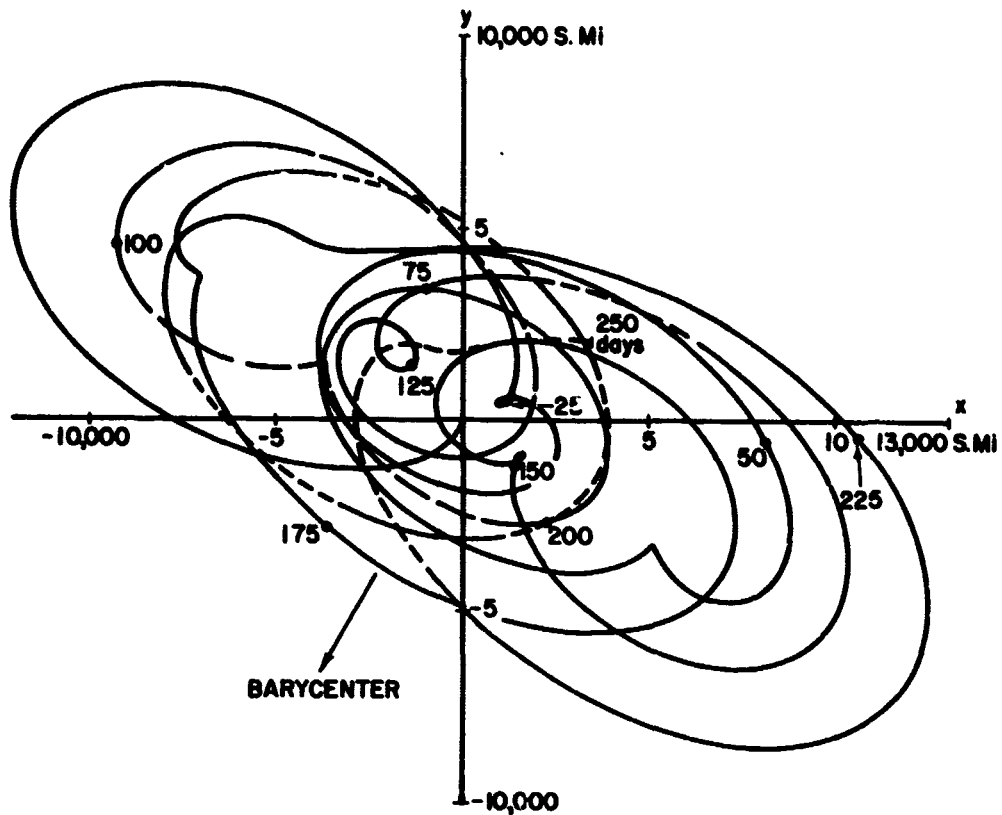


FIGURE 9a. L_4 ROTATING (x, y) -RESULTS FOR $\psi_0 = 180^\circ$
FROM 0 DAYS TO 250 DAYS

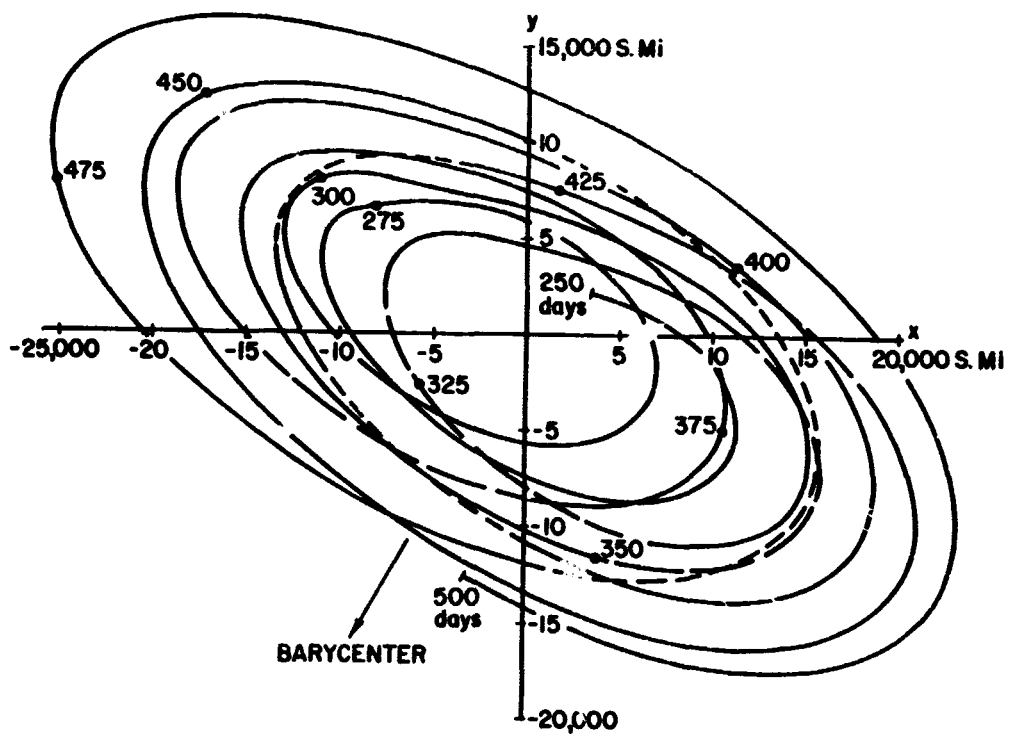


FIGURE 9b. L_4 ROTATING (x, y) -RESULTS FOR $\psi_0 = 180^\circ$
FROM 250 DAYS TO 500 DAYS

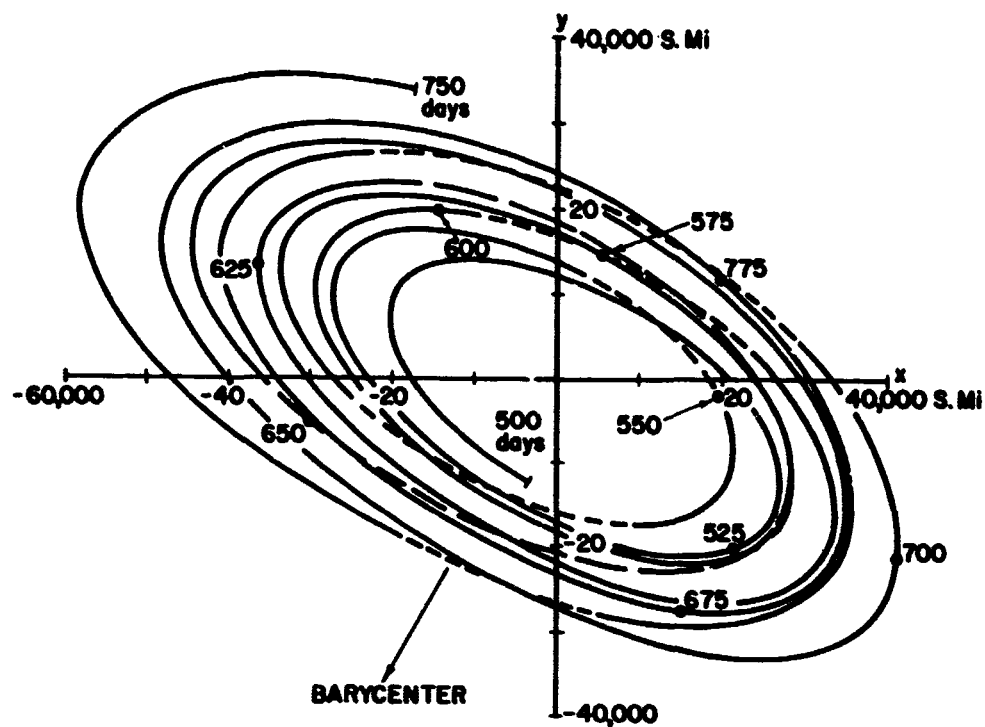


FIGURE 9c. L_4 ROTATING (x, y) -RESULTS FOR $\psi_0 = 180^\circ$ FROM 500 DAYS TO 750 DAYS

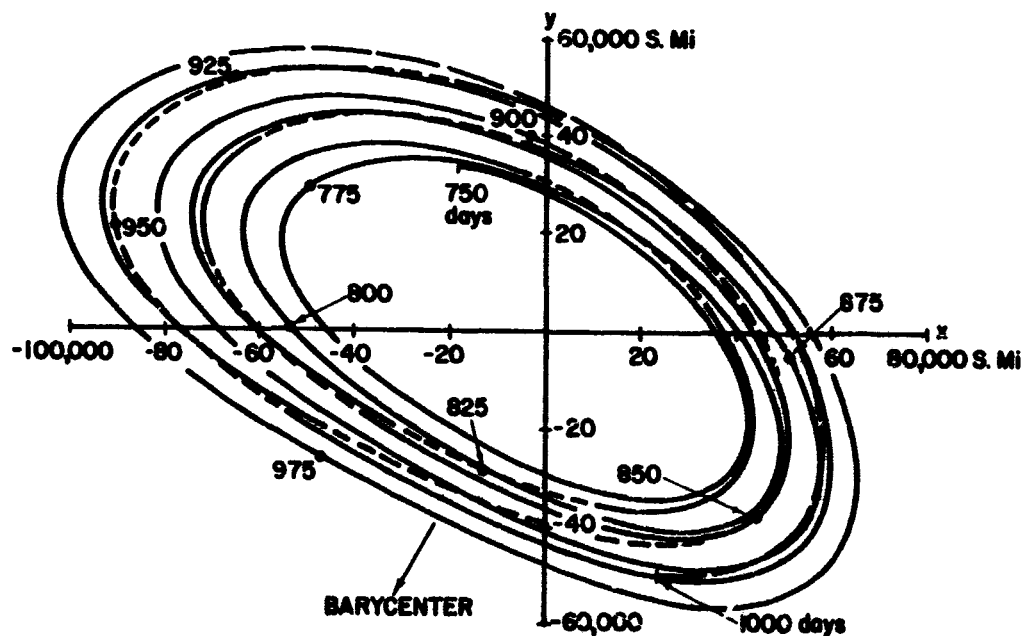


FIGURE 9d. L_4 ROTATING (x, y) -RESULTS FOR $\psi_0 = 180^\circ$ FROM 750 DAYS TO 1000 DAYS

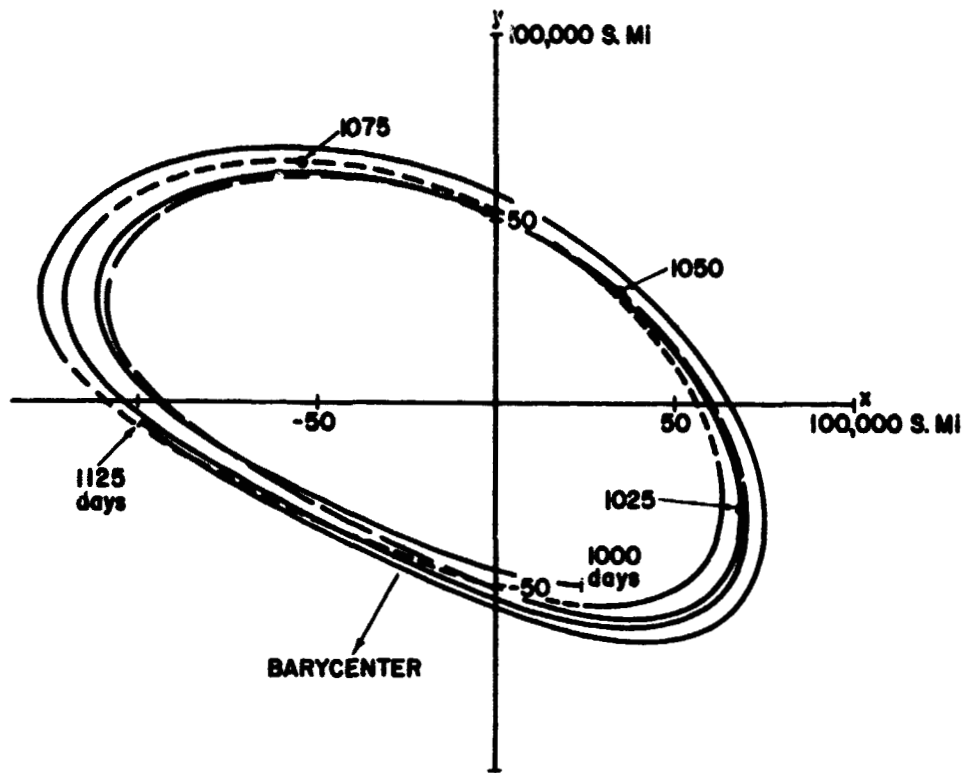


FIGURE 9e. L_4 ROTATING (x, y) -RESULTS FOR $\psi_0 = 180^\circ$ FROM 1000 DAYS TO 1125 DAYS

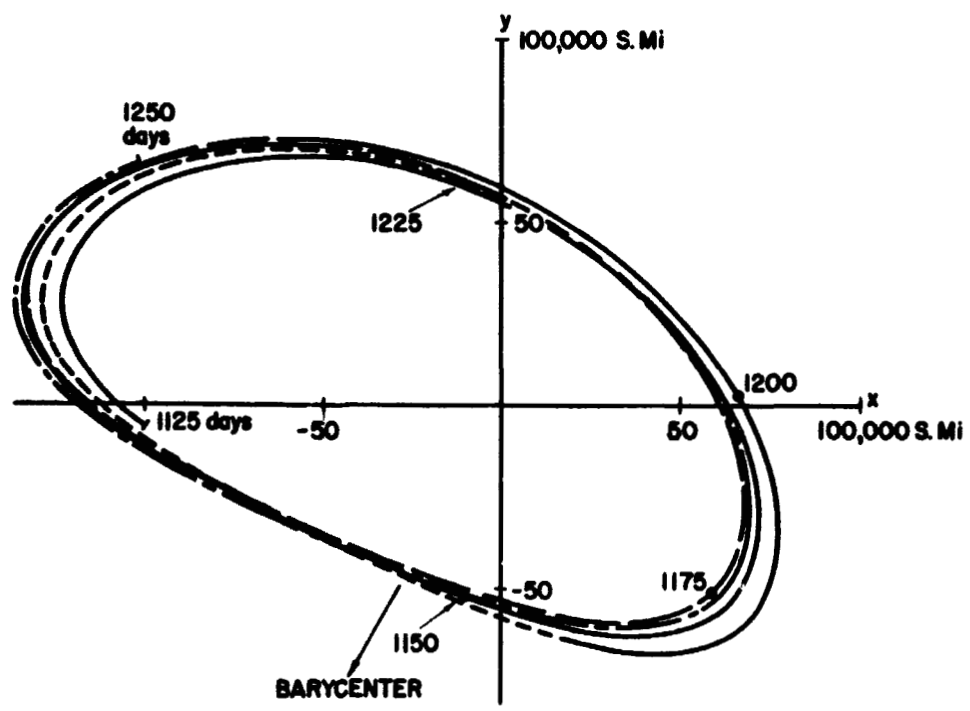


FIGURE 9f. L_4 ROTATING (x, y) -RESULTS FOR $\psi_0 = 180^\circ$ FROM 1125 DAYS TO 1250 DAYS

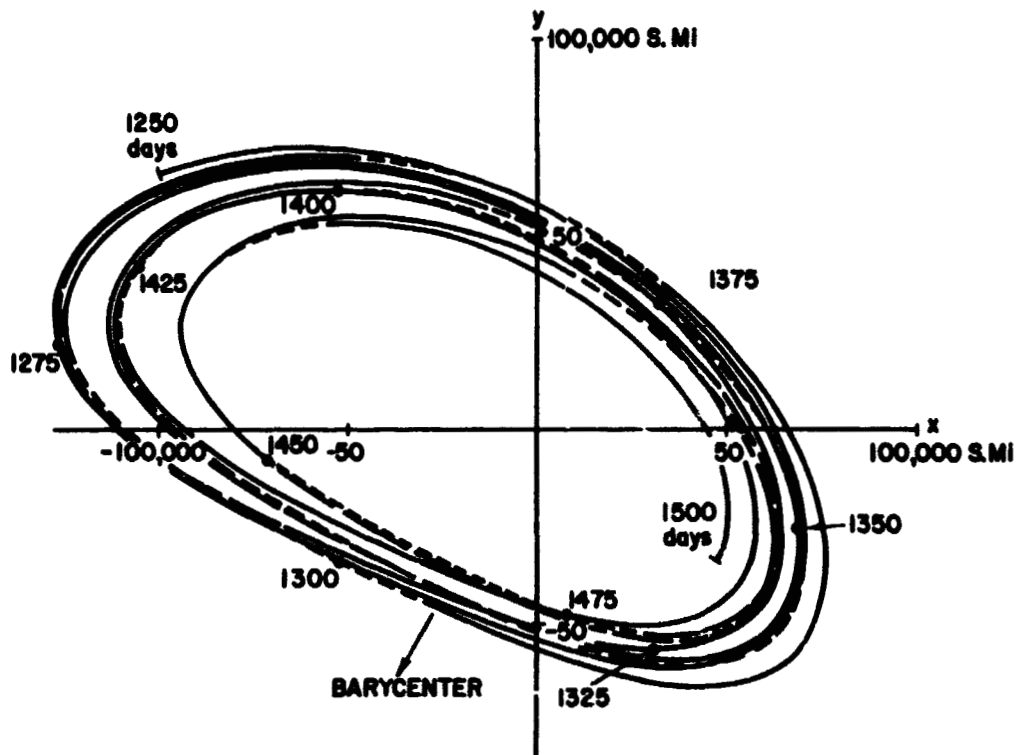


FIGURE 9g. L_4 ROTATING (x,y) -RESULTS FOR $\psi_0 = 180^\circ$ FROM 1250 DAYS TO 1500 DAYS

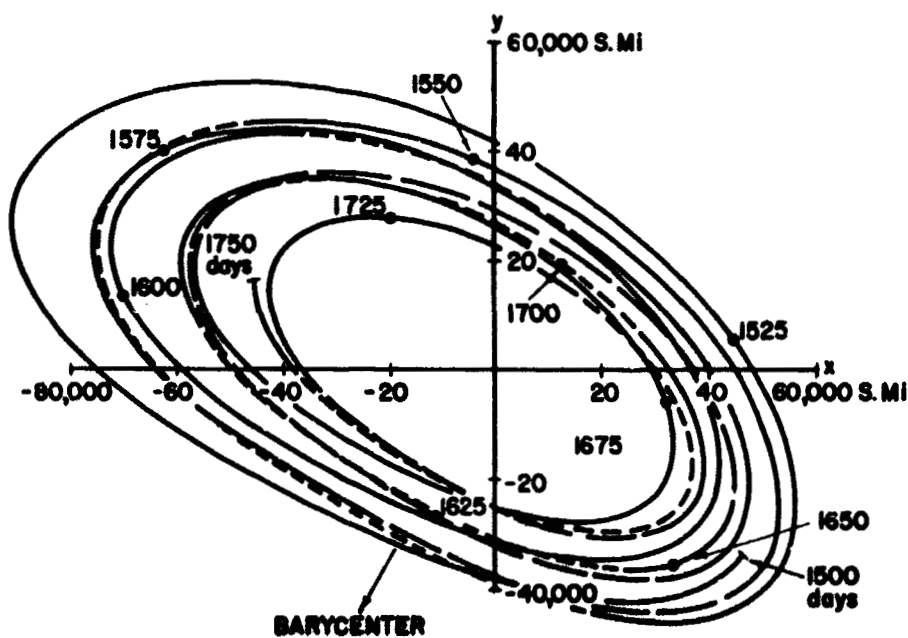


FIGURE 9h. L_4 ROTATING (x,y) -RESULTS FOR $\psi_0 = 180^\circ$ FROM 1500 DAYS TO 1750 DAYS

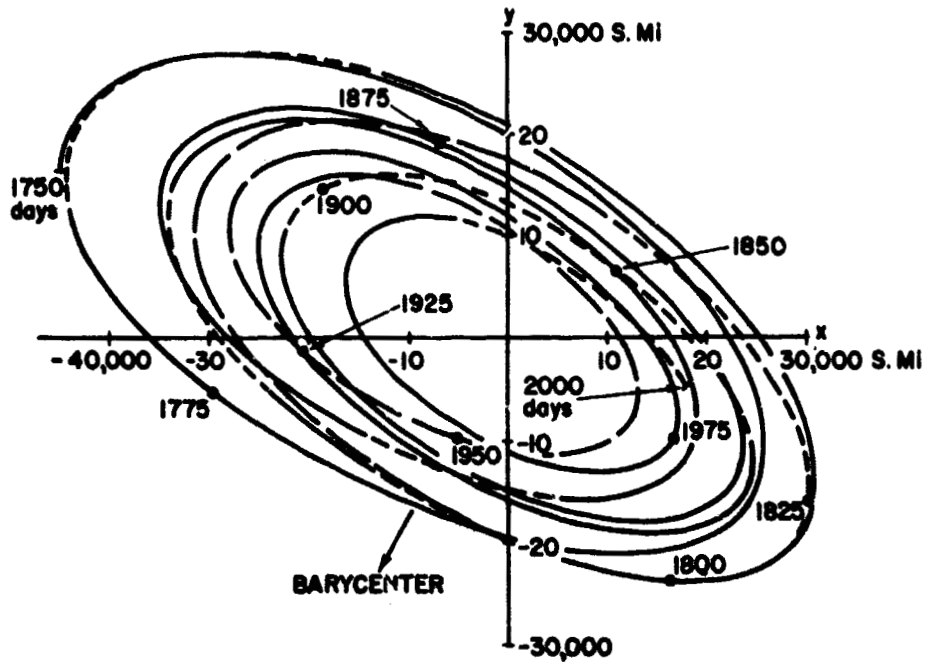


FIGURE 9i. L_4 ROTATING (x, y) -RESULTS FOR $\psi_0 = 180^\circ$ FROM 1750 DAYS TO 2000 DAYS

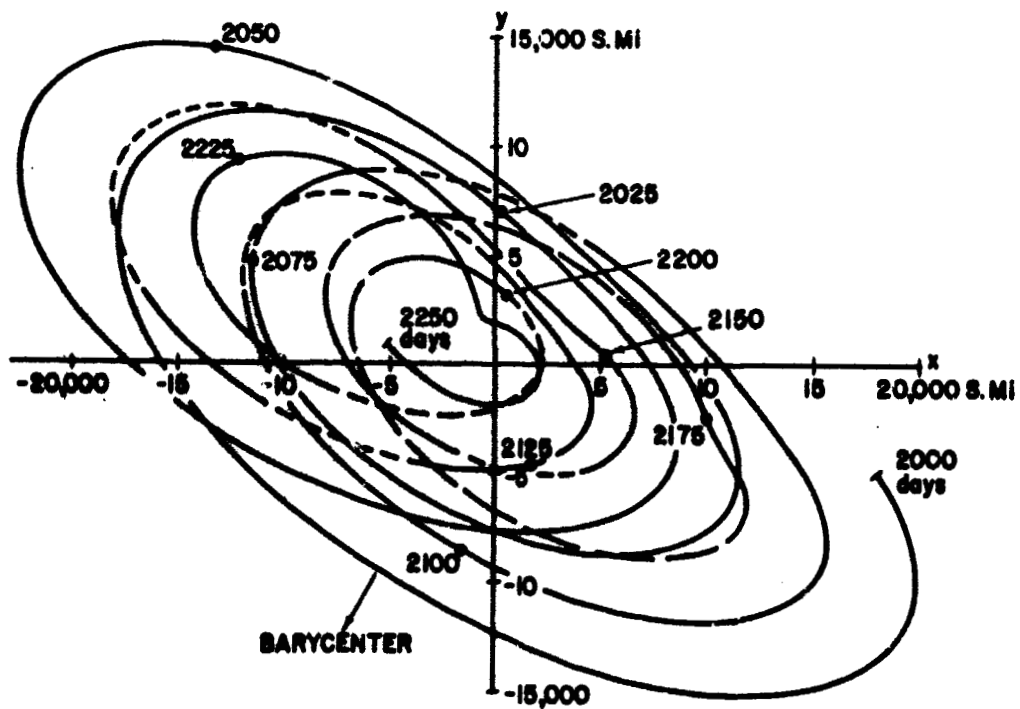


FIGURE 9j. L_4 ROTATING (x, y) -RESULTS FOR $\psi_0 = 180^\circ$ FROM 2000 DAYS TO 2250 DAYS

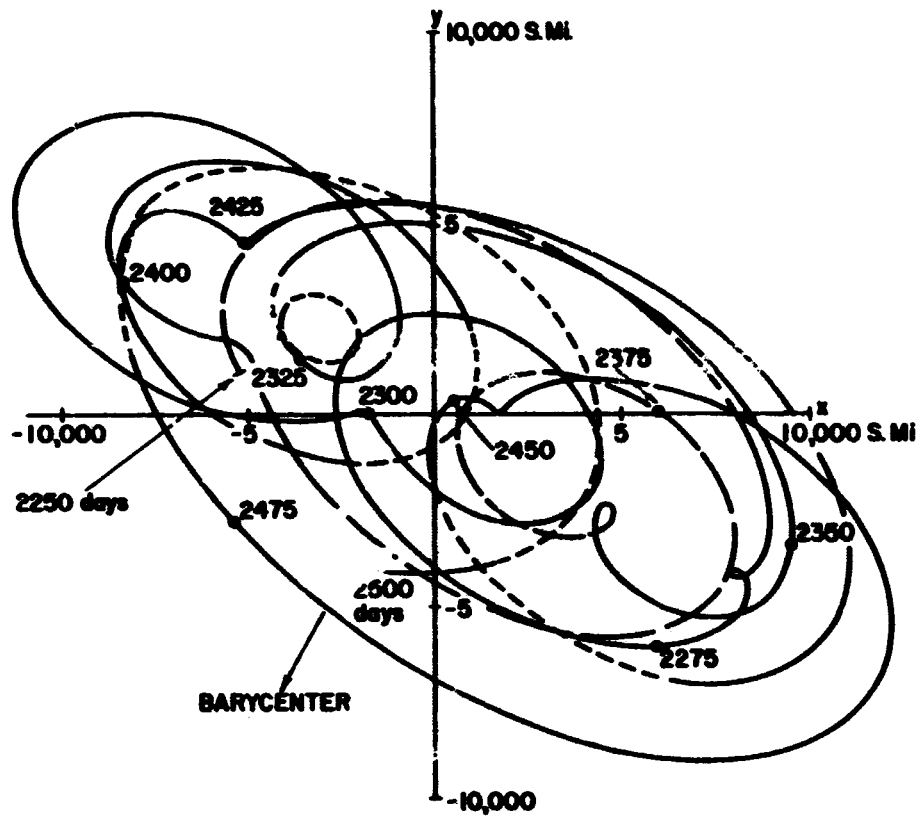


FIGURE 9k. L_4 ROTATING (x, y) -RESULTS FOR $\psi_0 = 180^\circ$
FROM 2250 DAYS TO 2500 DAYS

observed, i. e., an unstable motion. Between 1334 and 1335 days, the spacecraft makes a close pass of the moon and subsequently leaves the earth-moon system to take up a heliocentric orbit separate from the earth-moon system. It must be remembered that in the period from 0 days to 1335 days, the spacecraft is already in a heliocentric orbit since it is moving within the earth-moon system. The heliocentric motion is shown in Fig. 11 for about one year after the lunar encounter. The data for Fig. 11 were obtained by making a coordinate transformation from the rotating (x, y, z) -system to the (X, Y, Z) -heliocentric coordinate system.

For comparison purposes, the magnitude of the displacement from L_4 was determined and plotted versus time. The results of Ref. 5 are shown in Figs. 12 to 13. The results of the investigation reported in this chapter are shown in Figs. 14 to 15. It should be pointed out that there are some slight differences in constants used in the mathematical model of Ref. 5 and those used in this chapter. In Ref. 5, the earth-moon distance is taken to be 238,855 miles, the sun-barycenter distance is 92,913,600 miles, and the earth-moon ratio is 81.53. The corresponding constants used in this chapter are, respectively, 239,083 miles, 92,960,700 miles, and 81.3015. There are also slight differences in the angular velocities in addition to the inclusion of the nodal regression of the model discussed previously. Accounting for the slight differences in the constants used in the two mathematical models, it appears that the nodal regression has an important effect on the motion.

For the case in which $\psi_0 = 180^\circ$, the absolute value of the z -component of the motion does not exceed 3500 miles. The absolute value of the z -component for $\psi_0 = 225^\circ$ does not exceed 3700 miles prior to 1335 days.

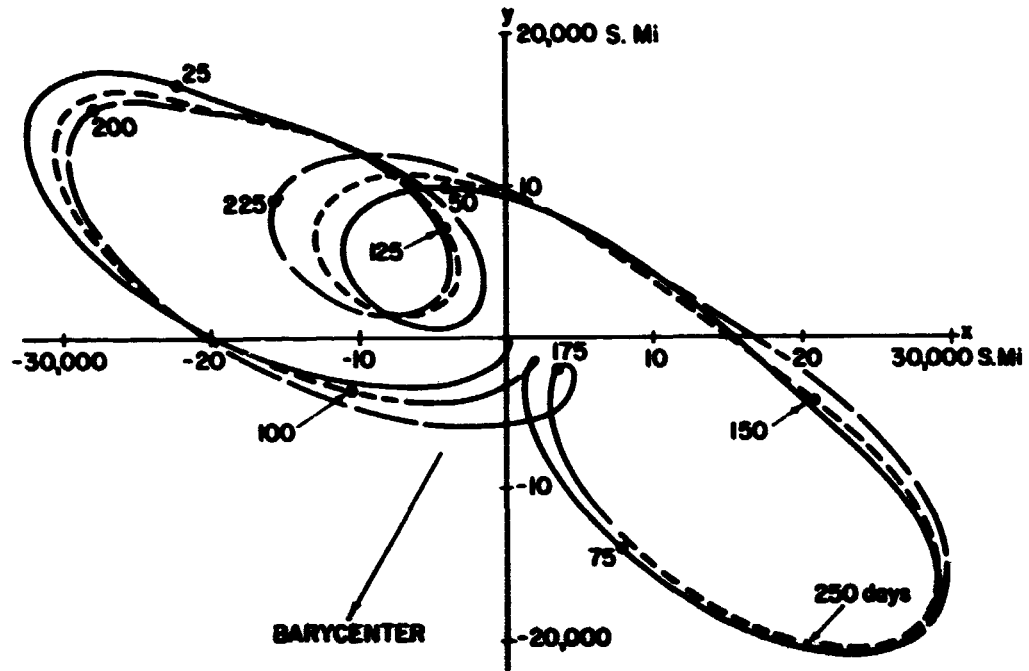


FIGURE 10a. L_4 ROTATING (x, y) -RESULTS FOR $\psi_0 = 225^\circ$ FROM 0 DAYS TO 250 DAYS

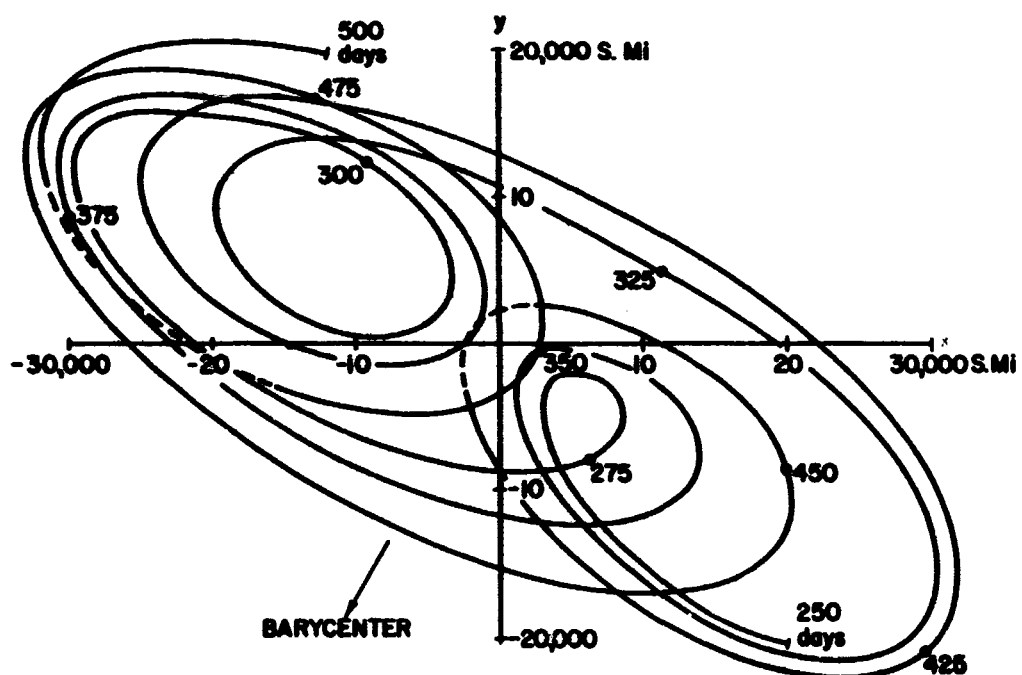


FIGURE 10b. L_4 ROTATING (x, y) -RESULTS FOR $\psi_0 = 225^\circ$ FROM 250 DAYS TO 500 DAYS

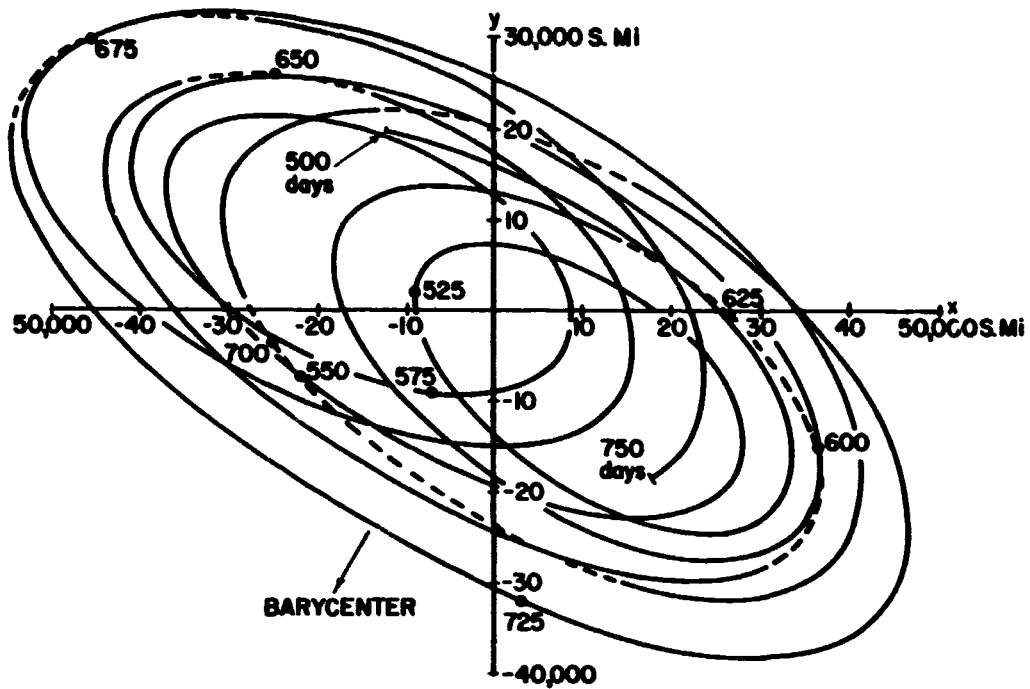


FIGURE 10c. L_4 ROTATING (x, y) -RESULTS FOR $\psi_0 = 225^\circ$ FROM 500 DAYS TO 750 DAYS

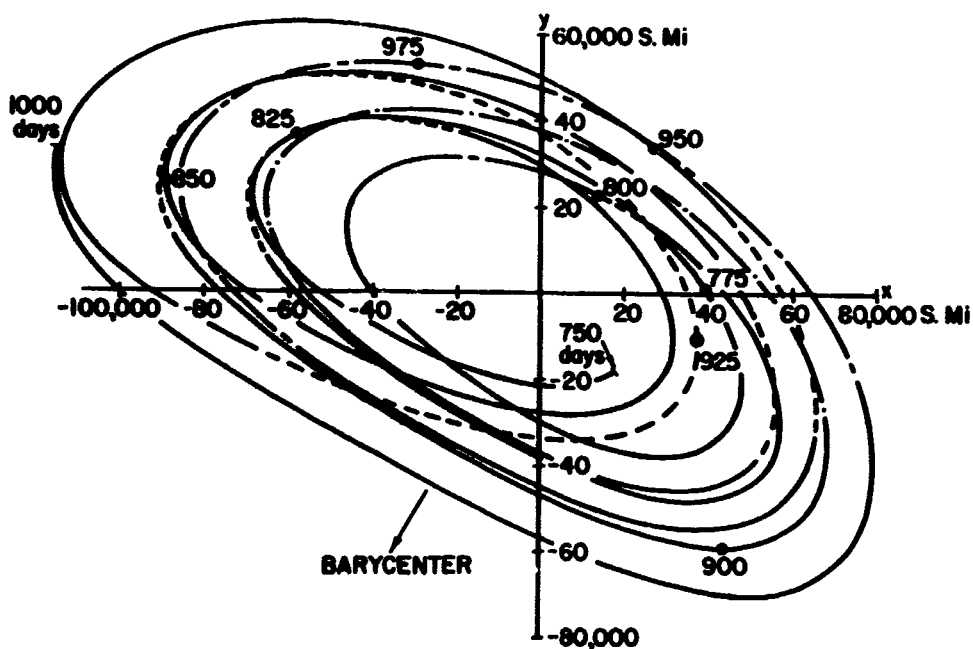


FIGURE 10d. L_4 ROTATING (x, y) -RESULTS FOR $\psi_0 = 225^\circ$ FROM 750 DAYS TO 1000 DAYS

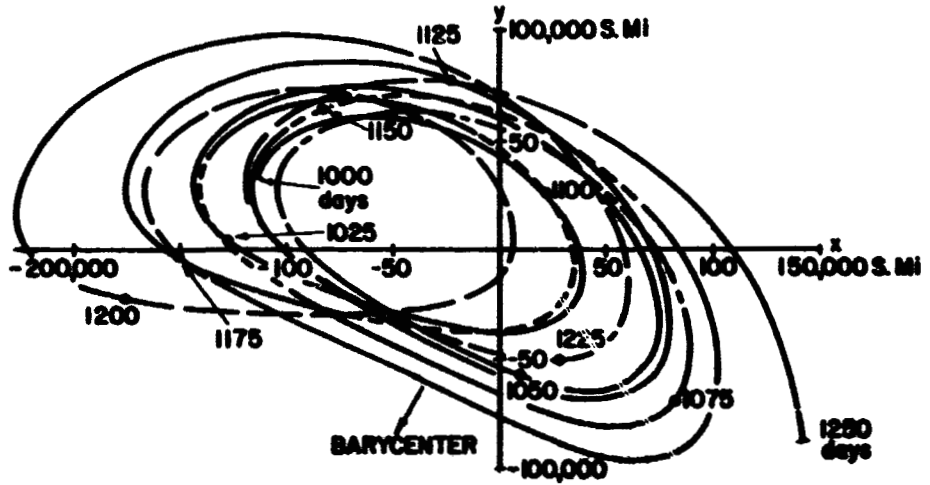


FIGURE 10e. L_4 ROTATING (x,y)-RESULTS FOR $\psi_0 = 225^\circ$ FROM 1000 DAYS TO 1250 DAYS

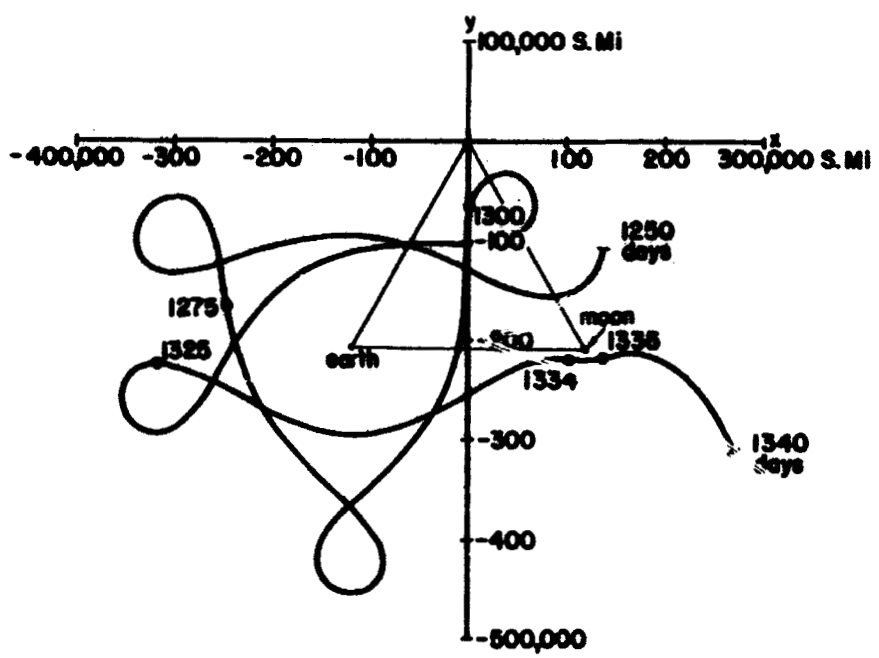


FIGURE 10f. L_4 ROTATING (x,y)-RESULTS FOR $\psi_0 = 225^\circ$ FROM 1250 DAYS TO 1340 DAYS

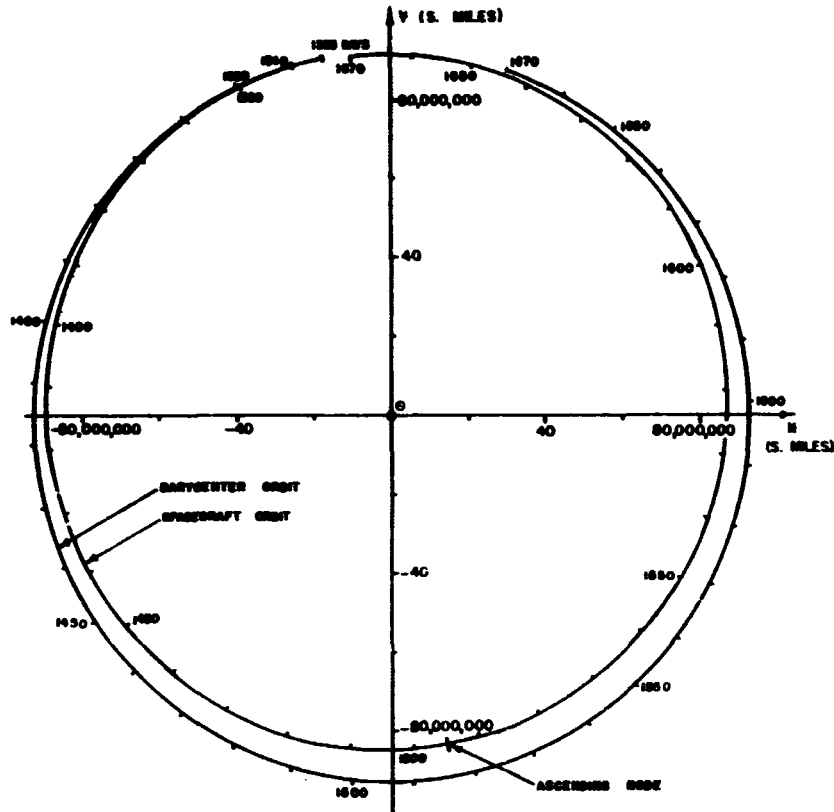


FIGURE 11. SPACECRAFT MOTION SUBSEQUENT TO LUNAR ENCOUNTER AT 1334 TO 1336 DAYS WITH $\psi_0 = 225^\circ$

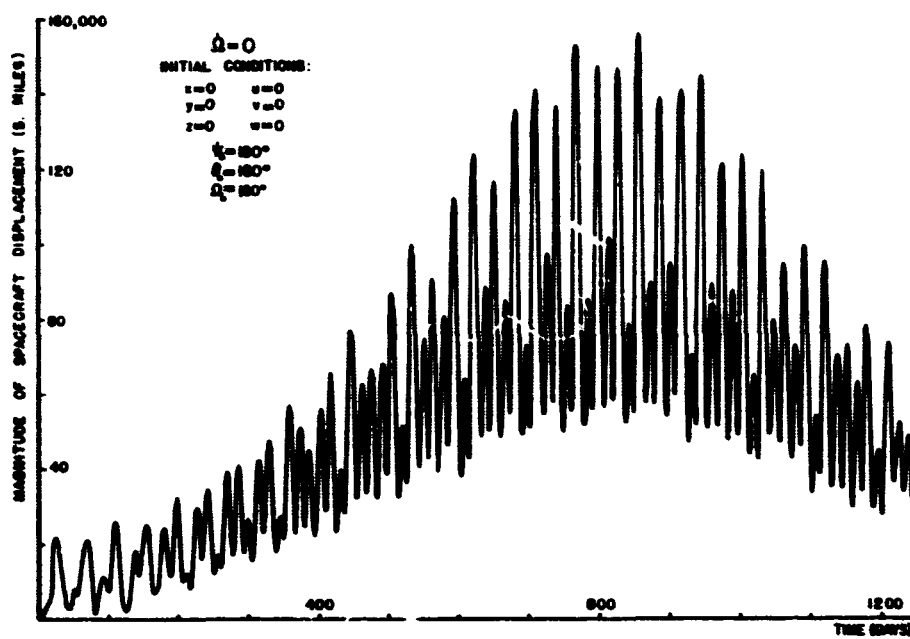


FIGURE 12a. MAGNITUDE OF DISPLACEMENT VECTOR VS. TIME

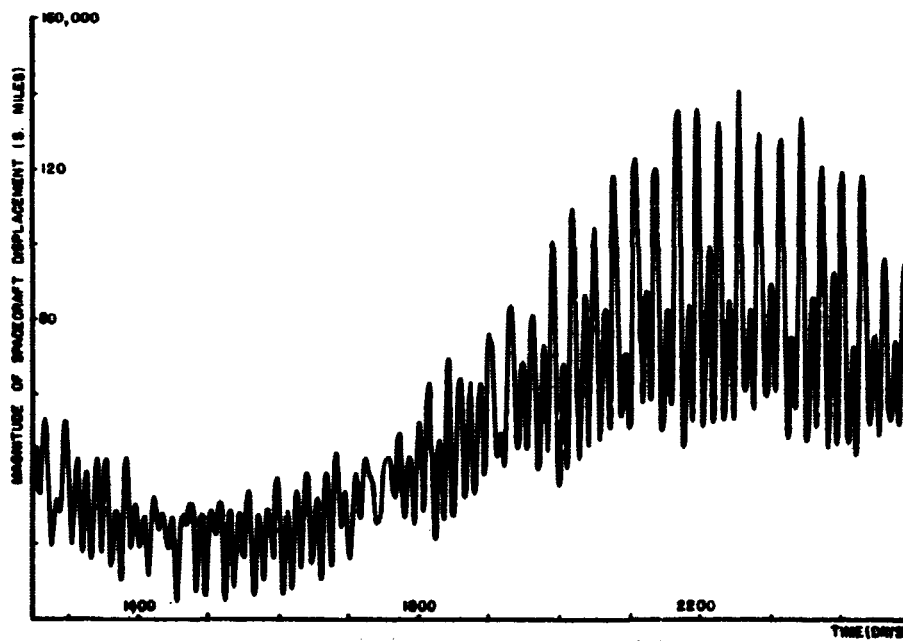


FIGURE 12b. MAGNITUDE OF DISPLACEMENT VECTOR VS. TIME

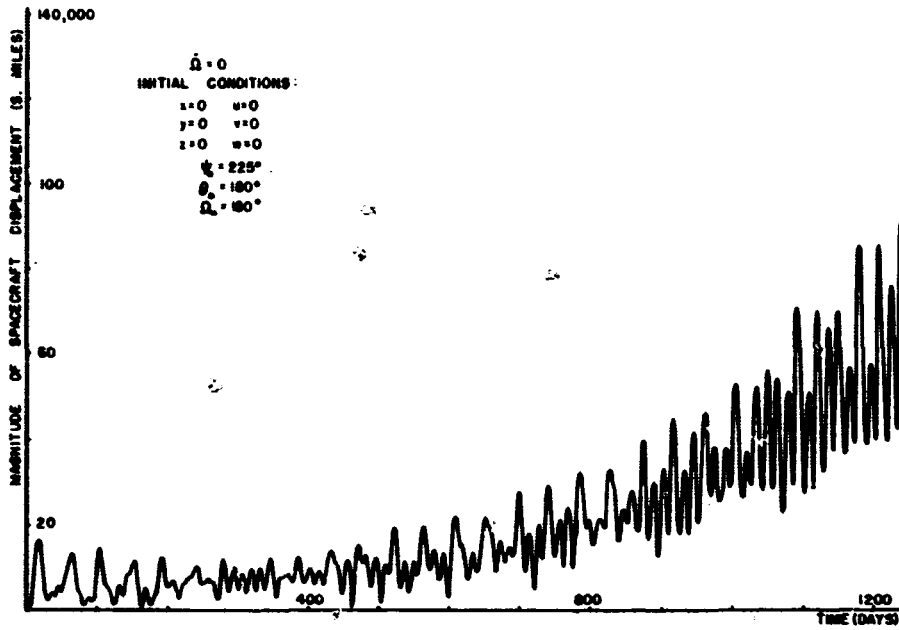


FIGURE 13a. MAGNITUDE OF DISPLACEMENT VECTOR VS. TIME

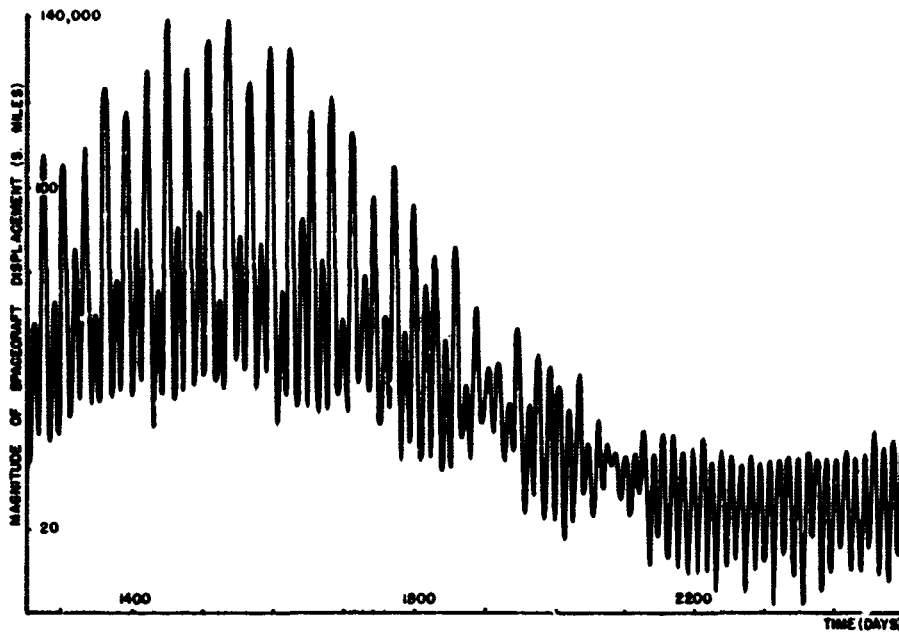


FIGURE 13b. MAGNITUDE OF DISPLACEMENT VECTOR VS. TIME

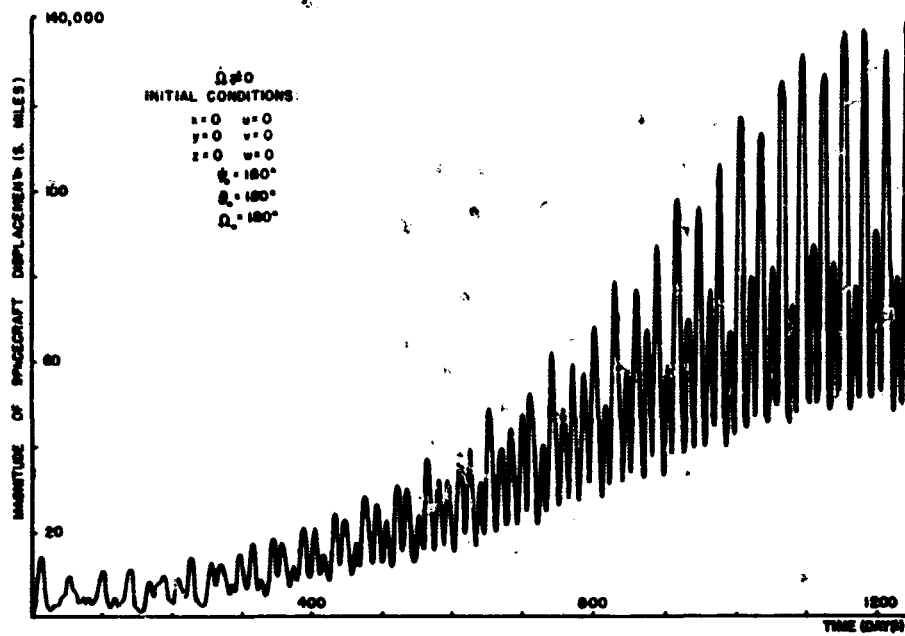


FIGURE 14a. MAGNITUDE OF DISPLACEMENT VECTOR VS. TIME

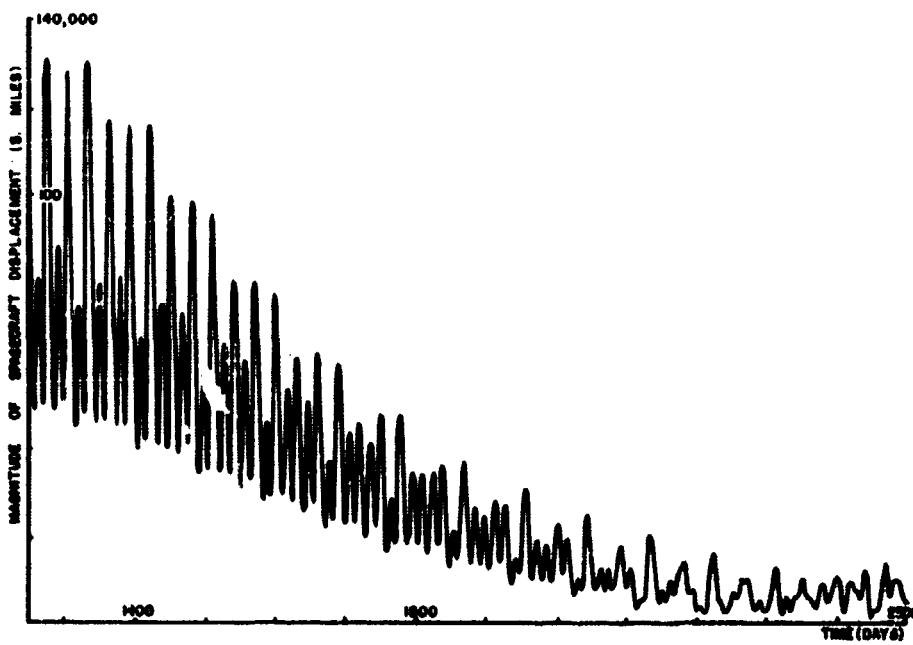
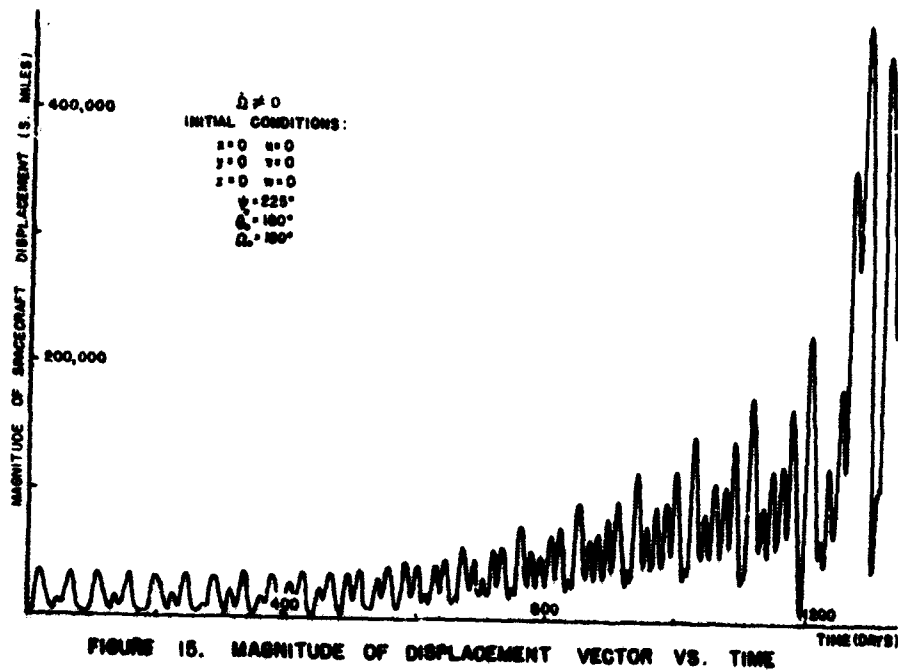


FIGURE 14b. MAGNITUDE OF DISPLACEMENT VECTOR VS. TIME



Case II: Nonrotating Coordinate System

Equations of motion. Because ephemeris information will be used in a subsequent mathematical model, it would be extremely difficult to use a rotating coordinate system for the equations of motion with such data. It would be necessary to determine from the ephemeris data items such as angular velocity and acceleration. This could be achieved, but the results would be subject to the inaccuracies associated with the numerical differencing of the position and velocity information. However, if the equations of motion are expressed with respect to a nonrotating coordinate system, the need for angular velocities is eliminated. The numerical integration was carried out in a nonrotating coordinate system and the results compared with those of Case I.

By combining Eqs. (7), (10), (25), and (26), the components of the equations of motion can be expressed in the nonrotating (X, Y, Z)- coordinate system as follows:

$$\begin{aligned}\ddot{X}_S &= -\frac{Gm_{\odot}(X_S - X_{\odot})}{r_{\odot S}^3} - \frac{Gm_{\oplus}(X_S - X_{\oplus})}{r_{\oplus S}^3} - \frac{Gm_{\text{J}}(X_S - X_{\text{J}})}{r_{\text{J}S}^3} - X_{\odot}\dot{\psi}^2 \\ \ddot{Y}_S &= -\frac{Gm_{\odot}(Y_S - Y_{\odot})}{r_{\odot S}^3} - \frac{Gm_{\oplus}(Y_S - Y_{\oplus})}{r_{\oplus S}^3} - \frac{Gm_{\text{J}}(Y_S - Y_{\text{J}})}{r_{\text{J}S}^3} - Y_{\odot}\dot{\psi}^2 \\ \ddot{Z}_S &= -\frac{Gm_{\odot}(Z_S - Z_{\odot})}{r_{\odot S}^3} - \frac{Gm_{\oplus}(Z_S - Z_{\oplus})}{r_{\oplus S}^3} - \frac{Gm_{\text{J}}(Z_S - Z_{\text{J}})}{r_{\text{J}S}^3}\end{aligned}$$

(44)

where

$$r_{\odot S} = \left[(X_S - X_{\odot})^2 + (Y_S - Y_{\odot})^2 + (Z_S - Z_{\odot})^2 \right]^{1/2}$$

$$r_{\oplus S} = \left[(X_S - X_{\oplus})^2 + (Y_S - Y_{\oplus})^2 + (Z_S - Z_{\oplus})^2 \right]^{1/2}$$

$$r_{\text{J}S} = \left[(X_S - X_{\text{J}})^2 + (Y_S - Y_{\text{J}})^2 + (Z_S - Z_{\text{J}})^2 \right]^{1/2}$$

Integration of the Eqs.(43) yields the position of the spacecraft in the (X, Y, Z)-nonrotating coordinate system.

Initial conditions. The initial conditions in this study will be such that when a coordinate transformation of the initial conditions is made from the (X, Y, Z)-coordinate system to the rotating (x, y, z)-system, the result will be the same as the initial conditions used in Case I. In Case I, the initial position and velocity relative to the (x, y, z)-coordinate system was zero, i. e., the spacecraft was placed at the libration point L_4 with the same velocity as L_4 . Therefore, the initial conditions relative to the nonrotating (X, Y, Z)-system are, from Eq. (12),

$$\begin{bmatrix} X_S \\ Y_S \\ Z_S \end{bmatrix} = A \begin{bmatrix} \xi_p \\ \eta_p \\ 0 \end{bmatrix} \quad (45)$$

where the matrix A is expressed by Eq. (13). Furthermore, since both sets of initial conditions in Case I are similar, i. e., $\Omega_0 = 180^\circ$ and $\theta_0 = 180^\circ$, the matrix A becomes

$$A = \begin{bmatrix} 1 & 0 & 0 \\ 0 & \cos i & \sin i \\ 0 & -\sin i & \cos i \end{bmatrix} \quad (46)$$

for the initial conditions only. Then

$$X_S = \xi_p, \quad Y_S = \eta_p \cos i, \quad Z_S = -\eta_p \sin i$$

The velocity of the spacecraft will be the same in the (ξ, η, ζ) -coordinate system as in the (x, y, z) -system since, as shown in Eq. (24),

$$\dot{x}_S = \dot{\xi}_S, \quad \dot{y}_S = \dot{\eta}_S, \quad \dot{z}_S = \dot{\zeta}_S$$

The components of the total velocity expressed in the rotating (ξ, η, ζ) -coordinate system are as follows:

$$\begin{bmatrix} \dot{X}_S \\ \dot{Y}_S \\ \dot{Z}_S \end{bmatrix} = A \begin{bmatrix} (\omega_\eta \zeta_S - \omega_\zeta \eta_S + \dot{\xi}_S) \\ (\omega_\zeta \xi_S - \omega_\xi \zeta_S + \dot{\eta}_S) \\ (\omega_\xi \eta_S - \omega_\eta \xi_S + \dot{\zeta}_S) \end{bmatrix} \quad (47)$$

Using the matrix A evaluated for the initial conditions, viz., Eq. (46), and the initial values of $\xi_S, \eta_S, \zeta_S, \dot{\xi}_S, \dot{\eta}_S,$ and $\dot{\zeta}_S$, the following expressions can be obtained:

$$\dot{X}_S = -(\dot{\Omega} \cos i + \dot{\Theta}) \eta_p$$

$$\dot{Y}_S = \xi_p (\dot{\Omega} + \dot{\Theta} \cos i)$$

$$\dot{Z}_S = -\xi_p \dot{\Theta} \sin i$$

The initial conditions are computed in double precision to avoid as much round-off error as possible. The initial conditions for $\Omega_0 = 180^\circ$ and $\theta_0 = 130^\circ$ are

$$\begin{aligned}
 X_S &= 116,630.86 \text{ mi} & \dot{X}_S &= - .5489 \text{ mi/sec} \\
 Y_S &= 206,206.07 \text{ mi} & \dot{Y}_S &= .3080 \text{ mi/sec} \\
 Z_S &= 18,584.80 \text{ mi} & \dot{Z}_S &= - .0278 \text{ mi/sec}
 \end{aligned}$$

Case II results and comparison with Case I. The integration of Eqs. (44) was carried out using the same single-step error range as in Case I. Although the integration was made in the barycentered (X, Y, Z)-coordinate system, the data were transformed to the (x, y, z)-libration-point-centered coordinate system to facilitate comparison with Case I. Tables 1 and 2 show the results of this comparison for the two different initial orientations used. For the case in which $\psi_0 = 180^\circ$ (Table 1), the solutions of the two different sets of differential equations are in good agreement throughout the 2500-day study. In fact, at 2500 days, where one might expect the largest disagreement, there is a difference of 1.76 miles in over 4000 miles. For $\psi_0 = 225^\circ$, there is good agreement until approximately 1200 days with a difference of 24 miles in 175,000 miles. As the spacecraft leaves the libration-point-centered motion, the discrepancy between the two coordinate systems becomes more noticeable, and is 6411 miles in 270,000 miles 5 days after the lunar encounter.

Since $\psi_0 = 180^\circ$ exhibits very good agreement over a long time span (2500 days), it appears that the discrepancy in the $\psi_0 = 225^\circ$ is not a result of a numerical instability. There are a number of possible causes for the discrepancy in the $\psi_0 = 225^\circ$ case. First of all, the discrepancy could be a result of inaccurate specification of initial conditions. The initial conditions in the rotating case were zero relative displacement and zero relative velocity; however, in the nonrotating case the initial conditions are computed. Since the trajectory which a spacecraft will follow is determined by the initial

Time (Days)		Rotating	Nonrotating	Absolute Difference	Time (Days)		Rotating	Nonrotating	Absolute Difference
100	x	-9270.09	-9270.09	0	1800	x	16,045.1	16,044.8	0.3
	y	4537.35	4537.35	0		y	-23,713.1	-23,712.8	0.3
	z	-1049.77	-1049.77	0		z	-1572.04	-1572.01	0.03
400	x	11,301.2	11,301.2	0	2000	x	17,872.6	17,872.7	0.1
	y	3598.06	3598.04	0.02		y	-4569.96	-4570.25	0.29
	z	-560.903	-560.904	0.001		z	3040.08	3040.04	0.04
800	x	-53,455.2	-53,454.8	0.4	2200	x	676.415	677.662	1.247
	y	515.571	515.621	0.05		y	3240.97	3240.06	0.91
	z	497.841	497.842	0.001		z	-215.638	-215.615	0.023
1200	x	65,871.2	65,870.7	0.5	2400	x	-8115.63	8114.59	1.04
	y	3027.65	3027.65	0		y	5954.66	5955.21	0.55
	z	-1627.22	-1627.20	0.02		z	-2662.14	-2662.13	0.01
1600	x	-70,031.3	-70,031.4	0.1	2500	x	-1777.06	-1776.78	0.28
	y	13,840.6	13,840.6	0		y	-4053.45	-4055.21	1.76
	z	-1182.80	-1182.78	0.02		z	-506.352	-506.337	0.015

Table 1. Comparison of Rotating and Nonrotating Data (Miles) for $\psi_0 = 180^\circ$

Time (Days)		Rotating	Nonrotating	Absolute Difference	Time (Days)		Rotating	Nonrotating	Absolute Difference
5	x	-157.663	-157.663	0	1000	x	-115,480	-115,478	2.0
	y	-1282.68	-1282.68	0		y	32,719.6	32,718.9	0.7
	z	22.8080	22.8080	0		z	37.4331	37.4509	0.0178
200	x	-27,972.1	-27,972.0	0.1	1200	x	-175,293	-175,317	24.0
	y	15,246.1	15,246.1	0		y	-22,339.4	-22,343.9	4.5
	z	149.047	149.047	0		z	-463.374	-463.242	0.132
400	x	-19,156.5	-19,156.5	0	1250	x	-140,456	-140,473	17.0
	y	2288.63	2288.72	0.09		y	-86,974.9	-86,994.4	19.5
	z	-747.020	-747.020	0		z	-2429.65	-2429.57	0.08
600	x	36,678.3	36,677.9	0.5	1300	x	1792.50	1321.95	470.55
	y	-14,940.4	-14,940.2	0.2		y	-65,908.4	-65,033.8	874.6
	z	-959.706	-959.703	0.003		z	-1183.59	-1198.59	15.0
800	x	13,560.1	13,560.5	0.4	1340	x	270,148	263,737	6411.0
	y	23,063.8	23,063.1	0.7		y	-313,821	-319,693	5872.0
	z	1051.92	1051.91	0.01		z	11,315.5	10,193.6	1121.9

Table 2. Comparison of Rotating and Nonrotating Data (Miles) for $\psi_0 = 225^\circ$

conditions, slightly inaccurate initial conditions will result in a trajectory differing from the accurate initial conditions. This problem was anticipated, however, and the initial conditions were computed in double precision.

On observing that the large discrepancy occurs when the spacecraft leaves a libration-point-centered motion, another possibility accounting for the discrepancy involves round-off error during this period. In any numerical integration method there will be some truncation error and round-off error. For the comparison under discussion, two sets of differential equations were integrated using the same numerical integration technique. These equations differ only in that they express the acceleration in rotating and nonrotating coordinate systems. Furthermore, since the form of the equations is different (even though the numerical integration should yield the same point in space), the round-off error encountered by numerically integrating these equations will not, in general, be the same for both sets of equations. One might note that the differential equations of motion referred to the rotating coordinate system are somewhat more complex than those for the nonrotating coordinate system [compare Eqs. (32) and (44)]. During periods after which the spacecraft has left the libration-point-centered motion, one might be determining small changes in a large distance, particularly when the spacecraft trajectory forms a cusp in the rotating system. Such is not the case in the nonrotating system. In the nonrotating system, there are no cusps and, furthermore, the trajectory is near elliptical. Thus, it is possible that round-off error of sufficient magnitude is being accumulated prior to and after departing from the libration-point-centered motion that the results in the rotating system are somewhat inaccurate.

From the considerations of the two previous paragraphs, it appears that the results in the rotating system are somewhat less accurate than those in the nonrotating system during the period in which the spacecraft is no longer on a libration-point-centered motion. Thus, the nonrotating system probably offers the more accurate results. Again, during the period of a libration-point-centered motion, the results of the two coordinate systems are much the same.

A check of the numerical integration procedure was made also by numerically integrating the differential equations of motion expressed in a nonrotating coordinate system for a particle in the two-body case. The primary body was taken to be a body with the mass of the earth. Since approximately 36,000 steps were necessary to get to the 2500-day mark in the mathematical model under discussion, the integration of the two-body case was carried out a comparable number of steps. By comparing the results with those obtained from the closed form solution of the two-body problem, it was found that the numerical integration results differed with the exact solution less than .1 mile in 4000 miles after 36,000 steps. From this comparison, it appears that the numerical integration procedure does give quite accurate results over long time periods.

Case III: Earth-Moon Orbital Plane Defined by Angular Momentum

Equations of motion and initial conditions. The equations of motion derived in Case II, Eqs. (44), will be used in this section, however, the initial conditions of position and velocity will differ from those used in Case II.

It will be assumed that the libration points are in the earth-moon orbital plane, i. e., the plane normal to the angular momentum vector and

passing through the earth-moon mass center. The total angular momentum of the earth-moon system with respect to the barycentered coordinate system is the sum of the earth's angular momentum and the angular momentum of the moon. However, it is shown in Appendix B that the total angular momentum of the system can be computed from the angular momentum of the moon, viz., Eqs. (B-13). Furthermore, as also shown in Appendix B, the inclination and longitude of the ascending node can be computed from the angular momentum per unit mass of the moon, viz., Eqs. (B-15) and (B-16). The position of the moon in the orbital plane, viz., the angle θ^* (see Fig. B-1), is given by Eqs. (B-5). The position and velocity of the moon can be determined from

$$\begin{bmatrix} X_D \\ Y_D \\ Z_D \end{bmatrix} = A \begin{bmatrix} r_{BD} \\ 0 \\ 0 \end{bmatrix}, \quad \begin{bmatrix} \dot{X}_D \\ \dot{Y}_D \\ \dot{Z}_D \end{bmatrix} = A \begin{bmatrix} 0 \\ \omega_\zeta r_{BD} \\ \omega_\eta r_{BD} \end{bmatrix}.$$

In order to compare the results, the same initial angles will be used in this case as in the two previous cases, viz., $\Omega_0 = 180^\circ$ and $\theta_0 = 180^\circ$.

The initial position and velocity of the moon are

$$\begin{aligned} X_D &= r_{BD} & \dot{X}_D &= 0 \\ Y_D &= 0 & \dot{Y}_D &= r_{BD}(\dot{\Omega} + \dot{\theta} \cos i) \\ Z_D &= 0 & \dot{Z}_D &= r_{BD} \dot{\theta} \sin i \end{aligned} \quad (48)$$

The initial orientation and velocity are illustrated in Fig. 16. It is important to note that the velocity of the moon is composed of the velocity due to circular orbit motion and that due to the regressional motion. The angular momentum per unit mass of the moon is, for the specified initial conditions,

$$\begin{aligned}
h_{X_D} &= 0 \\
h_{Y_D} &= -r_{B_D}^2 \dot{\theta} \sin i \\
h_{Z_D} &= r_{B_D}^2 (\dot{\Omega} + \dot{\theta} \cos i) \\
h_D &= r_{B_D}^2 (\dot{\theta}^2 + 2\dot{\Omega} \dot{\theta} \cos i + \dot{\Omega}^2)^{1/2}
\end{aligned} \tag{49}$$

Then the inclination of the earth-moon orbital plane, i^* , is (from Eq. (B-15))

$$\cos i^* = \frac{\dot{\Omega} + \dot{\theta} \cos i}{(\dot{\theta}^2 + 2\dot{\Omega} \dot{\theta} \cos i + \dot{\Omega}^2)^{1/2}} \tag{50}$$

It is important to note that i^* is not equal to i . The situation is illustrated in Fig. 17. If, however, $\dot{\Omega}$ equals zero, the case of Ref. 4, then i^* is equal to i , i. e., the earth-moon plane in Ref. 4 is the plane defined by the angular momentum.

Since the inclinations of the orbital plane and the earth-moon plane are not equal, the question arises as to which plane should contain the libration point. Since the libration point was assumed to be in the earth-moon plane in Case I and Case II, it seems logical to determine the resultant motion assuming that the libration point is in the orbital plane. Only one set of initial conditions will be used in this case, namely

$$\Omega_0 = 180^\circ, \quad \psi_0 = 225^\circ, \quad \theta_0 = 180^\circ$$

Also, it will be assumed that the spacecraft will be initially placed at the libration point L_4 where L_4 is assumed to lie in the earth-moon orbital plane. The primary reason for using this set of initial conditions is because of the instability observed in the previous cases for this set. Evaluation of Eq. (50) yields $i^* = 5.17075^\circ$. Recall that i was selected as 5.15° .

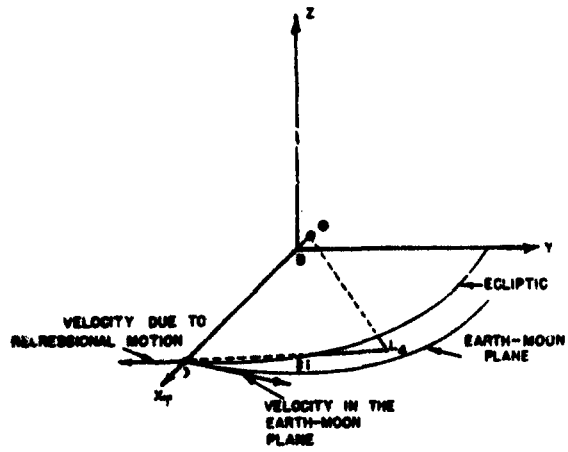


FIGURE 16. INITIAL ORIENTATION OF THE EARTH-MOON SYSTEM WITH L_4 ASSUMED TO EXIST IN THE EARTH-MOON PLANE

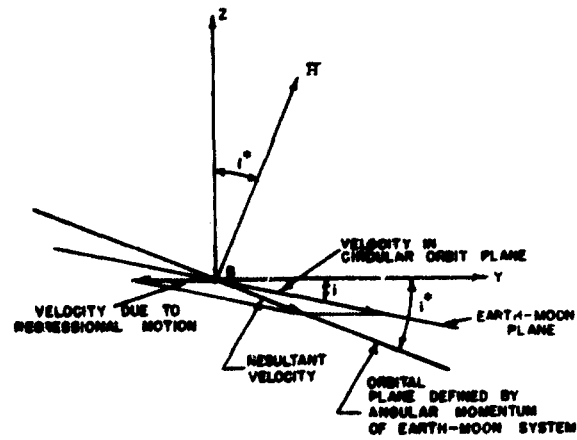


FIGURE 17. ORIENTATION OF THE EARTH-MOON ORBIT PLANE DEFINED BY THE ANGULAR MOMENTUM

Using the results for the angular momentum expressed by Eqs. (49), it follows that $\cos \Omega_o^* = -1$ and $\tan \Omega_o^* = 0$. Therefore, $\Omega_o^* = \Omega_o = 180^\circ$ where Ω_o^* is the ascending node location of the earth-moon orbital plane. In a similar manner, $\theta_o^* = \theta_o = 180^\circ$. The initial position of the spacecraft is given by Eq. (C-3), in which ξ_p and η_p have the same numerical value as in Cases I and II and the matrix A is evaluated at θ_o^* , Ω_o^* , and i^* . For the initial position of the spacecraft, i. e., $x_S = 0$, $y_S = 0$, $z_S = 0$, it follows that $X_S = \xi_p$, $Y_S = \eta_p \cos i^*$, and $Z_S = \eta_p \sin i^*$. The angular velocity of the earth-moon line in the orbital plane is given by Eq. (C-6) and can be used to determine the following condition:

$$r_{B\mathcal{D}} \dot{\theta}^* = \dot{Y}_p \cos i^* - \dot{Z}_p \sin i^* \quad (51)$$

The libration point L_4 is an angle ϕ ahead of the earth-moon line, i. e.,

$$\tan \phi = \frac{\eta_p}{\xi_p} \quad (52)$$

Also, the barycenter - L_4 distance is a constant and is determined from

$$r_{BL} = \left[\xi_p^2 + \eta_p^2 \right]^{1/2}. \quad (53)$$

The initial velocity of the spacecraft is expressed by Eq. (C-10), in which r_{BL} , i. e., the barycenter - L_4 distance, is a constant and $\dot{r}_{B\mathcal{D}} = 0$. Furthermore, the initial velocity components $\dot{x}_S = 0$, $\dot{y}_S = 0$ and $\dot{z}_S = 0$ will lead to the following conditions:

$$\begin{aligned}\dot{X}_S &= -\sin \phi (r_{BL} \dot{\theta}^*) \\ \dot{Y}_S &= \cos \phi \cos i^* (r_{BL} \dot{\theta}^*) \\ \dot{Z}_S &= -\cos \phi \sin i^* (r_{BL} \dot{\theta}^*)\end{aligned}$$

Equations (51), (52), and (53) yield

$$\begin{aligned}\dot{\theta}^* &= 2.651045902 \times 10^{-6} \text{ rad/sec} \\ r_{BL} &= 382,432.8 \text{ km} \\ &= 237,632.3 \text{ mi} \\ \phi &= 60.60656^\circ\end{aligned}$$

The initial position and velocity of the spacecraft computed from Eqs. (C-3) and (C-10) are

$$\begin{aligned}X_S &= 187,699.5 \text{ km} & \dot{X}_S &= -.88333448 \text{ km/sec} \\ &= 116,239.6 \text{ mi} & &= -.5488775 \text{ mi/sec} \\ \\ Y_S &= 331,846.3 \text{ km} & \dot{Y}_S &= .49558 \text{ km/sec} \\ &= 206,199.3 \text{ mi} & &= .30794 \text{ mi/sec} \\ \\ Z_S &= -30,029.6 \text{ km} & \dot{Z}_S &= -.04485 \text{ km/sec} \\ &= -18,659.5 \text{ mi} & &= -.02787 \text{ mi/sec.}\end{aligned}$$

Assuming that L_4 lies in the circular orbit plane, that is, Case II, the initial conditions were

$$\begin{aligned} X_S &= 187,699.5 \text{ km} & \dot{X}_S &= - .88333442 \text{ km/sec} \\ &= 116,239.6 \text{ mi} & &= - .54887750 \text{ mi/sec} \end{aligned}$$

$$\begin{aligned} Y_S &= 331,857.2 \text{ km} & \dot{Y}_S &= .49558 \text{ km/sec} \\ &= 206,206.1 \text{ mi} & &= .30794 \text{ mi/sec} \end{aligned}$$

$$\begin{aligned} Z_S &= - 29,909.4 \text{ km} & \dot{Z}_S &= - .04485 \text{ km/sec} \\ &= - 18,584.8 \text{ mi} & &= - .02787 \text{ mi/sec.} \end{aligned}$$

The initial velocity is much the same in the two cases with only a difference in the eighth decimal place in \dot{X} . There is a difference of approximately 6 miles (10 km) in the initial Y displacement, but there is a difference of approximately 75 miles (120 km) in Z.

Case III results and comparison with Case I. The integration was performed in the barycentered coordinate system, however, a coordinate transformation to the (x, y, z)-system located in the earth-moon plane was made at the printout for comparison with Case I. The results differed only slightly from Case I prior to 1200 days, in fact, it was impossible to discern a difference in the plots for both cases. After 1200 days, the two trajectories begin to noticeably diverge and the motion for the period from 1250 days to 1500 days is shown in Fig. 18. Note that although the spacecraft does come almost as close to the moon as in Case I, it does not leave the earth-moon system, but continues on a trajectory which keeps it in the earth-moon system. It is important to note that even with this set of initial conditions in the orbital plane defined by the angular momentum, the motion is unstable. There has not been a significant change in the motion throughout the stable period.

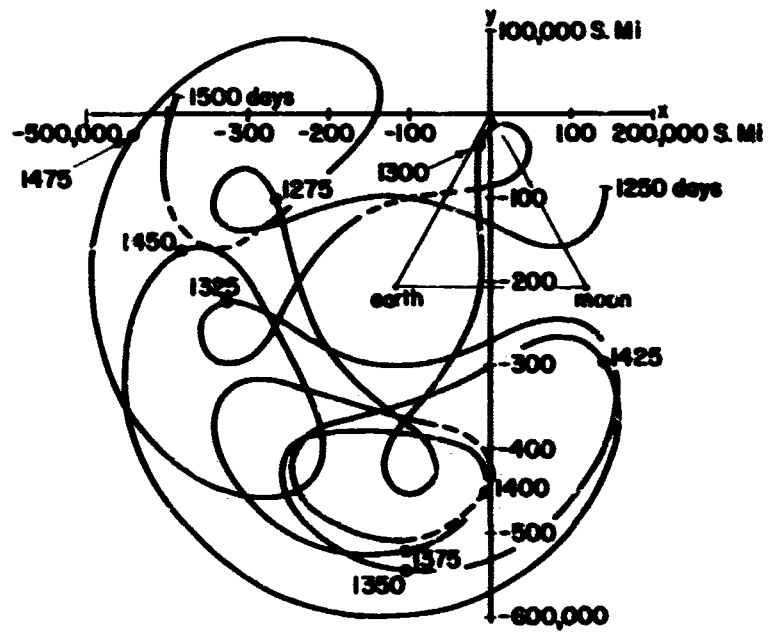


FIGURE 18. L_4 ROTATING (x, y) -RESULTS FOR $\psi_0 = 225^\circ$ FROM 1250 DAYS TO 1500 DAYS USING THE EARTH-MOON ORBITAL PLANE

Case IV: Orientation Corresponding to JD 2,439,501.0

Using the computer program for the integration of the differential equations expressed in the rotating (x, y, z)-coordinate system, viz., Eqs. (32), an initial orientation of the earth-moon-sun system was supplied which corresponded to the orientation of the system on Julian Date 2,439,501.0 (January 10, 1967; 12^h GMT). This corresponds to the initial values for the angles Ω , θ , and ψ of $\Omega_0 = 43^\circ$, $\theta_0 = 242^\circ$ and $\psi_0 = 109^\circ$. The results are displayed in a total displacement from L_4 versus elapsed time plot in Fig. 19. The spacecraft is in a libration-point-centered motion throughout the 1770 day period considered in this four-body model. These results are compared to the "real world" model in a later section.

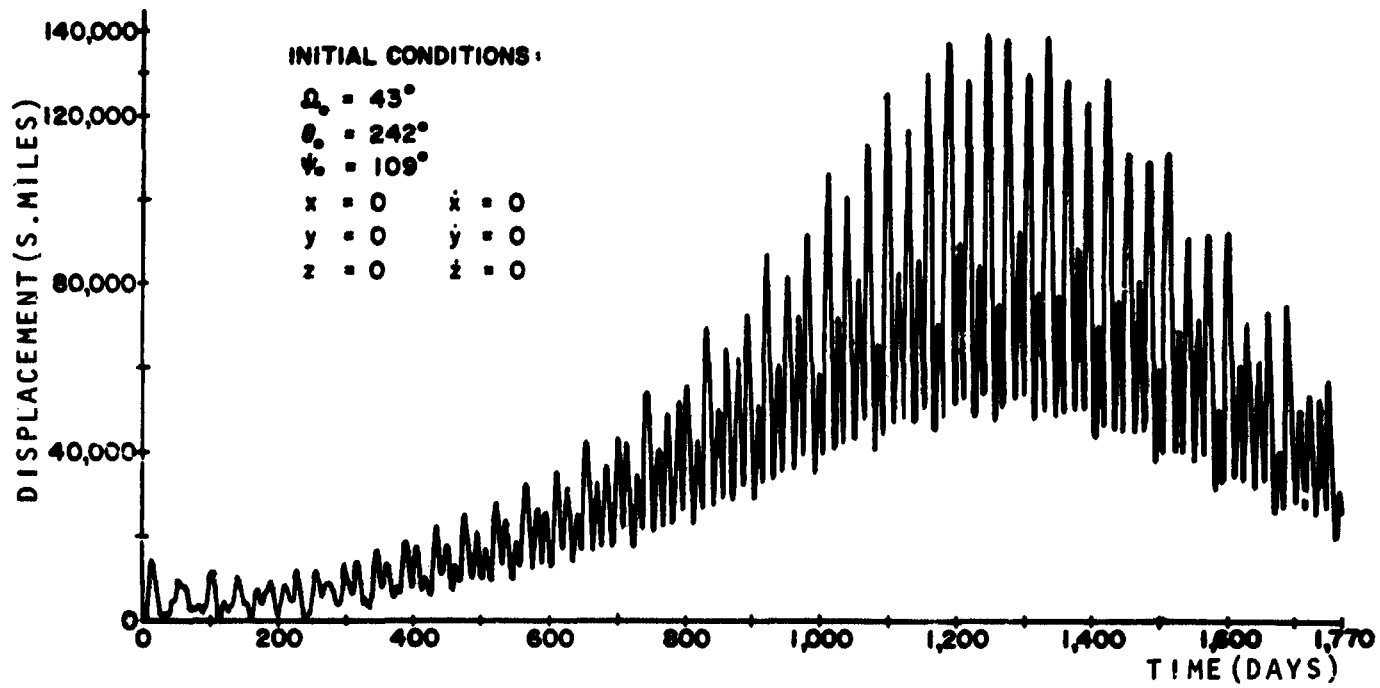


FIGURE 19. MAGNITUDE OF SPACECRAFT DISPLACEMENT VECTOR VS. TIME FOR ORIENTATION CORRESPONDING TO JD 2439501.0

CHAPTER IV

MATHEMATICAL MODEL UTILIZING EPHEMERIS INFORMATION

Mathematical Model

In the previous analysis, assumptions concerning the orbits of the sun, moon, and earth were made, viz., the orbits were assumed to be circular. As stated previously, these orbits are not in reality circular, nor are they exactly elliptical. In fact, they are not really closed orbits, i. e., they do not return to the same point in space after each revolution around the sun or the barycenter. Rather than make an assumption regarding two-body elliptical motion in this mathematical model, ephemeris information will be used to obtain, to a very good degree of accuracy, the actual position of the members of the solar system. This information is stored on the Jet Propulsion Laboratory (JPL) Ephemeris Tapes for use on digital computers. These ephemeris tapes will be discussed more fully in a subsequent section.

As stated previously, Newton's Three Laws of Motion and the Law of Gravitation will be accepted as postulates, it will be assumed that all the bodies under consideration are point masses, the mass of the spacecraft is very small, that there are no external forces on the solar system, and that there is no solar radiation pressure on the spacecraft. Relativistic effects will also be excluded.

The Jet Propulsion Laboratory Ephemeris Tapes directly provide the geometric position and velocity of all the major planets (except earth), the

barycenter, and the moon. Therefore, all the major planets could be included in this analysis since the information is readily obtainable. It seems reasonable to assume, however, that certain bodies will have a much smaller effect than others and can be neglected in order to prevent unnecessary computations which would needlessly increase the computer time required.

Study of Table A-1 in Appendix A reveals that the sun is the major perturbing influence on a spacecraft at the triangular libration points in the earth-moon system. The planets Venus, Jupiter, and Saturn exert a stronger influence than the other planets. The effects of Mercury and Mars are similar and can be as small as the effects of Uranus or Neptune and as large as Venus; however, the effect of Pluto is about one-onehundredth that of Uranus or Neptune. Further study would show that the effects of Uranus or Neptune are approximately the same order of magnitude as the effect of the noncentral gravitational field of the earth at the triangular point. Therefore if the planets Uranus and Neptune are included, then the noncentral gravitational fields of the earth and moon should be included also. Inclusion of the noncentral effects would probably become noticeable only after many years and it would also complicate the mathematical model to a considerable extent. Therefore, the three outer planets Uranus, Neptune, and Pluto, will be excluded along with the noncentral force components due to gravitational attraction. The effects of all other bodies, e.g., sun, Mercury, etc., will be included.

In this mathematical model, the triangular libration points are assumed to exist in the earth-moon orbital plane, i. e., the plane defined by the angular momentum of the earth-moon system. It is necessary to define an earth-moon orbital plane in order to locate the triangular libration points under investigation. In the restricted three-body problem, the libration points exist in a

plane defined by the angular momentum of the system. Furthermore, since the libration points of the restricted three-body problem are considered herein with the addition of perturbing forces, i. e. , forces which cause the motion to deviate from the three-body case, it seems logical to use the earth-moon orbital plane for the location of the libration points in the mathematical model under discussion. It is important to note at this point that angular momentum plays an important, although often unrecognized, part in orbital mechanics. Two-body motion takes place in a plane defined by the angular momentum, a plane which has a fixed orientation in space since there are no external forces on the two-body system. In addition, the orbit elements used in the expressions for the time rates of change of the orbit elements locate the instantaneous orientation of a plane defined by the angular momentum of the body under consideration.

In Ref. 7, ephemeris positions are used in a 180-day study beginning October 27, 1963, and also in a 475 day study beginning July 2, 1964 (the data are also presented in Ref. 16). The spacecraft coordinates are presented in a libration-point-centered coordinate system. The numerical integration was carried out using the General Electric N-Body Trajectory Program with an initial velocity equal in magnitude to that of the moon. However, the orientation of the earth-moon system is determined by computing the cross product of two consecutive lunar position vectors. It appears from the considerations of the previous paragraph that determining the orientation by the angular momentum vector is preferred to using two consecutive radius vectors.

Equations of Motion

If the equations of motion in the "real world" model were expressed in a rotating coordinate system located at the libration point of interest, it would be necessary to determine angular velocities and angular accelerations [see Eq. (11)]. Furthermore, these quantities would have to be computed from the position-velocity information stored on the ephemeris tapes and would increase the necessary computer time considerably. However, expressing the equations of motion in a nonrotating coordinate system eliminates the need for angular velocities and angular accelerations. It was found in Case II of the modified restricted four-body model that the nonrotating and rotating equations of motion gave results which compared very well during the period in which the spacecraft continued on a libration-point-centered motion. Furthermore, it was concluded that after the spacecraft departed from the libration-point-centered motion, the nonrotating equations of motion yielded results which were more accurate than the results of the rotating equations of motion. With these considerations, the differential equations of motion in the "real world" model of this chapter will be derived in a nonrotating barycentered coordinate system.

Because of the assumption regarding external forces on the solar system, viz., that they do not exist, the center of mass of the solar system will move in a straight line with constant velocity relative to an absolute coordinate system. Since the center of mass is moving with constant velocity, Newton's Second Law will be valid if referenced to a nonrotating coordinate system at the center of mass of the solar system. In Fig. 20 the (x_C, y_C, z_C) -nonrotating coordinate system is shown with origin at the solar system

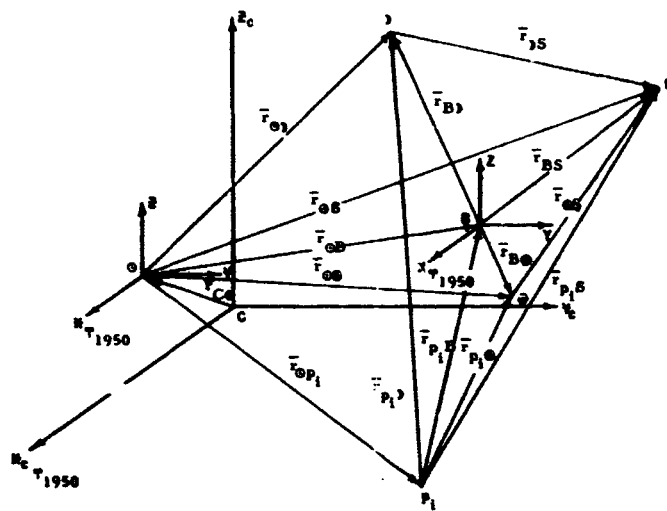


FIGURE 20. VECTOR REPRESENTATION OF POSITIONS

center of mass. The vector distances involved are also shown. The equations of motion, with respect to the (X_C, Y_C, Z_C) -system are

$$m_S \ddot{\bar{r}}_{CS} = - \frac{G m_{\odot} m_S \bar{r}_{\odot S}}{r_{\odot S}^3} - \frac{G m_{\oplus} m_S \bar{r}_{\oplus S}}{r_{\oplus S}^3} - \frac{G m_{\text{J}} m_S \bar{r}_{\text{J}S}}{r_{\text{J}S}^3} - \sum_i \frac{G m_{p_i} m_S \bar{r}_{p_i S}}{r_{p_i S}^3} \quad (54)$$

where $\sum_i \frac{G m_{p_i} m_S \bar{r}_{p_i S}}{r_{p_i S}^3}$ indicates the summation of all forces on the spacecraft

due to bodies other than the earth, the moon, and the sun. The position of the spacecraft can be expressed as

$$\bar{r}_{CS} = \bar{r}_{CB} + \bar{r}_{BS} \quad (55)$$

where the components of the vectors are expressed in the (X_C, Y_C, Z_C) -coordinate system or in a nonrotating (X, Y, Z) -barycentered system, the axes of which are parallel to their counterparts in the (X_C, Y_C, Z_C) -system. Therefore,

$$\dot{\bar{r}}_{CS} = \dot{\bar{r}}_{CB} + \dot{\bar{r}}_{BS} \quad (56)$$

$$\ddot{\bar{r}}_{CS} = \ddot{\bar{r}}_{CB} + \ddot{\bar{r}}_{BS} \quad (57)$$

Equation (57) can also be written as

$$\ddot{\bar{r}}_{BS} = \ddot{\bar{r}}_{CS} - \ddot{\bar{r}}_{CB} \quad (58)$$

Since $\ddot{\bar{r}}_{CS}$ is given by Eq. (54), knowledge of the acceleration of the barycenter with respect to the solar system mass center permits determination of

the spacecraft acceleration with respect to the barycenter. The mass times acceleration of the moon is given by

$$m_{\text{J}} \ddot{\bar{r}}_{\text{CJ}} = \bar{F}_{e_{\text{J}}} - \frac{Gm_{\text{J}}m_{\text{E}}\bar{r}_{\text{JE}}}{r_{\text{JE}}^3} \quad (59)$$

where $\bar{F}_{e_{\text{J}}}$ is the sum of all forces on the moon except the earth. The mass times acceleration of the earth is given as

$$m_{\text{E}} \ddot{\bar{r}}_{\text{CE}} = \bar{F}_{e_{\text{E}}} + \frac{Gm_{\text{E}}m_{\text{J}}\bar{r}_{\text{JE}}}{r_{\text{JE}}^3} \quad (60)$$

where $\bar{F}_{e_{\text{E}}}$ is the sum of all forces on the earth except that due to the moon. Adding Eqs. (59) and (60) yields

$$m_{\text{J}} \ddot{\bar{r}}_{\text{CJ}} + m_{\text{E}} \ddot{\bar{r}}_{\text{CE}} = \bar{F}_{e_{\text{J}}} + \bar{F}_{e_{\text{E}}} \quad (61)$$

The location of the barycenter in the $(X_{\text{C}}, Y_{\text{C}}, Z_{\text{C}})$ -coordinate system is, by definition,

$$\bar{r}_{\text{CB}} = \frac{m_{\text{J}}\bar{r}_{\text{CJ}} + m_{\text{E}}\bar{r}_{\text{CE}}}{m_{\text{J}} + m_{\text{E}}} \quad (62)$$

Taking the second derivative with respect to time yields

$$\ddot{\bar{r}}_{\text{CB}} = \frac{m_{\text{J}}\ddot{\bar{r}}_{\text{CJ}} + m_{\text{E}}\ddot{\bar{r}}_{\text{CE}}}{m_{\text{J}} + m_{\text{E}}} \quad (63)$$

Therefore by combining Eqs. (61) and (63), the following expression can be obtained:

$$\ddot{\bar{r}}_{\text{CB}} = \frac{1}{m_{\text{J}} + m_{\text{E}}} (\bar{F}_{e_{\text{J}}} + \bar{F}_{e_{\text{E}}}) \quad (64)$$

Combining Eqs. (54), (58), and (64) yields

$$\begin{aligned}
 \ddot{\bar{r}}_{BS} = & -\frac{Gm_{\odot}\bar{r}_{\odot S}}{r_{\odot S}^3} - \frac{Gm_{\oplus}\bar{r}_{\oplus S}}{r_{\oplus S}^3} - \frac{Gm_{J}\bar{r}_{J S}}{r_{J S}^3} - \sum_i \frac{Gm_{p_i}\bar{r}_{p_i S}}{r_{p_i S}^3} \\
 & - \frac{1}{m_{\oplus} + m_J} \left[-\frac{Gm_{\oplus}m_{\odot}\bar{r}_{\odot\oplus}}{r_{\odot\oplus}^3} - \sum_i \frac{Gm_{\oplus}m_{p_i}\bar{r}_{p_i\oplus}}{r_{p_i\oplus}^3} \right. \\
 & \left. - \frac{Gm_Jm_{\odot}\bar{r}_{\odot J}}{r_{\odot J}^3} - \sum_i \frac{Gm_Jm_{p_i}\bar{r}_{p_i J}}{r_{p_i J}^3} \right] \quad (65)
 \end{aligned}$$

Rearranging Eq. (65) will lead to the following result:

$$\begin{aligned}
 \ddot{\bar{r}}_{BS} = & -\frac{Gm_{\odot}\bar{r}_{\odot S}}{r_{\odot S}^3} - \frac{Gm_{\oplus}\bar{r}_{\oplus S}}{r_{\oplus S}^3} - \frac{Gm_J\bar{r}_{J S}}{r_{J S}^3} - \sum_i \frac{Gm_{p_i}\bar{r}_{p_i S}}{r_{p_i S}^3} \\
 & + \frac{Gm_{\odot}}{m_J + m_{\oplus}} \left(\frac{m_{\oplus}\bar{r}_{\odot\oplus}}{r_{\odot\oplus}^3} + \frac{m_J\bar{r}_{\odot J}}{r_{\odot J}^3} \right) \\
 & + \sum_i \left[\frac{Gm_{p_i}}{m_J + m_{\oplus}} \left(\frac{m_{\oplus}\bar{r}_{p_i\oplus}}{r_{p_i\oplus}^3} + \frac{m_J\bar{r}_{p_i J}}{r_{p_i J}^3} \right) \right] \quad (66)
 \end{aligned}$$

All vectors in Eq. (66) are expressed in the (X, Y, Z)-barycentered coordinate system. Expressing Eq. (66) in component form yields

$$\begin{aligned}
\ddot{X}_S = & -\frac{Gm_{\odot}(X_S - X_{\odot})}{r_{\odot S}^3} - \frac{Gm_{\oplus}(X_S - X_{\oplus})}{r_{\oplus S}^3} - \frac{Gm_{J}(X_S - X_J)}{r_{JS}^3} \\
& - \sum_i \frac{Gm_{p_i}(X_S - X_{p_i})}{r_{p_i S}^3} + \frac{Gm_{\odot}}{m_J + m_{\oplus}} \left[\frac{m_{\oplus}(X_{\oplus} - X_{\odot})}{r_{\odot\oplus}^3} \right. \\
& \left. + \frac{m_J(X_J - X_{\odot})}{r_{\odot J}^3} \right] + \sum_i \left[\frac{Gm_{p_i}}{m_J + m_{\oplus}} \left(\frac{m_{\oplus}(X_{\oplus} - X_{p_i})}{r_{p_i\oplus}^3} \right. \right. \\
& \left. \left. + \frac{m_J(X_J - X_{p_i})}{r_{p_i J}^3} \right) \right]
\end{aligned}$$

$$\begin{aligned}
\ddot{Y}_S = & -\frac{Gm_{\odot}(Y_S - Y_{\odot})}{r_{\odot S}^3} - \frac{Gm_{\oplus}(Y_S - Y_{\oplus})}{r_{\oplus S}^3} - \frac{Gm_J(Y_S - Y_J)}{r_{JS}^3} \\
& - \sum_i \frac{Gm_{p_i}(Y_S - Y_{p_i})}{r_{p_i S}^3} + \frac{Gm_{\odot}}{m_J + m_{\oplus}} \left[\frac{m_{\oplus}(Y_{\oplus} - Y_{\odot})}{r_{\odot\oplus}^3} \right. \\
& \left. + \frac{m_J(Y_J - Y_{\odot})}{r_{\odot J}^3} \right] + \sum_i \left[\frac{Gm_{p_i}}{m_J + m_{\oplus}} \left(\frac{m_{\oplus}(Y_{\oplus} - Y_{p_i})}{r_{p_i\oplus}^3} \right. \right. \\
& \left. \left. + \frac{m_J(Y_J - Y_{p_i})}{r_{p_i J}^3} \right) \right]
\end{aligned}$$

$$\begin{aligned}
\ddot{Z}_S = & - \frac{Gm_{\odot}(Z_S - Z_{\odot})}{r_{\odot S}^3} - \frac{Gm_{\oplus}(Z_S - Z_{\oplus})}{r_{\oplus S}^3} - \frac{Gm_J(Z_S - Z_J)}{r_{J S}^3} \\
& - \sum_i \frac{Gm_{P_i}(Z_S - Z_{P_i})}{r_{P_i S}^3} + \frac{Gm_{\odot}}{m_J + m_{\oplus}} \left[\frac{m_{\oplus}(Z_{\oplus} - Z_{\odot})}{r_{\oplus \odot}^3} \right. \\
& \left. + \frac{m_J(Z_J - Z_{\odot})}{r_{\odot J}^3} \right] + \sum_i \left[\frac{Gm_{P_i}}{m_J + m_{\oplus}} \left(\frac{m_{\oplus}(Z_{\oplus} - Z_{P_i})}{r_{P_i \oplus}^3} \right. \right. \\
& \left. \left. + \frac{m_J(Z_J - Z_{P_i})}{r_{P_i J}^3} \right) \right]
\end{aligned} \tag{67}$$

where

$$r_{\odot S} = \left[(X_S - X_{\odot})^2 + (Y_S - Y_{\odot})^2 + (Z_S - Z_{\odot})^2 \right]^{1/2}$$

$$r_{\oplus S} = \left[(X_S - X_{\oplus})^2 + (Y_S - Y_{\oplus})^2 + (Z_S - Z_{\oplus})^2 \right]^{1/2}$$

$$r_{J S} = \left[(X_S - X_J)^2 + (Y_S - Y_J)^2 + (Z_S - Z_J)^2 \right]^{1/2}$$

$$r_{P_i S} = \left[(X_S - X_{P_i})^2 + (Y_S - Y_{P_i})^2 + (Z_S - Z_{P_i})^2 \right]^{1/2}$$

Numerical integration of Eqs. (67) with specified initial conditions yields the position of the spacecraft in the (X, Y, Z)-barycentered coordinate system. The coordinates of the natural bodies are provided by the ephemeris tape.

The integration of Eqs. (67) could be performed in an equatorial coordinate system centered at the earth-moon barycenter provided, of course, that it is nonrotating. However, in this particular study, it is advantageous to compute in the (X, Y, Z)-coordinate system since the motion takes place very nearly in the ecliptic. This allows one to display the (X, Y)-motion as representative of the total motion since the Z-component of the displacement is much less than $(X^2 + Y^2)^{1/2}$. In the equatorial coordinate system, such displays could not be made since all three components of the displacement would be large.

It should be noted that large amounts of computer time were required for integration of Eqs. (67). This is largely attributable to reading the tape and interpolation of the tape data.

Jet Propulsion Laboratory Ephemeris Tapes

Acquisition of the Jet Propulsion Laboratory Ephemeris Tapes has provided The University of Texas with a valuable research aid. The Ephemeris Tapes consist of a set of nine magnetic tapes for the time span between the year 1950 and the year 2000 (Ref. 27). The heliocentric positions and velocities of all the planets except the earth are stored on the tapes in double precision (about 24 decimal places). In addition to these bodies, the position and velocity of the barycenter is included. The positions and velocities are geometrical, i. e., the effects of aberration have been removed. The positions and velocities are stored in Astronomical Units and Astronomical Units

per day in increments varying from one day to two days. The second and fourth differences are also included on the tapes for interpolation to a date not stored on the tape. The interpolation is accurate to twelve decimal places. Furthermore, the information is stored as a function of the Julian Date, i. e., given a Julian Date, the position and velocity of any body can be determined either directly from the position and velocity data stored on the tape or by interpolation. The positions of the moon are stored on the tapes at half-day intervals in a geocentric equatorial coordinate system in which the distances are given in earth radii. From the heliocentric position of the barycenter and the geocentric position of the moon, the heliocentric position of the earth can be determined from Eq. (B-7) in Appendix B. The heliocentric coordinate system used is a rectangular system in which the X_e -axis points in the direction of the vernal equinox of 1950, the Y_e -axis lies in a plane parallel to the equatorial plane of the earth at Epoch 1950, and the Z_e -axis is mutually perpendicular. The orientation of the axis system is shown in Fig. 21. Since, as stated previously, it is somewhat more convenient to use a coordinate system in which the Y axis is in the Ecliptic of Epoch 1950, the transformation to this system is made by

$$\begin{aligned} X &= X_e \\ Y &= Y_e \cos \epsilon + Z_e \sin \epsilon \\ Z &= Z_e \sin \epsilon + Y_e \cos \epsilon \end{aligned} \tag{68}$$

as shown in Fig. 22. It is important to note that the vernal equinox of Epoch 1950 and the Ecliptic of Epoch 1950 are fixed, and, therefore, the (X, Y, Z) -coordinate system is nonrotating. If the vernal equinox of date and ecliptic

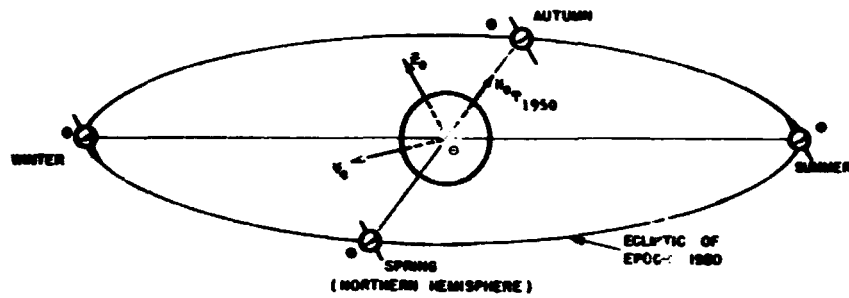


FIGURE 21. ORIENTATION OF COORDINATE SYSTEM USED IN THE EPHEMERIS TAPES

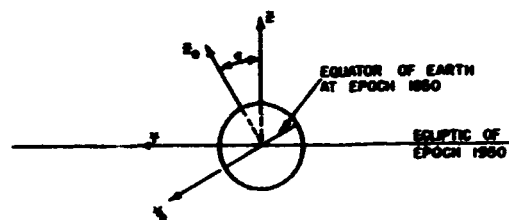


FIGURE 22. RELATION BETWEEN EQUATORIAL AND ECLIPTIC COORDINATE SYSTEMS

of date were used, the (X, Y, Z)-coordinate system would be rotating since the vernal equinox moves westward along the celestial sphere. The value for ϵ , given by Ref. 28, is

$$\epsilon = .40920619 \text{ radians} \quad .$$

This is the obliquity of the ecliptic at the Epoch 1950.

Constants

Since the ephemeris data are stored on the tapes in Astronomical Units and Astronomical Units per day, the integration was made in the units of Astronomical Units and days. Therefore, it was necessary to use compatible units with the gravitational parameter of the bodies involved (the gravitational parameter is the product of the universal gravitational constant and the mass of the body). The gravitational parameters which were used in this investigation are given in Ref. 23 and have been generally accepted for use in trajectory calculations. These constants are given in Table 3. Although the integration is performed in Astronomical Units, a conversion to customary engineering units is made at the printout. In order to make the conversion, it is necessary to know the value of the Astronomical Unit; the value given by Ref. 23 is 1 A. U. = 149,599,000.0 km and is the value used in this study. The conversion from kilometers to miles is 1 km = .62136996 mi. Since the lunar data stored on the tape are in earth radii, rather than Astronomical Units, the value of earth radii suggested for use with the Ephemeris Tapes, as given by Ref. 28, is 1 Earth Radii = 6378.327 km. This value does disagree slightly with that of Ref. 23.

Body	Symbol	Gravitation Parameter (Gm_{p_i})	
		A. U. ³ /day ²	km ³ /sec ²
Sun	☉	$2.959122093 \times 10^{-4}$	$1.32715445 \times 10^{11}$
Mercury	☿	4.835167×10^{-11}	2.168553×10^4
Venus	♀	$7.2431725 \times 10^{-10}$	3.2485340×10^5
Earth	♁	8.887552×10^{-10}	3.9860320×10^5
Moon	☾	$Gm_{\text{☾}} = \frac{Gm_{\text{♁}}}{81.3015}$	
Mars	♂	9.582649×10^{-11}	4.297780×10^4
Jupiter	♃	2.825234×10^{-7}	1.267106×10^8
Saturn	♄	8.454635×10^{-8}	3.791870×10^7
Uranus	♅	1.293945×10^{-8}	5.803292×10^6
Neptune	♆	1.566585×10^{-8}	7.026072×10^6
Pluto	♇	7.397895×10^{-10}	3.317886×10^5

Table 3. Gravitation Parameters of the Major Bodies in the Solar System

Transformation to Libration-Point-Centered Rotating System

It is informative to observe the motion in a coordinate system which is centered at the libration point of interest. In order to do this, it is necessary to make a coordinate transformation from the (X, Y, Z)-system data which results from the numerical integration of the equations of motion. Assuming that an (x, y, z)-coordinate system has its origin at the libration point of interest (as shown in Fig. C-1 in Appendix C) with the x-axis being parallel to the earth-moon line and lying in earth-moon orbital plane, the z-axis being perpendicular to the orbital plane, the y-axis being mutually perpendicular, then the relation between the (X, Y, Z)-position and the (x, y, z)-position is given by Eqs. (C-3) for L_4 , viz.,

$$\begin{bmatrix} X_S \\ Y_S \\ Z_S \end{bmatrix} = A \begin{bmatrix} x_S + \xi_p \\ y_S + \eta_p \\ z_S \end{bmatrix}$$

where the transformation matrix A given by Eq. (13) is evaluated at Ω^* , θ^* , and i^* .

The (X, Y, Z)-spacecraft coordinates are known from the numerical integration procedure and the angles Ω^* , θ^* , and i^* , necessary to determine the transformation matrix A, are determined from the angular momentum of the earth-moon system. Then for the L_4 -libration point

$$\begin{bmatrix} x_S \\ y_S \\ z_S \end{bmatrix} = A \begin{bmatrix} X_S \\ Y_S \\ Z_S \end{bmatrix} - \begin{bmatrix} \xi_p \\ \eta_p \\ 0 \end{bmatrix} \quad (69)$$

Assuming the libration point of interest to be defined by the instantaneous earth-moon distance, then ξ_p and η_p are time dependent since r_{\oplus} varies with time. In addition, the angles Ω^* and i^* are also time dependent since the earth-moon orbital plane does not have a fixed orientation in space. The transformation to an (x, y, z) -rotating coordinate system at L_5 will be the same as Eq. (69) with the exception that η_p is replaced by $-\eta_p$.

Case I: Initial Date JD 2,439,501.0 (January 10, 1967; 12^hGMT)

Orientation of the solar system and the earth-moon system. In the previous mathematical model, it was necessary to choose an initial orientation of the model in addition to supplying the initial position and velocity of the spacecraft. In the "real world" model considered in this chapter, choosing the initial date, i. e., the date at which the spacecraft is placed at the L_4 - or L_5 -position of the earth-moon system, will fix the orientation of the model. The date chosen for this study was Julian Date 2,439,501.0 or January 10, 1967, 12 hours Greenwich Mean Time. This date was chosen because of its location on the tape and not because of any particular aspect of the solar system orientation. This is the first record on the tape; the final record begins in June, 1974. The configuration of the solar system when the spacecraft is assumed to be placed at the triangular libration point is shown in Fig. 23.

For the assumed spacecraft insertion date, the orientation of the earth-moon system is computed from the angular momentum of the system. Using the angular momentum per unit mass of the moon in Eqs. (B-15) and (B-16) yields i^* and Ω^* of the earth-moon orbital plane. The angle θ^* is determined from Eqs. (B-5). The orientation of the earth-moon system is shown in Fig. 24. The inclination, i^* , of the earth-moon orbital plane at insertion

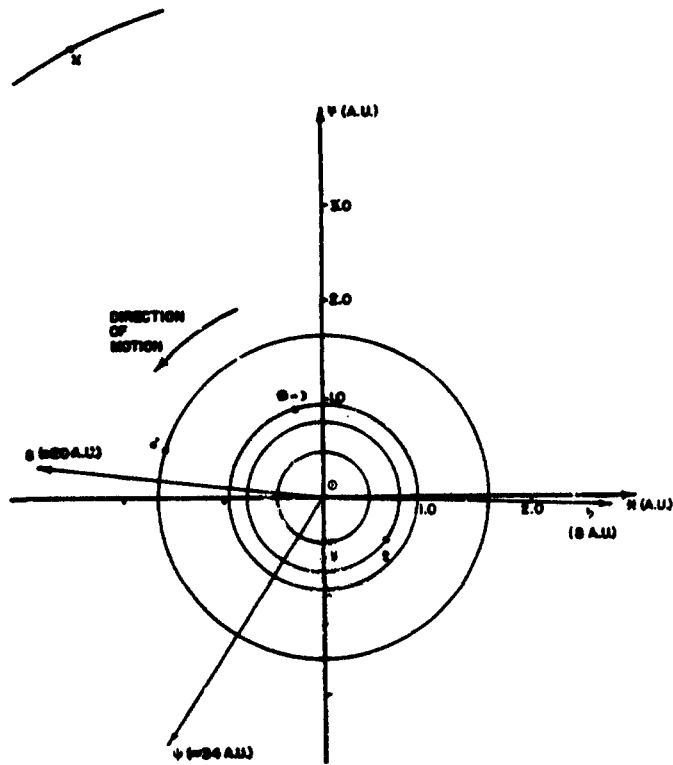


FIGURE 23. SOLAR SYSTEM ORIENTATION AT
J.D. 2439501.0 (JAN. 10, 1967; 12^h GMT)

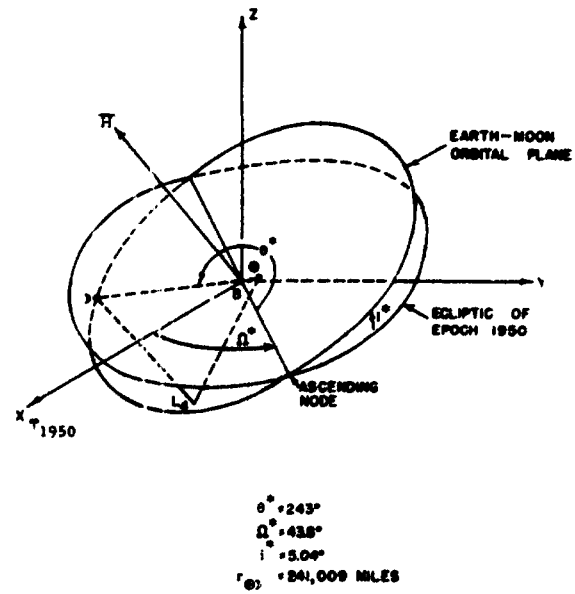


FIGURE 24. ORIENTATION OF THE EARTH-MOON
SYSTEM ON JULIAN DATE 2439501.0
(JAN. 10, 1967; 12^h GMT)

is 5.04° . The longitude of the ascending node, Ω^* , is 43.8° and the angle θ^* , locating the moon in the orbital plane, is 242.6° . The distance between the earth and the moon at insertion, $r_{\oplus\text{D}}$, is 241,008.5 miles. The lunar velocity component in the radial direction, r_{BD} , is 2248.13 miles/day and the lunar velocity component in the tangential direction, i. e., the \bar{e}_η -component as shown in Fig. C-2 or $r_{\text{BD}}\dot{\theta}^*$, is 54,001.02 miles/day. Furthermore, the value of ξ_p is 117,575.9 miles and the value of η_p is 208,719.5 miles. The lunar in-plane angular velocity, $\dot{\theta}^*$, is $13^\circ/\text{day}$ and the barycenter-sun distance, $r_{\text{B}\odot}$, is 91,414,830 miles.

Since, as stated previously, the earth-moon orbital plane does not have a fixed orientation in space, the angles i^* and Ω^* vary with time. To illustrate how they vary, and, in turn, the motion of the (x, y, z) -coordinate system, Ω^* is plotted versus time in Fig. 25 and i^* is shown versus time in Fig. 26. In addition, ξ_p and η_p are plotted versus time in Figs. 27 and 28 respectively.

Initial conditions and results with inclusion of \dot{r}_{BL} . If \dot{r}_{BL} is included, i. e., the radial-velocity component of the libration point necessary to maintain the equilateral configuration in the three-body sense (see Appendix C), then \dot{r}_{BL} is computed from the radial velocity component of the moon, Eq. (C-8), and is 2262.08 miles/day. Also, the tangential-velocity component in the earth-moon orbital plane $r_{\text{BL}}\dot{\theta}^* = 54,336.17$ miles/day where r_{BL} is the distance to the triangular point and is 239,558 miles. The initial position and velocity relative to the (x, y, z) -libration-point-centered coordinate system is assumed to be $x_S = y_S = z_S = 0$ and $\dot{x}_S = \dot{y}_S = \dot{z}_S = 0$. The initial (X, Y, Z) -position and velocity of the spacecraft were computed from Eqs. (C-3) and C-10) and yield

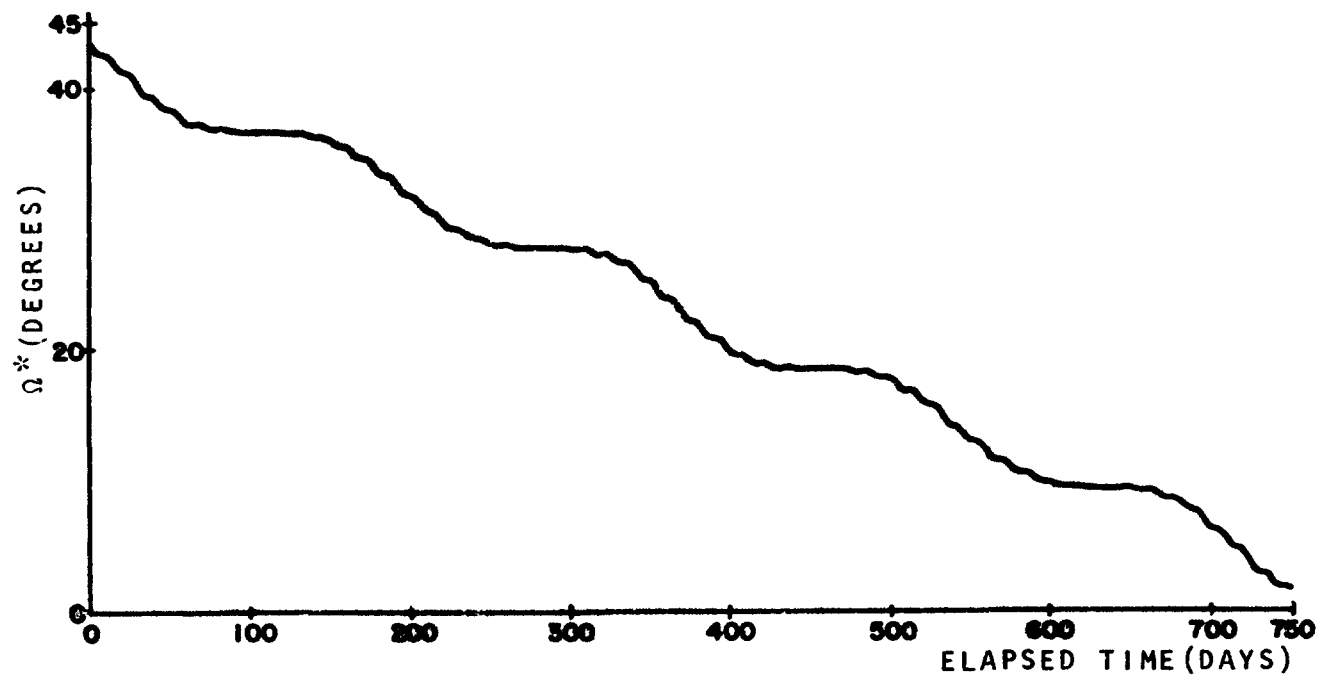


FIGURE 25. Ω^* OF THE EARTH-MOON ORBITAL PLANE FOR 750 DAY PERIOD BEGINNING JD 2439501.0

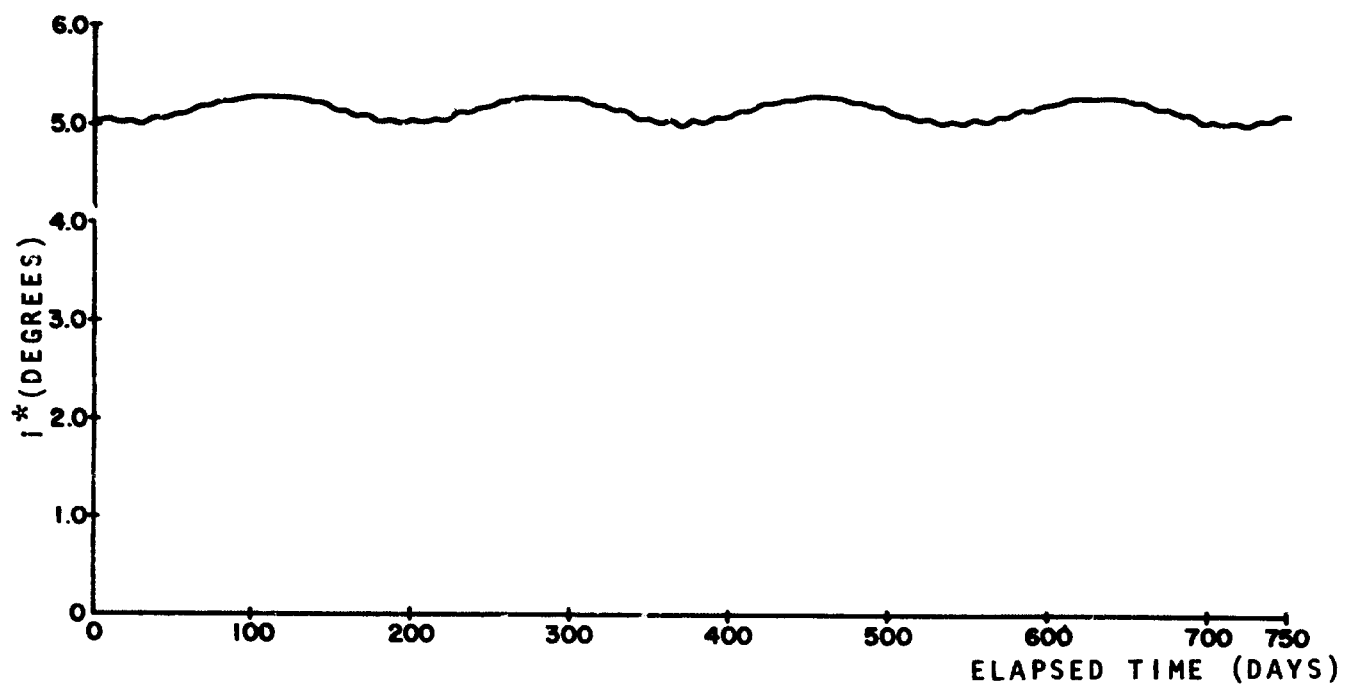


FIGURE 26. i^* OF THE EARTH-MOON ORBITAL PLANE FOR 750 DAY PERIOD BEGINNING JD 2439501.0

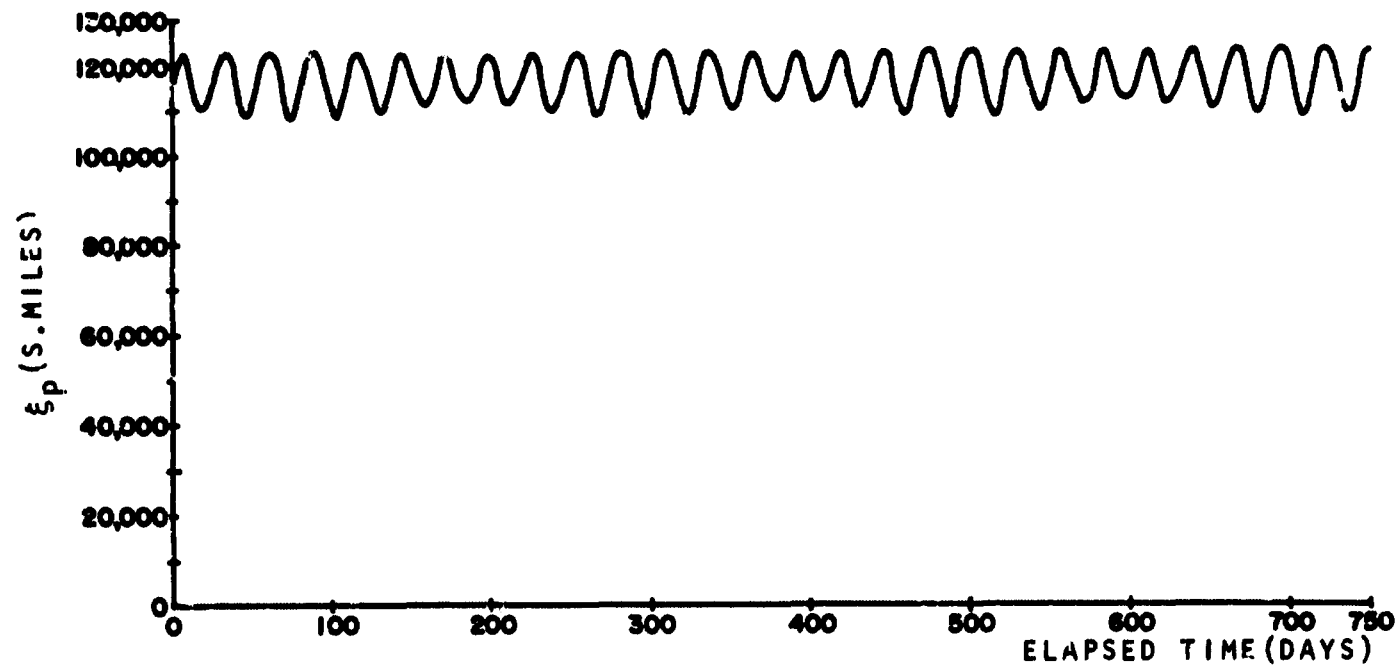


FIGURE 27. ξ_p FOR 750 DAY PERIOD BEGINNING JD 2439501.0

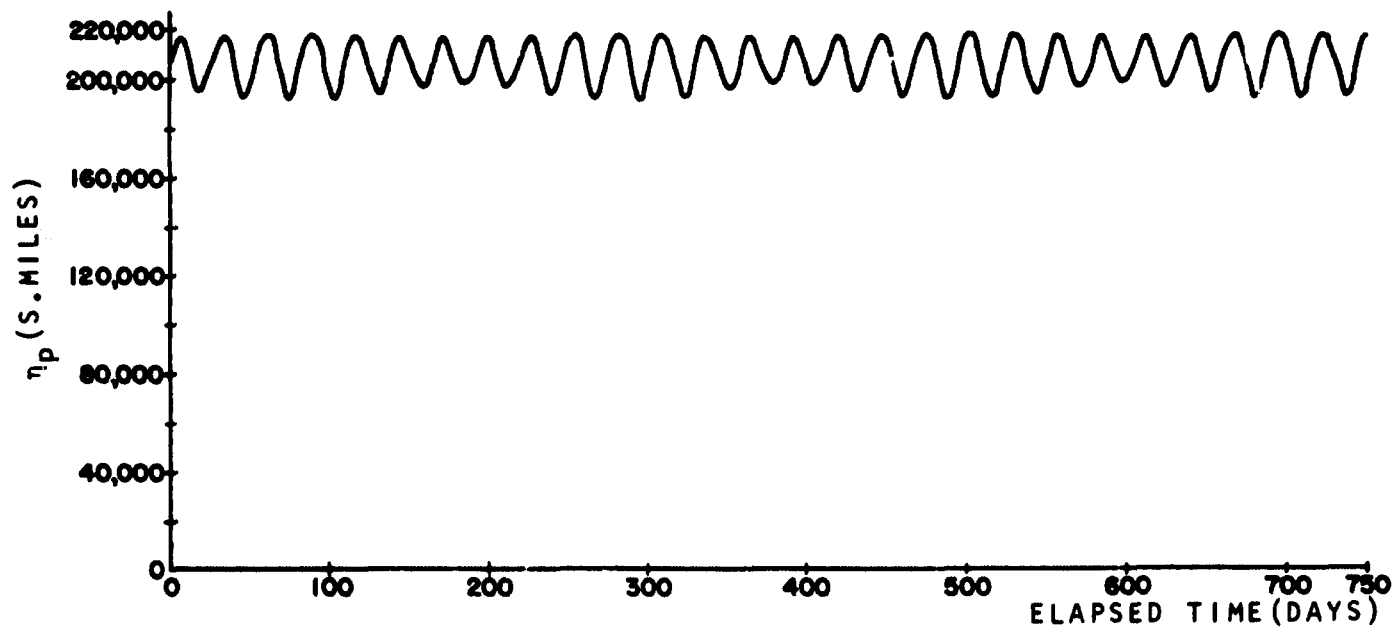


FIGURE 28. η_p FOR 750 DAY PERIOD BEGINNING JD 2439501.0

$$\begin{array}{ll}
 X_S = 232,851 \text{ mi} & \dot{X}_S = 14,531 \text{ mi/day} \\
 Y_S = -53,461 \text{ mi} & \dot{Y}_S = 52,349 \text{ mi/day} \\
 Z_S = -17,610 \text{ mi} & \dot{Z}_S = 2,444 \text{ mi/day.}
 \end{array}$$

Equations (67) were numerically integrated using the Adams-Moulton method with the Runge-Kutta starter. The step size used throughout the integration was either .15 days or .075 days until 725 days after spacecraft insertion into the libration orbit. After 725 days, the step size was reduced considerably. The single-step-error range was specified to be a maximum value of 1×10^5 and a minimum value of 5×10^{-11} .

The results of the integration are shown in Figs. 29. As can be seen from Fig. 29a and 29b, the trajectory of the spacecraft is much the same after each revolution around the barycenter. In Fig. 29c the trajectory is considerably different and has expanded to a much larger envelope of motion. Fig. 29d shows that the spacecraft makes a close lunar pass between 729 days and 730 days, after which time it appears that the spacecraft may leave the earth-moon system. The closest approach to the moon occurs at 729.895 days when the spacecraft is approximately 2100 miles from the lunar surface. Obviously, the spacecraft is no longer on an L_4 -point-centered orbit. The absolute value of the Z-component of spacecraft displacement does not exceed 30,000 miles in the 750-day period considered.

A coordinate transformation of the barycentered position data was made to the (x, y, z) - L_4 -centered coordinate system. It should again be pointed out that this coordinate system does not remain a fixed distance from the barycenter. It is both translating and rotating; it is translating because ξ_p and η_p are functions of time. Equations (69) are the transformation equations

and the results of the transformation are given in Figs. 30. The shape of the trajectory relative to the (x, y, z) -system is quite similar to those observed in the previous mathematical model, viz., the modified restricted four-body model. Again, as in previous cases, the envelope of motion expands considerably with each 250-day period as seen in Figs. 30a and 30b. Note in Fig. 30c that the spacecraft leaves a libration-point-centered motion and experiences a near encounter with the moon as expected from the (X, Y, Z) -data. The absolute value of the z -component does not exceed 2500 miles prior to 730 days. In the period from 730 to 750 days, it does attain a maximum value of about 8100 miles.

Figure 31 shows the total displacement of the spacecraft from the L_4 point versus time. This plot is quite similar to those in the restricted four-body models as one would expect because of the similarity between the (x, y) motion.

The magnitude of the spacecraft angular momentum vector is shown in Fig. 32. Note that the close lunar pass causes a very large reduction of the magnitude of the angular momentum vector. As the spacecraft nears the moon, the gravitational force of the moon produces a very large torque about the barycenter. Since the time rate of change of the angular momentum vector is equal to this torque, there is a very large time rate of change of the angular momentum vector. The data show that not only is there a very large slope of the angular momentum versus time curve (Fig. 32), but there is also a very rapid change in the direction of the angular momentum vector. At some time during the pass, the torque will be zero, i. e., the slope is zero, after which time the torque is in the opposite direction. Because of insufficient data, the minimum may have a magnitude less than that shown.

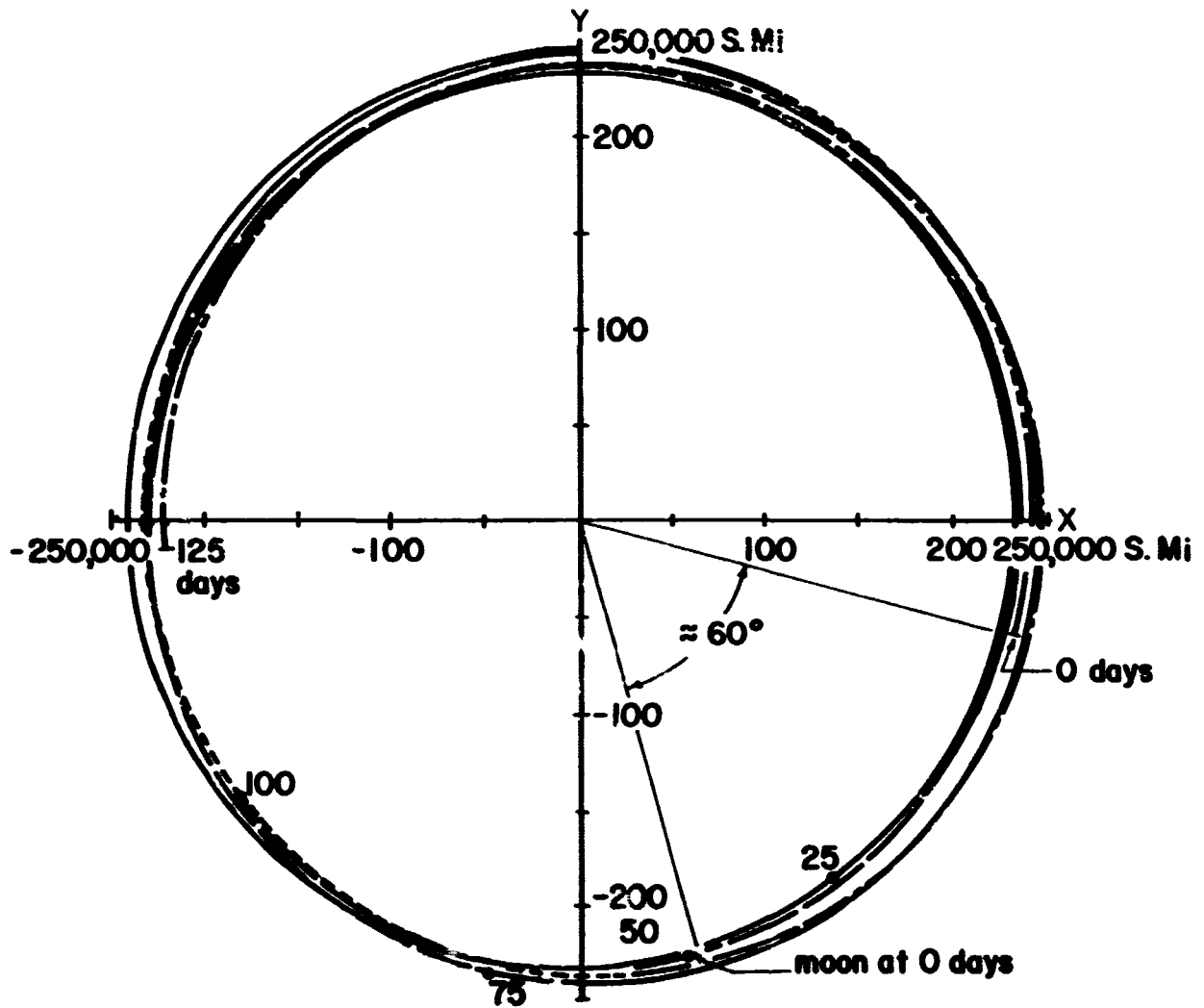


FIGURE 29a. L_4 NONROTATING (X, Y) -RESULTS FOR INITIAL JD 2439501.0 FROM 0 DAYS TO 125 DAYS

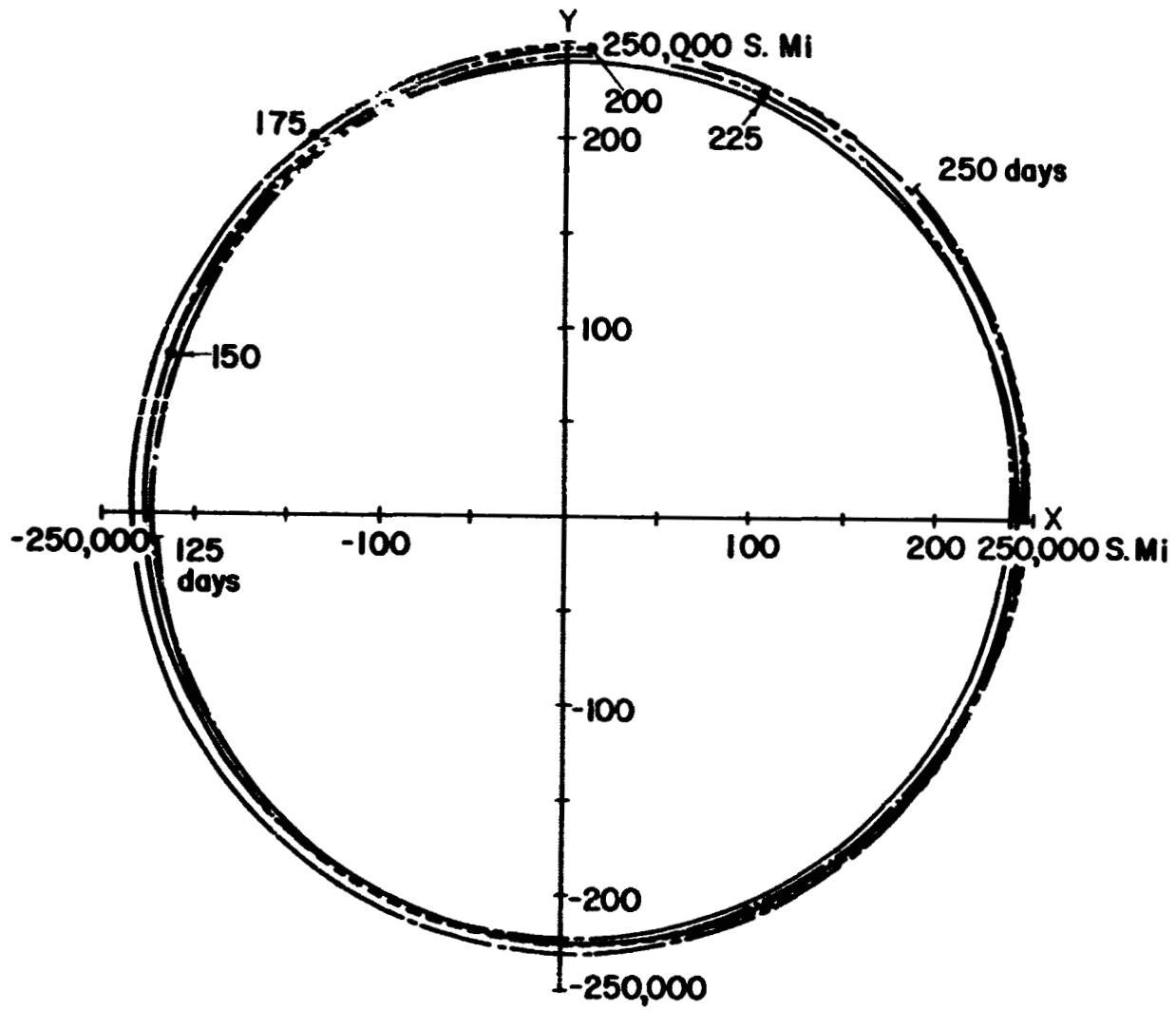


FIGURE 29b. L_4 NONROTATING (X,Y)-RESULTS FOR INITIAL
 JD 2439501.0 FROM 125 DAYS TO 250 DAYS

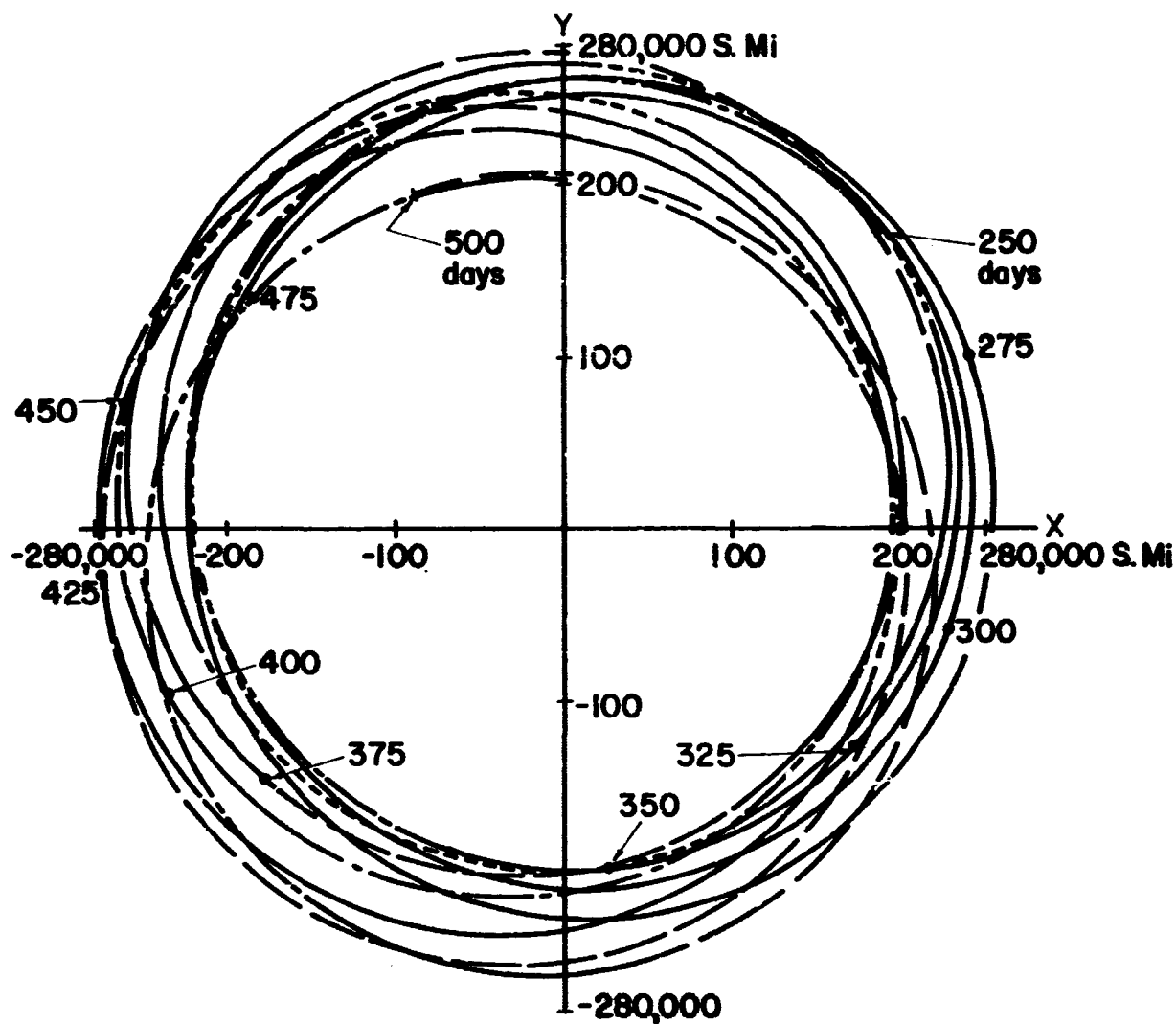


FIGURE 29c. L_4 NONROTATING (X, Y)-RESULTS FOR INITIAL
 JD 2439501.0 FROM 250 DAYS TO 500 DAYS

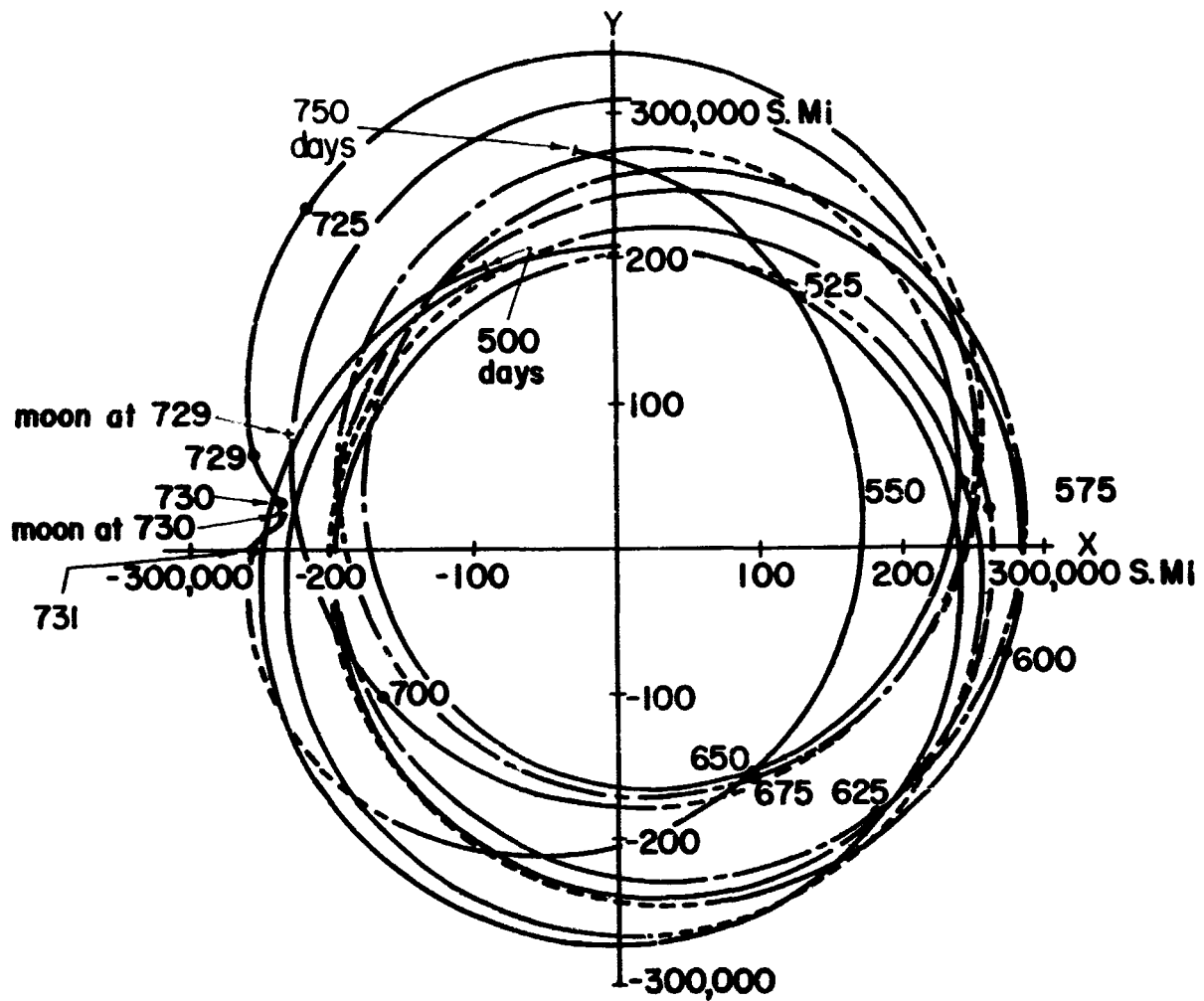


FIGURE 29d. L_4 NONROTATING (X, Y)-RESULTS FOR INITIAL
 JD 2439501.0 FROM 500 DAYS TO 750 DAYS

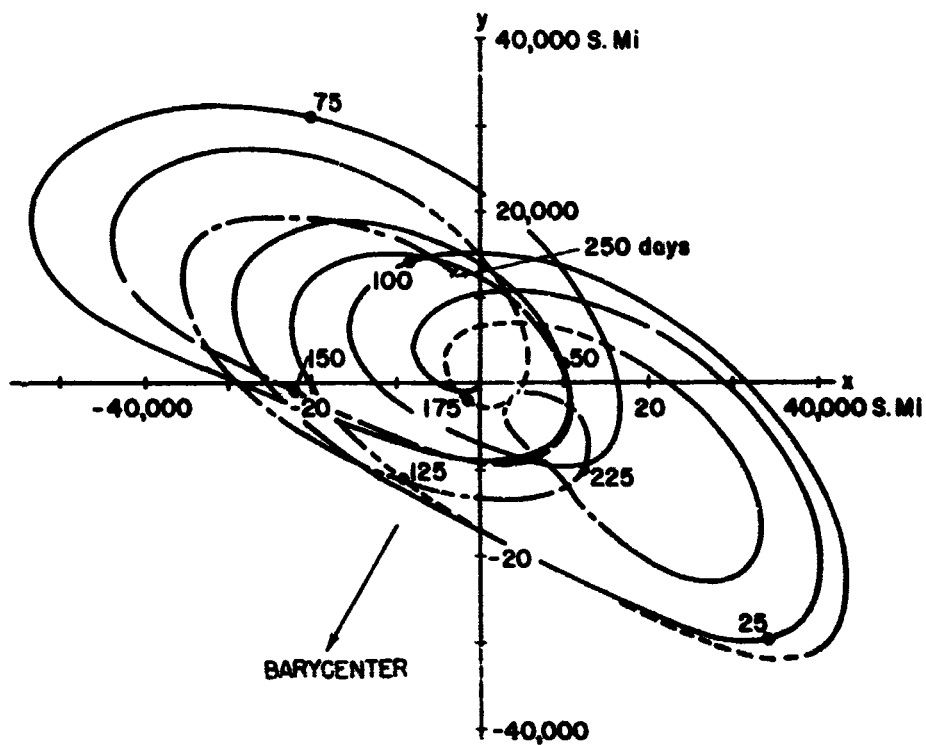


FIGURE 30a. L_4 ROTATING (x, y) -RESULTS FOR INITIAL JD 2439501.0 FROM 0 DAYS TO 250 DAYS

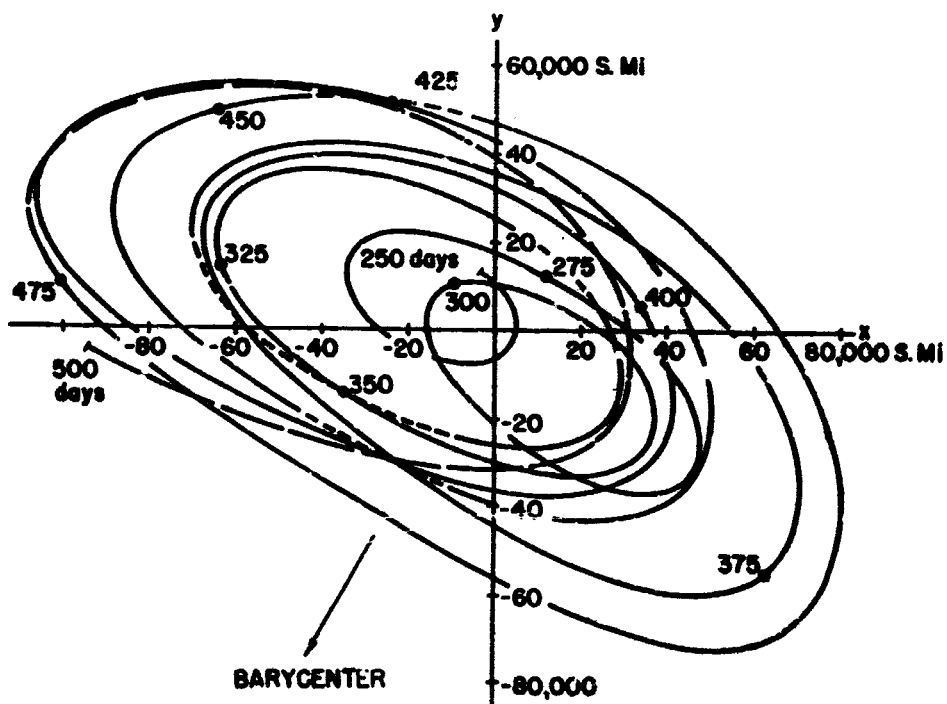


FIGURE 30b. L_4 ROTATING (x, y) -RESULTS FOR INITIAL JD 2439501.0 FROM 250 DAYS TO 500 DAYS

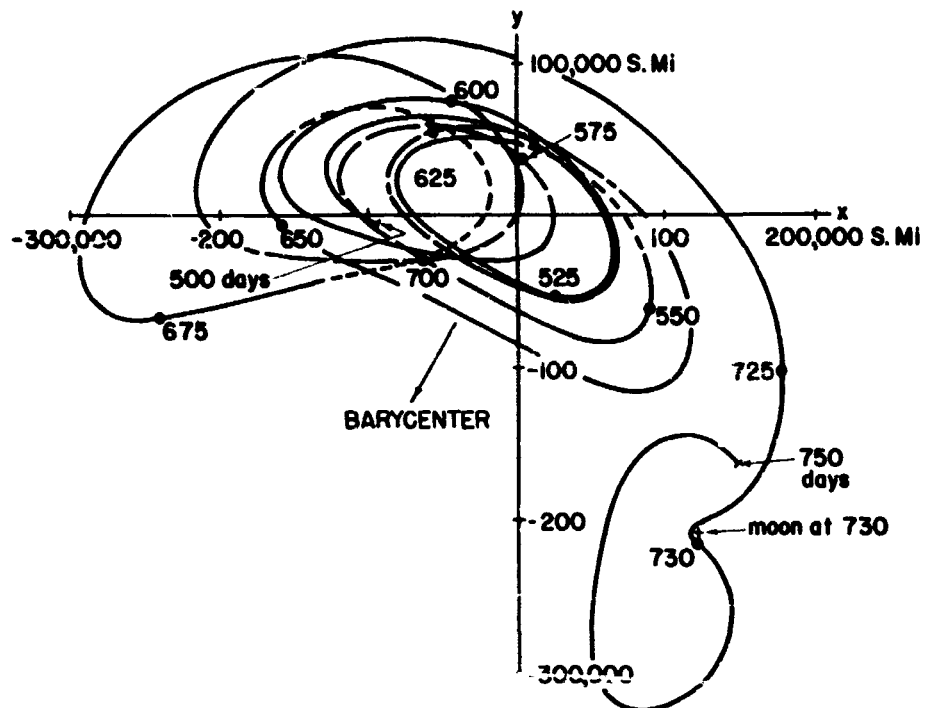


FIGURE 30c. L_4 ROTATING (x, y) -RESULTS FOR INITIAL
 JD 2439501.0 FROM 500 DAYS TO 750 DAYS

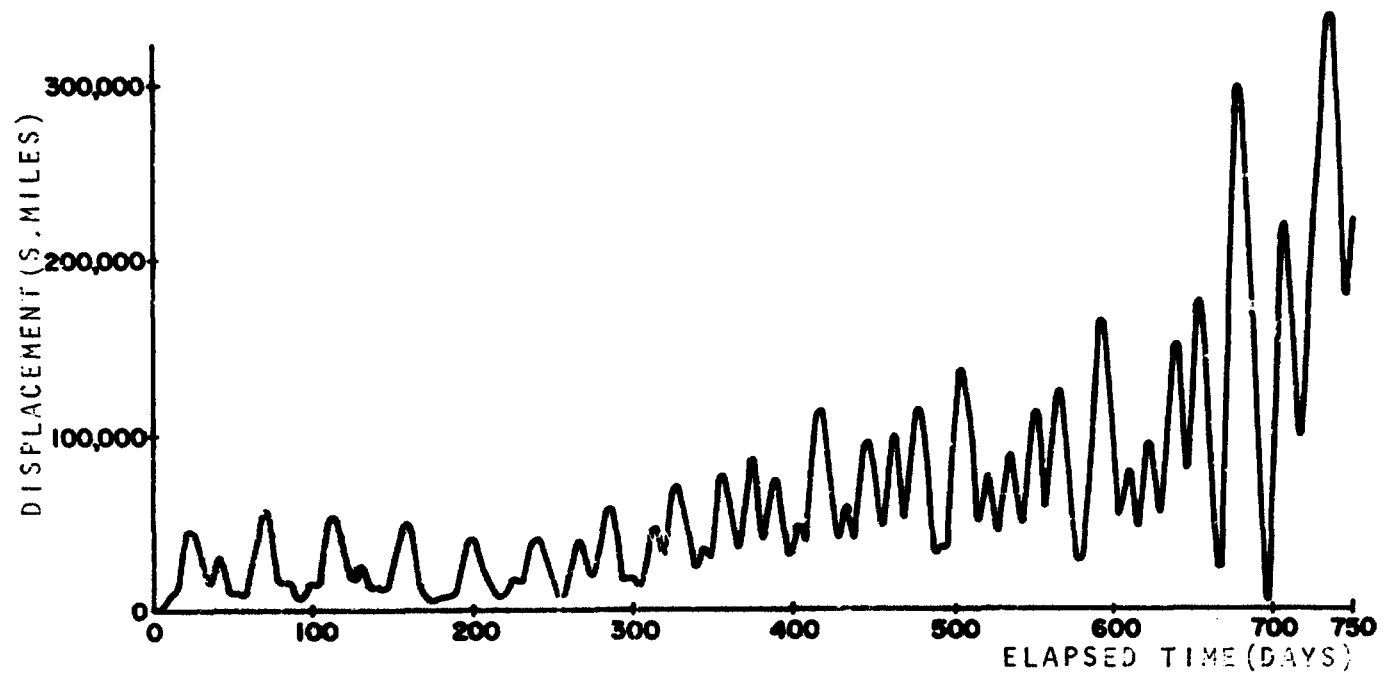


FIGURE 31. MAGNITUDE OF DISPLACEMENT VECTOR FROM L_4 VS. TIME FOR INITIAL JD 2439501.0

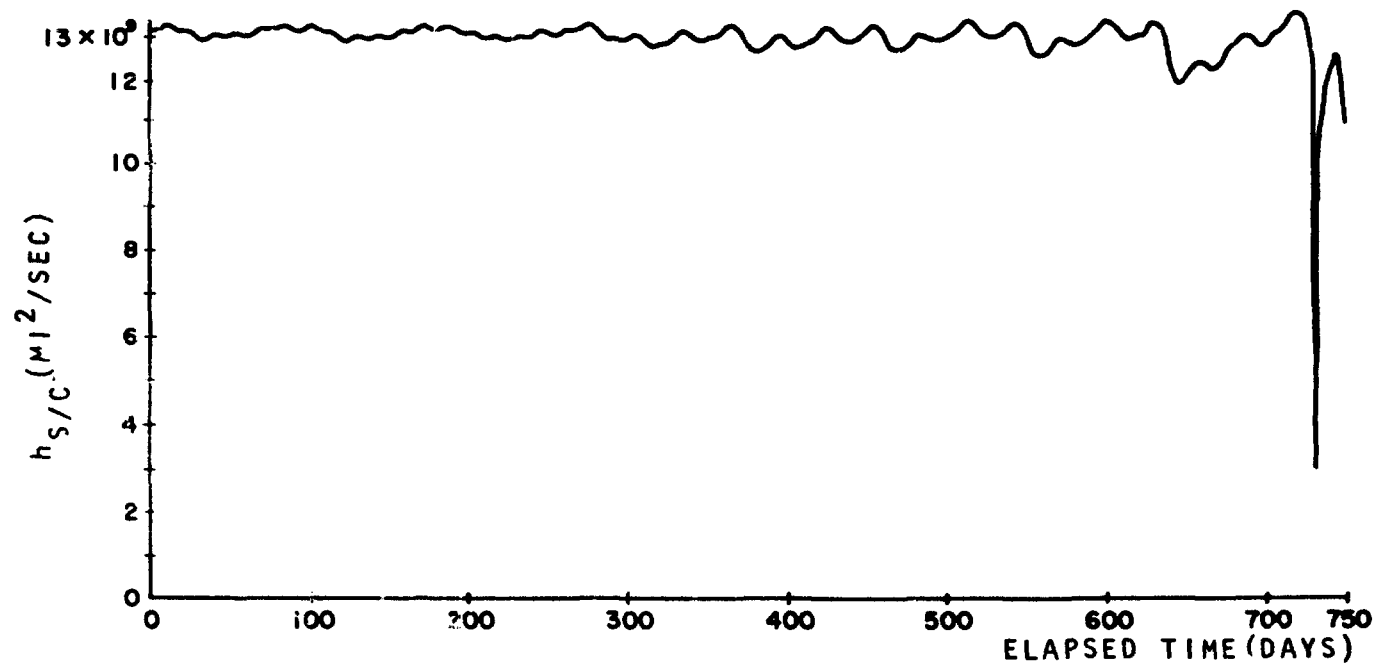


FIGURE 32. MAGNITUDE OF SPACECRAFT ANGULAR MOMENTUM VECTOR RELATIVE TO THE BARYCENTER VS. TIME FOR INITIAL JD 2439501.0

Initial conditions and results with $\dot{r}_{BL} = 0$. To determine the effect which \dot{r}_{BL} has on the subsequent motion, the equations were integrated with the same initial orientation and the same initial conditions relative to the (x, y, z)-coordinate system as in the previous section. In this case, however, \dot{r}_{BL} was set to zero. The spacecraft will have the same initial position as in the previous section, but the velocity will be different. The initial velocity of the spacecraft in the (X, Y, Z)-coordinate system is

$$\dot{X}_S = 12,332 \text{ mi/day}$$

$$\dot{Y}_S = 52,854 \text{ mi/day}$$

$$\dot{Z}_S = 2611 \text{ mi/day}$$

The step size for the first 100 days of the integration was .3 days. The step size was reduced to .15 days after 100 days in order to stay within the specified single-step-error range which was the same as the previous case.

The results of the integration are shown in Figs. 33. The trajectory in the (X, Y)-plane is quite similar to the previous case which included \dot{r}_{BL} , except that the envelope of motion throughout the first 250 days (Fig. 33a and 33b) is slightly larger with \dot{r}_{BL} equal to zero. In Fig. 33c, which illustrates the motion for the period from 250 days to 500 days, the envelope of motion expands considerably, and, in Figs. 33d and 33e it is seen that the spacecraft is in an orbit with an orbital period which is smaller than during the first 250 days. In fact, the spacecraft orbit in the period after 500 days takes the spacecraft within 60,000 miles of the barycenter during the 500-day to 600-day period (see Fig. 33d). The barycenter orbit of the spacecraft has a radius at closest approach of about 50,000 mi during the 600-day to 698-day period, whereas, the farthest approach does not change considerably. The radius at

farthest approach is between 210,000 miles and 200,000 miles. It seems conceivable that at some later date the spacecraft may make a close pass of the moon because of the difference in the orbital periods of the moon and spacecraft and because the spacecraft has a farthest approach of 200,000 mi.

The (x, y) -components of the spacecraft motion are shown in Figs. 34. Note that in Fig. 34b the spacecraft begins to leave the libration-point-centered motion near the end of the 500-day period. In Fig. 34c one can see that the spacecraft has definitely begun to move on an entirely different trajectory within the earth-moon system and is no longer on a libration-point-centered motion.

The magnitude of the angular momentum vector relative to the barycenter is shown in Fig. 35. Note the correspondence between the sudden decrease in the angular momentum magnitude and the spacecraft's departing from a libration-point-centered motion.

It is important to note that the spacecraft leaves the libration-point-centered motion with \dot{r}_{BL} equal to zero approximately 200 days prior to the case in which \dot{r}_{BL} is computed from the lunar radial velocity. In both cases, viz., the case in which \dot{r}_{BL} is zero and the case in which \dot{r}_{BL} is not zero, the spacecraft leaves the libration-point-centered motion. However, the period in which the spacecraft has a libration-point-centered motion is extended by the inclusion of the \dot{r}_{BL} .

Case II: Initial Date JD 2,439,796.735 (November 2, 1967; 5^h.64 GMT)

Method of determining initial date. In the previous chapter, the case in which $\psi_0 = 180^\circ$ exhibited a stable motion for a period of 2500 days. The initial orientation of that model was such that the sun, moon, and earth were along the same line in that order. It would be of interest to determine the

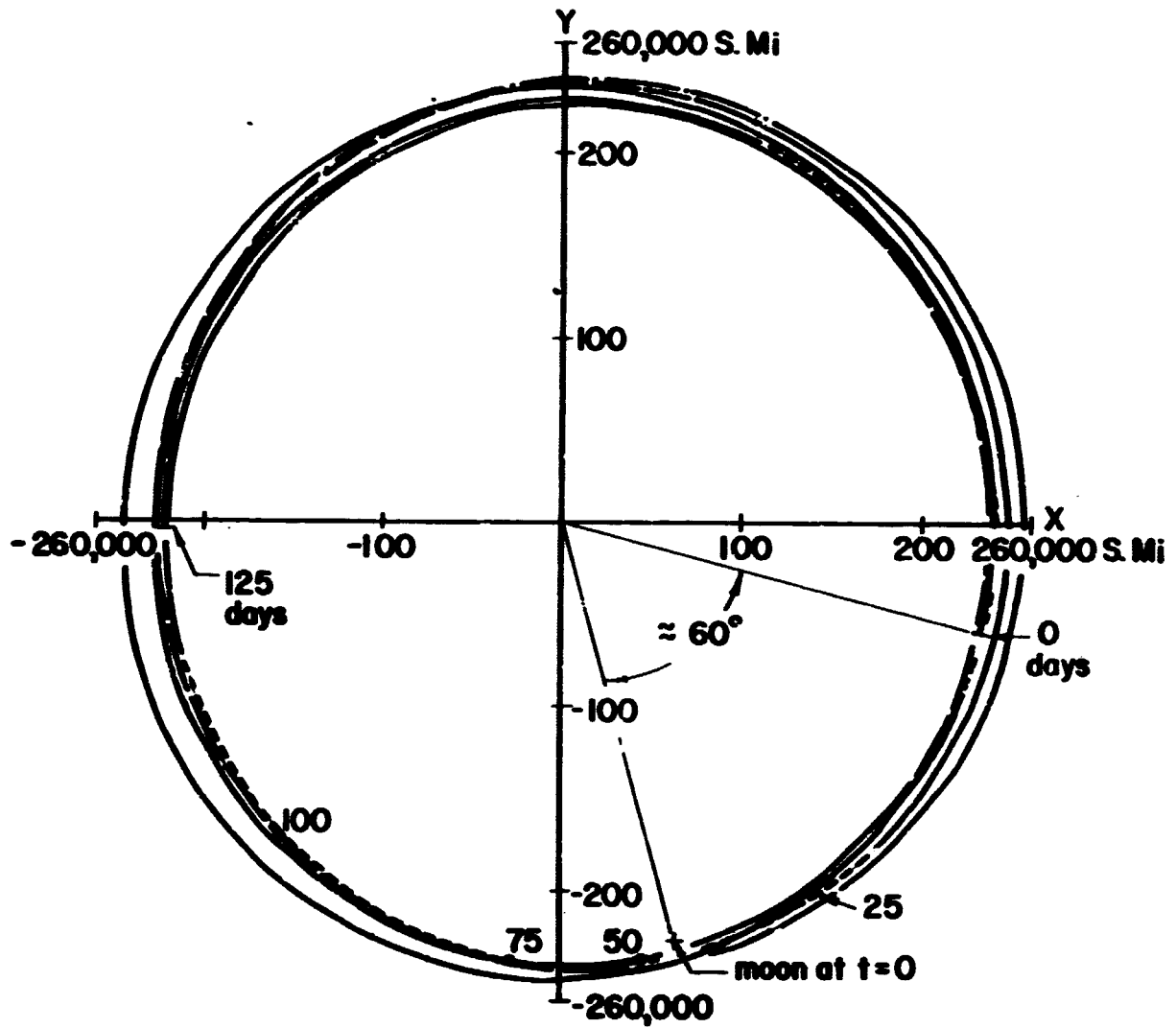


FIGURE 33a. L_4 NONROTATING (X, Y)-RESULTS FOR INITIAL
 JD 2439501.0 AND $i_{BL} = 0$ FROM 0 DAYS TO 125 DAYS

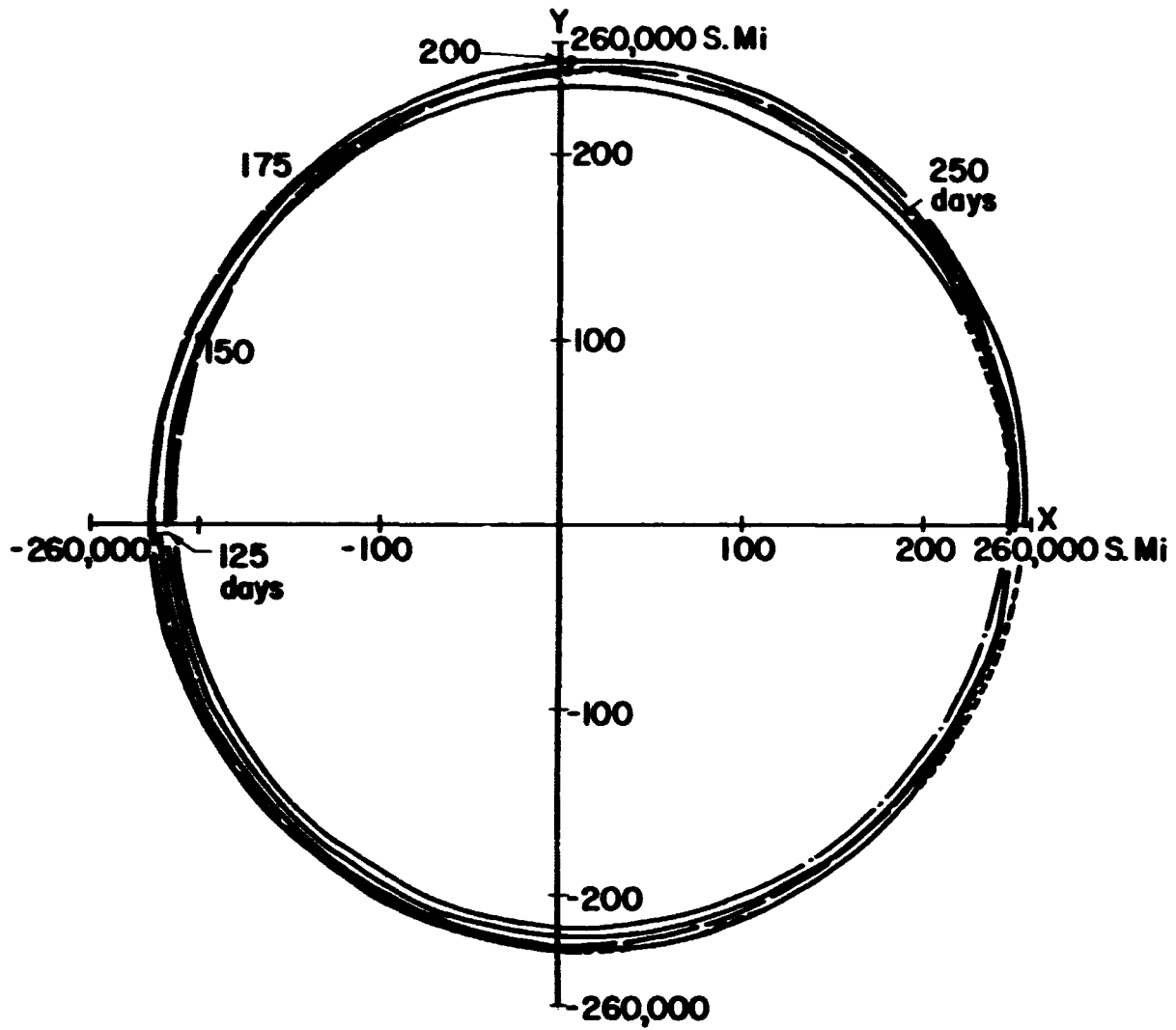


FIGURE 33b. L_4 NONROTATING (X, Y)-RESULTS FOR INITIAL
 JD 2439501.0 AND $t_{BL}=0$ FROM 125 DAYS TO 250 DAYS

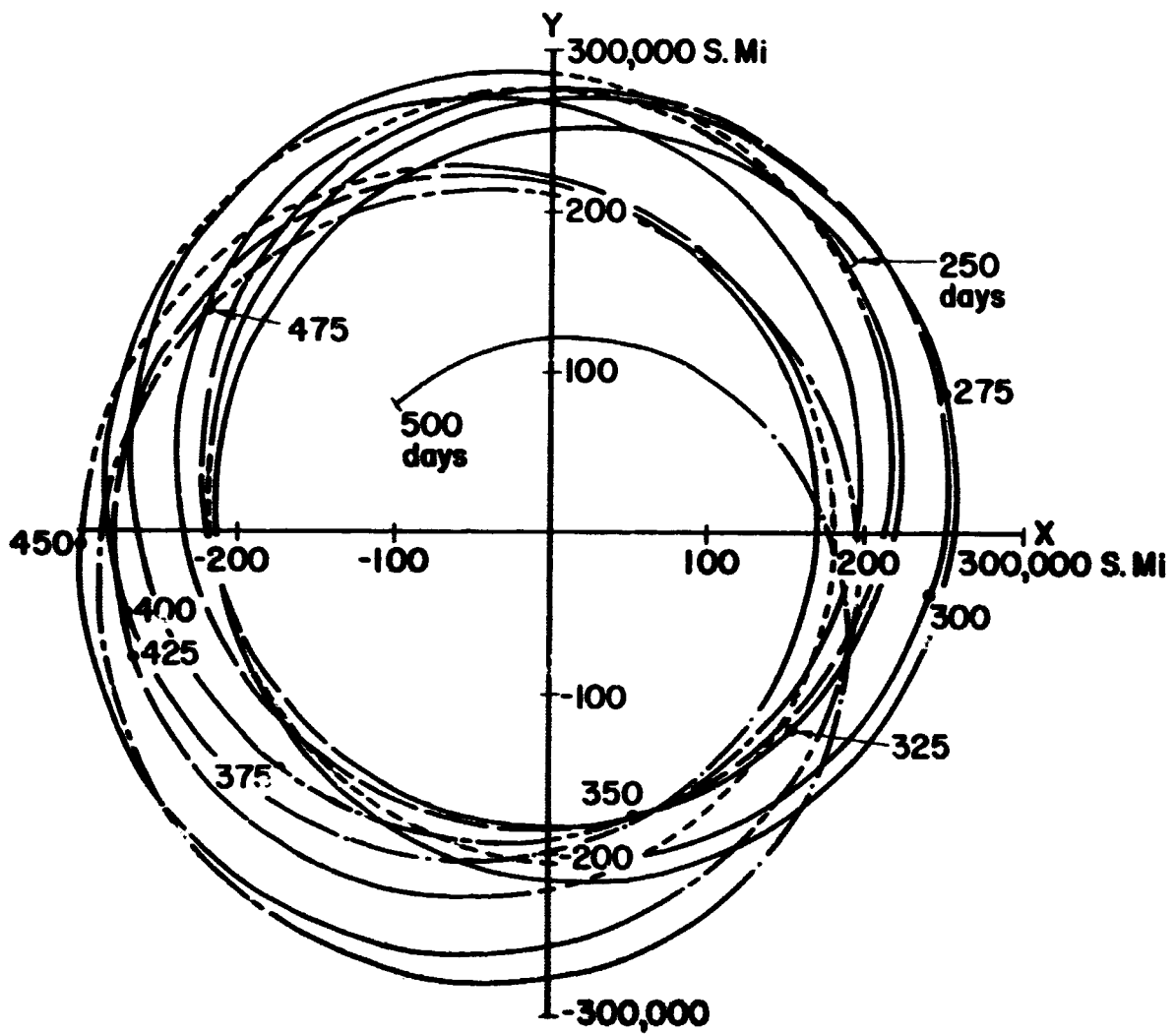


FIGURE 33c. L_4 NONROTATING (X, Y)-RESULTS FOR INITIAL
 JD 2439501.0 AND $r_{BL} = 0$ FROM 250 DAYS TO 500 DAYS

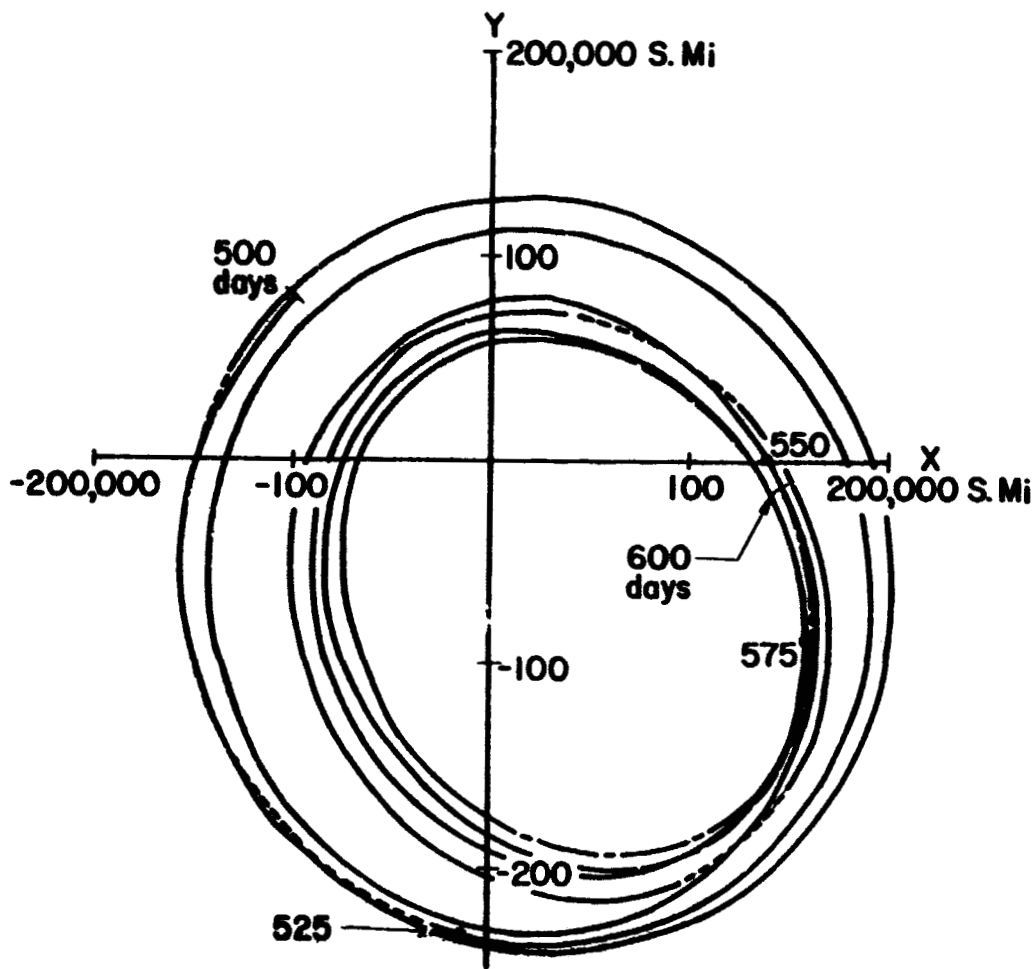


FIGURE 33d. L_1 NONROTATING (X, Y)-RESULTS FOR INITIAL
 JD 2439501.0 AND $\dot{r}_{BL}=0$ FROM 500 DAYS TO
 600 DAYS

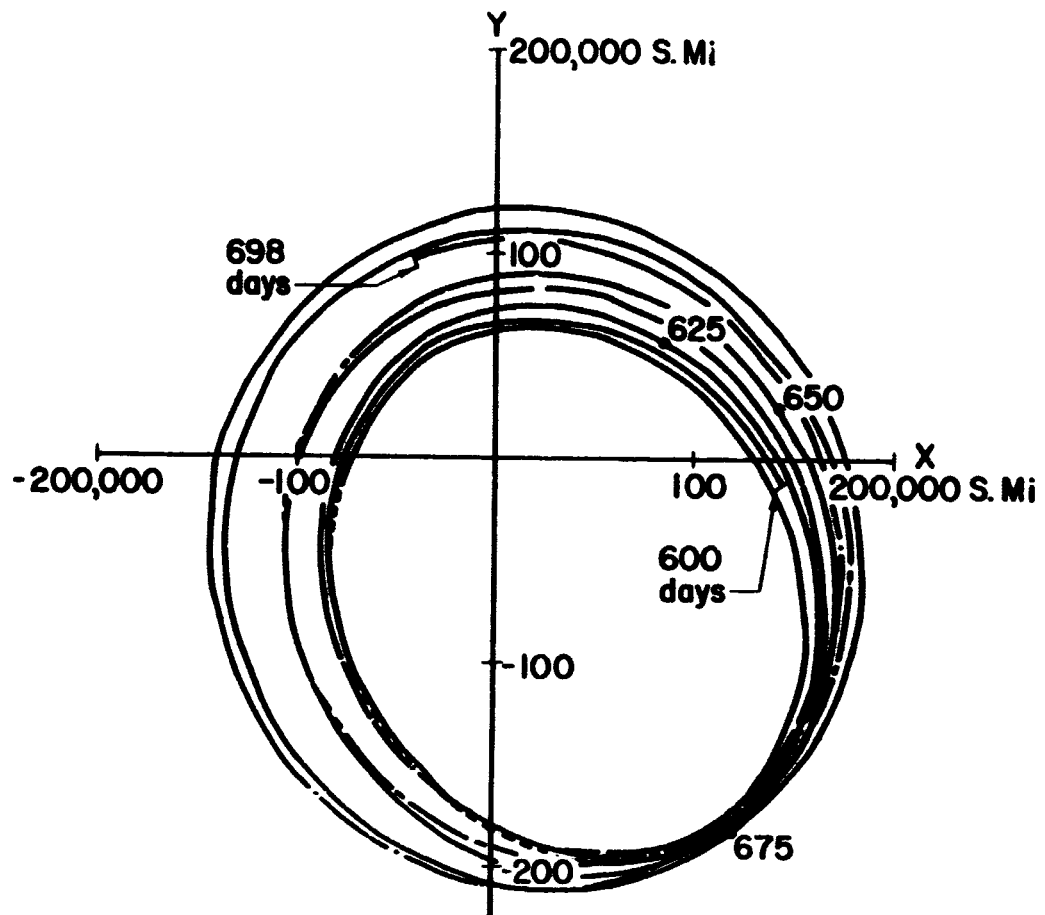


FIGURE 33e. L_4 NONROTATING (X, Y)-RESULTS FOR INITIAL JD 2439501.0 AND $\dot{r}_{BL} = 0$ FROM 600 DAYS TO 698 DAYS

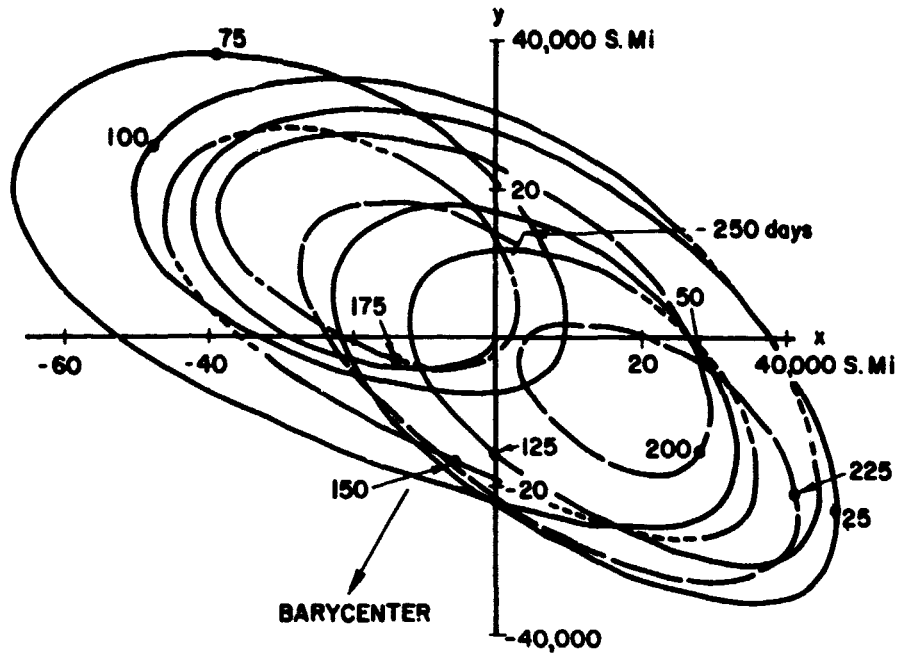


FIGURE 34a. L_4 ROTATING (x, y) -RESULTS FOR INITIAL JD 2439501.0 AND $\dot{r}_{BL}=0$ FROM 0 DAYS TO 250 DAYS

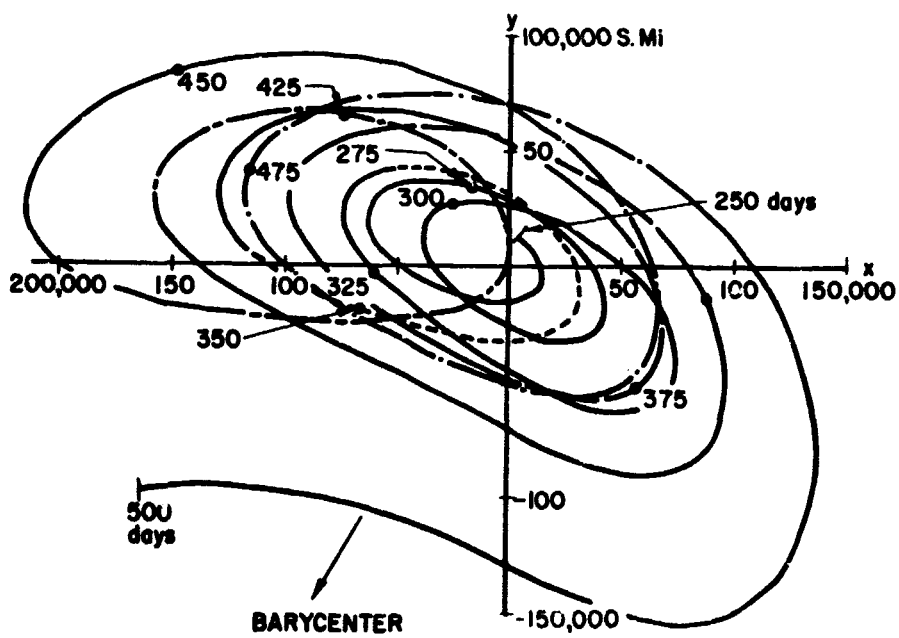


FIGURE 34b. L_4 ROTATING (x, y) -RESULTS FOR INITIAL JD 2439501.0 AND $\dot{r}_{BL}=0$ FROM 250 DAYS TO 500 DAYS

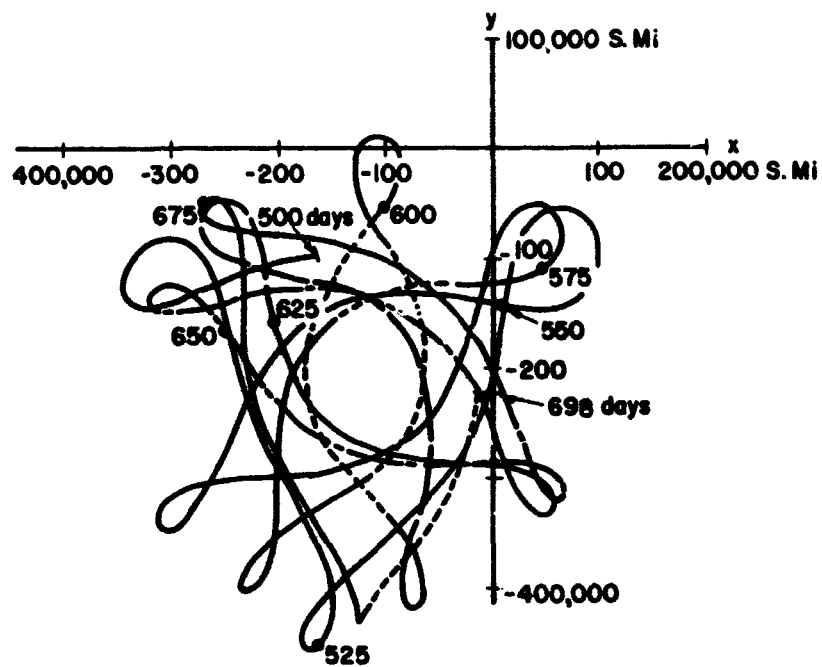


FIGURE 34c. L_4 ROTATING (x, y) -RESULTS FOR INITIAL JD 2439501.0 AND $\dot{\phi}_{BL}=0$ FROM 500 DAYS TO 698 DAYS

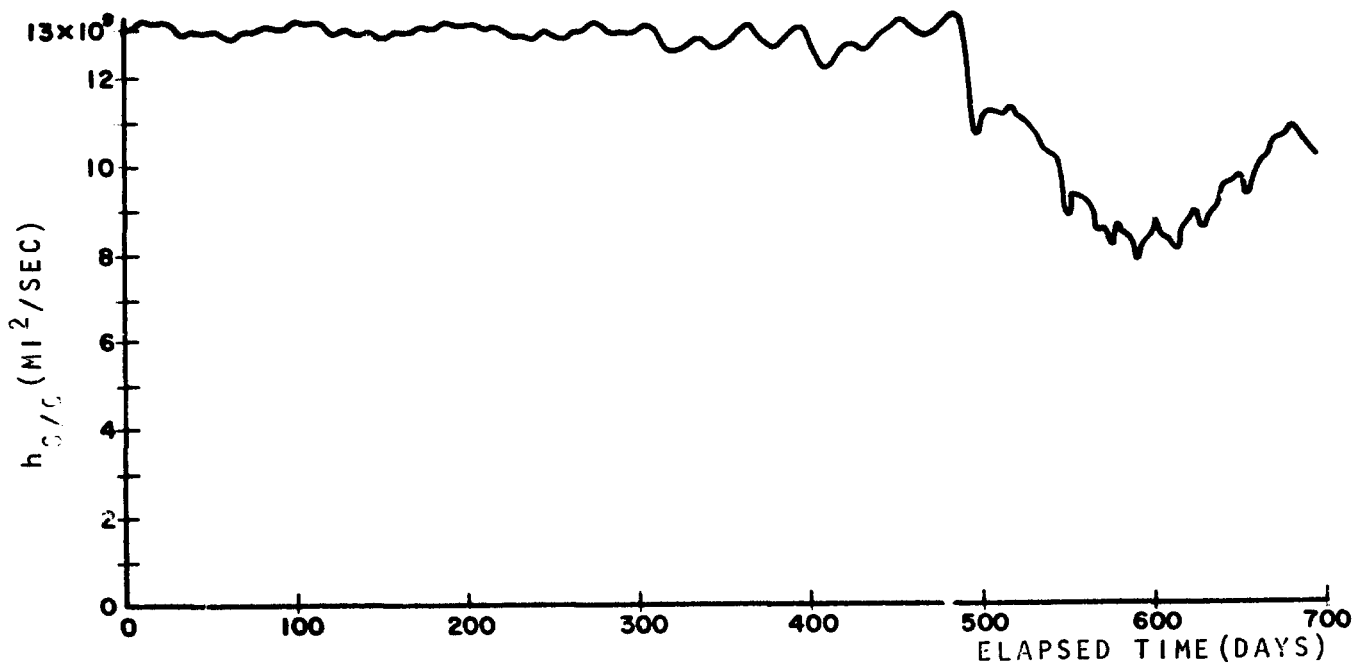


FIGURE 35. MAGNITUDE OF SPACECRAFT ANGULAR MOMENTUM VECTOR RELATIVE TO THE BARYCENTER VS. TIME FOR INITIAL JD 2439501.0 AND $\dot{r}_{BL}=0$

resultant motion in the model of this chapter with that initial orientation. Note that this initial orientation corresponds to either the orientation during a solar eclipse or of new moon. However, the earth, moon, and sun will not, in general, be exactly colinear. Furthermore, one can approximate the colinear orientation with the solar eclipse better than with the new moon orientation. It is possible for the earth, moon, and sun to be colinear during either a total or an annular eclipse. This cannot occur with the new moon orientation unless a solar eclipse also occurs. The eclipse will be annular or total depending almost entirely on how far the moon is from the earth. With these considerations, it was decided to use the solar eclipse orientation to approximate the $\psi_0 = 180^\circ$ case of the previous chapter. In addition, the solar eclipse chosen must be one in which the sun is at the ascending node, i. e., the sun is moving into the northern hemisphere of the earth-moon orbital plane. This is the situation for $\psi_0 = 180^\circ$ in the previous chapter. To facilitate matters, it was necessary to choose a date on the ephemeris tape which is near the beginning of that tape. A list of solar eclipses can be found in Ref. 3. During the year 1967 (the first year on the ephemeris tape used), two solar eclipses occur, viz., May 9 and November 2. The May 9 eclipse occurs when the sun is at the descending node, however, the November 2 eclipse occurs when the sun is at the ascending node.

As stated previously, when solar eclipses occur, the centers of the sun, the moon, and the earth are not, in general, precisely along the same line. However, an eclipse--total, annular, or partial--can occur when these bodies are not along the same line. To simulate as accurately as possible the initial orientation of the $\psi_0 = 180^\circ$ case in the previous chapter, it was necessary to determine when the sun, the moon, and the earth were

approximately colinear. Since three points define a plane, one can define an earth-moon-sun plane. Extending the sun-moon line past the earth, there will be a perpendicular distance between the terrestrial center and the sun-moon line (see Fig. 36). This perpendicular distance, d , can be determined by first noting that

$$r_{\oplus}^2 = r_{\oplus\ominus}^2 + r_{\ominus\odot}^2 - 2r_{\oplus\ominus}r_{\ominus\odot}\cos\alpha$$

where r_{\oplus} , $r_{\oplus\ominus}$, and $r_{\ominus\odot}$ are known at any instant of time since the coordinates of the sun, the moon, and the earth are known at any time from the ephemeris tapes. Then

$$\cos\alpha = \frac{-r_{\oplus}^2 + r_{\oplus\ominus}^2 + r_{\ominus\odot}^2}{2r_{\oplus\ominus}r_{\ominus\odot}} = \frac{x + r_{\ominus\odot}}{r_{\oplus\ominus}} \quad (70)$$

where x is the distance from the moon to the point of intersection, P , of the line from the earth which is perpendicular to the sun-moon line (see Fig. 36).

Then

$$x = r_{\oplus\ominus}\cos\alpha - r_{\ominus\odot}$$

$$d = (r_{\oplus}^2 - x^2)^{1/2}$$

where $\cos\alpha$ is given by Eq. (70).

A program was written to compute the distance d in addition to the latitude and longitude of the sun and moon as measured in the (X, Y, Z) -coordinate system. This information was computed at .01 day increments beginning at Julian Date 2,439,795.5 (November 1, 1967; 0^h GMT). At this date the distance d is 67,646 miles. The moon is .7^o above the (X, Y) -plane and the sun is .00166^o above that plane. Since d is so large, obviously the

longitude of the sun and moon are quite different. The moon is, in fact, at a longitude of 200° measured from the X-axis in the (X, Y)-plane; the sun is at a longitude of 217.6° . At Julian Date 2,439,796.0, d is 40,787 miles while the latitude and longitude of the moon are, respectively, $.0135^{\circ}$ and 207.6° . The latitude of the sun is $.00168^{\circ}$ and longitude is 218.1° . Note that the latitude of the moon is decreasing while that of the sun is increasing. From the earth-moon orbital plane, the sun will appear to be quite near to this orbital plane, but moving in a direction which will take it into the northern hemisphere of the plane. This is the aforementioned condition that the sun be at the ascending node. The distance d is plotted in Fig. 37 for the period from Julian Date 2,439,796.7 to Julian Date 2,439,796.78. As expected, the sun-moon line does not pass through the center of the earth. However, the minimum distance which d attains is approximately at Julian 2,439,796.735 (see Fig. 37). At this time, the latitude of the moon is -1° with a longitude of 218° . The solar latitude is $.0017^{\circ}$ and a longitude of 218° . It is of interest to note that the length of the moon's umbral cone is approximately 231,000 miles during this eclipse orientation. The diameter of this cone at the earth's distance is approximately 800 miles or radius of 400 miles. However, the earth center is approximately 3950 miles from the sun-moon line. The radius of the earth is approximately 3960 miles, therefore, a locus of points on the surface of the earth will be along the sun-moon line, and, furthermore, these are in the umbra. Therefore, a total solar eclipse has occurred, confirming the data in Ref. 3.

Orientation of the solar system and the earth-moon system. The orientation of the solar system on the chosen initial date of Julian Date 2,439,796.735 or November 2, 1967, 5.64 hours Greenwich Mean Time, is

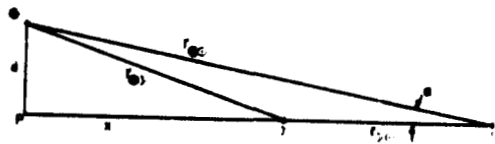


FIGURE 36. DETERMINATION OF d

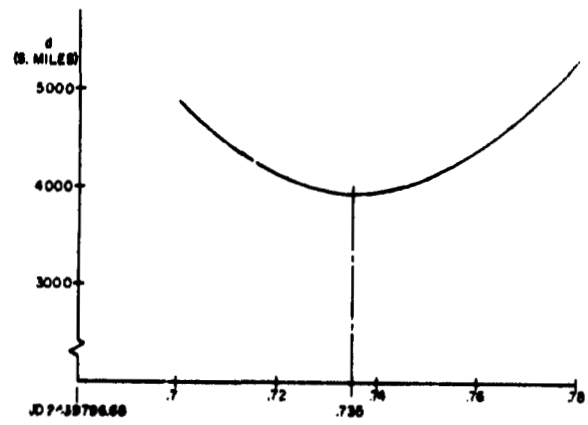


FIGURE 37. d VS. TIME FOR JD 2439796.68 TO JD 2439796.70

shown in Fig. 38. For this initial date, the inclination, i^* , between the Ecliptic of the Epoch 1950 and the instantaneous earth-moon orbital plane is 5.28° , the longitude of the ascending node, Ω^* , is 27.7° , and the angle θ^* locating the moon in the orbital plane is 191.1° . The distance between the earth and the moon at insertion, r_{\oplus} , is 221,825.7 miles. The lunar velocity component in the radial direction, $\bar{r}_{B\oplus}$, is 196.25 miles/day and the lunar velocity component $r_{B\oplus}\dot{\theta}^*$ is 58,480.5 miles/day. Also, ξ_p is 108,217.6 miles and η_p is 192,106.7 miles. The lunar in-plane angular velocity, $\dot{\theta}^*$, is $15.3^\circ/\text{day}$ and the barycenter-sun distance, $r_{B\odot}$, is 92,236,915 miles. The variation of Ω^* and i^* with time are shown in Figs. 25 and 26, respectively, where Julian Date 2,439,795.735 is at 295 days elapsed time from Julian Date 2,439,501.0.

Note that the moon is slightly past perigee since $\dot{r}_{B\oplus}$ is positive. Therefore, although the initial orientation of the sun, the moon, and the earth is such that it very nearly coincides with that of $\psi_0 = 180^\circ$ in the previous chapter, the earth-moon distance for Julian Date 2,439,796.735 is approximately 20,000 miles less than the $\psi_0 = 180^\circ$ case.

Initial conditions and results in nonrotating and rotating coordinate systems for spacecraft placement at L_4 . The velocity component \dot{r}_{BL} is included in this case and is 197.5 miles/day. The in-plane tangential velocity component of L_4 , $r_{BL}\dot{\theta}^*$, is 58,843.5 miles/day. The distance from the barycenter to L_4 is 220,490 miles. The initial position and velocity of the spacecraft is assumed to be zero relative to the (x, y, z)- L_4 -centered coordinate system. Thus, the initial (X, Y, Z)-position and velocity of the spacecraft were computed from Eqs. (C-3) and C-10), and were

$$\begin{array}{ll}
 X_S = 35,641 \text{ mi} & \dot{X}_S = 58,047 \text{ mi/day} \\
 Y_S = 216,735 \text{ mi} & \dot{Y}_S = 9,497 \text{ mi/day} \\
 Z_S = 19,279 \text{ mi} & \dot{Z}_S = 1,719 \text{ mi/day}
 \end{array}$$

Equations (67) were numerically integrated as in Case I. The initial step size was .2 days which was subsequently halved about 100 days later.

The results of the integration are shown in Figs. 39. Note how the orbit changes with each revolution around the barycenter in Fig. 39c. In Figs. 39c, it can be seen that the spacecraft is in a near elliptical orbit with a radius of closest approach to the barycenter of approximately 70,000 miles. This sudden change in the orbit is caused by a close lunar pass between 579 days and 580 days. The absolute value of the Z-component of spacecraft displacement does not exceed 30,000 miles.

The motion as it appears in the rotating (x, y, z)-coordinate system is shown in Figs. 40. Figure 40b exhibits an unusual character between 400 days and 450 days. In Fig. 40c it is seen that the spacecraft has begun an entirely different type of motion than in the 0 to 500 day period. The spacecraft has left the libration-point-centered motion and, as indicated by the (X, Y)-data, experiences a close pass of the moon between 579 days and 580 days. The absolute value of the z-component of displacement does not exceed 3000 miles during the stable motion; it does not exceed 20,000 miles during the unstable period (after about 575 days).

The magnitude of the angular momentum vector relative to the barycenter is shown in Fig. 41. Note the sudden decrease in angular momentum between 579 to 580 days during the lunar pass. This was observed also in Fig. 32 for the Julian Date 2,439,501.0 case during the near lunar pass.

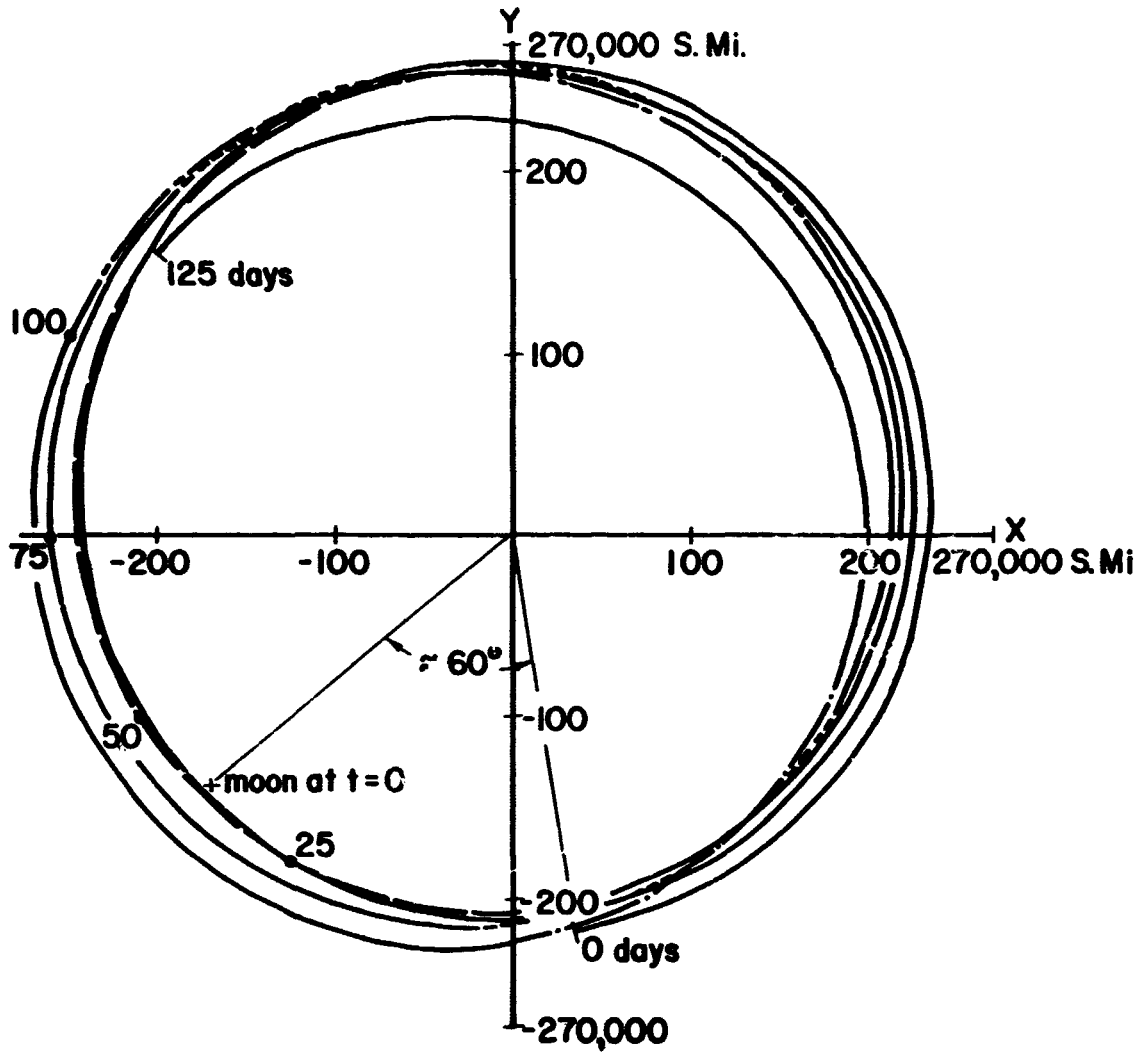


FIGURE 39a. L_4 NONROTATING (X,Y)-RESULTS FOR INITIAL
 JD 2439796.735 FROM 0 DAYS TO 125 DAYS

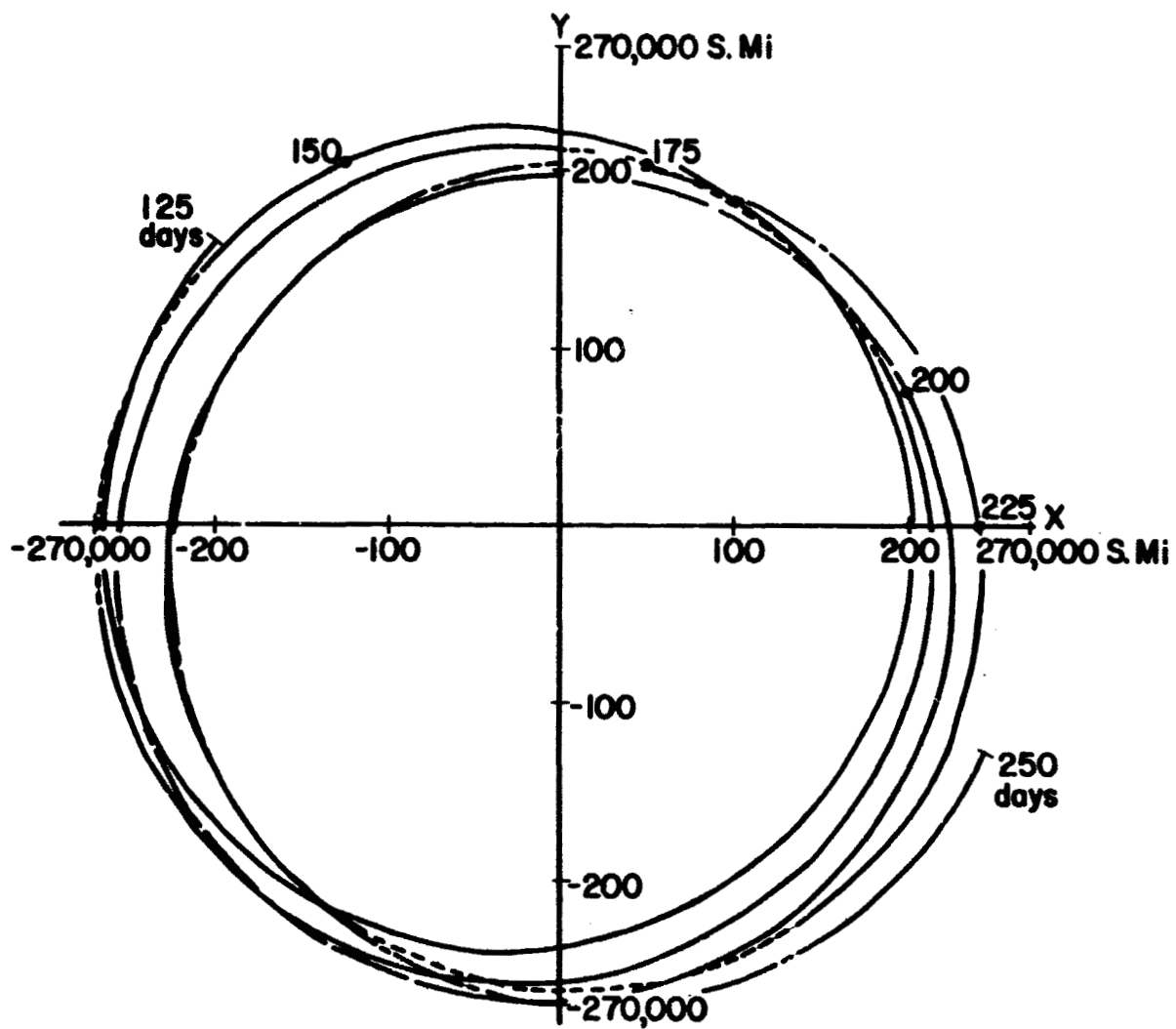


FIGURE 39b. L_4 NONROTATING (X,Y)-RESULTS FOR INITIAL
 JD 2439796.735 FROM 125 DAYS TO 250 DAYS

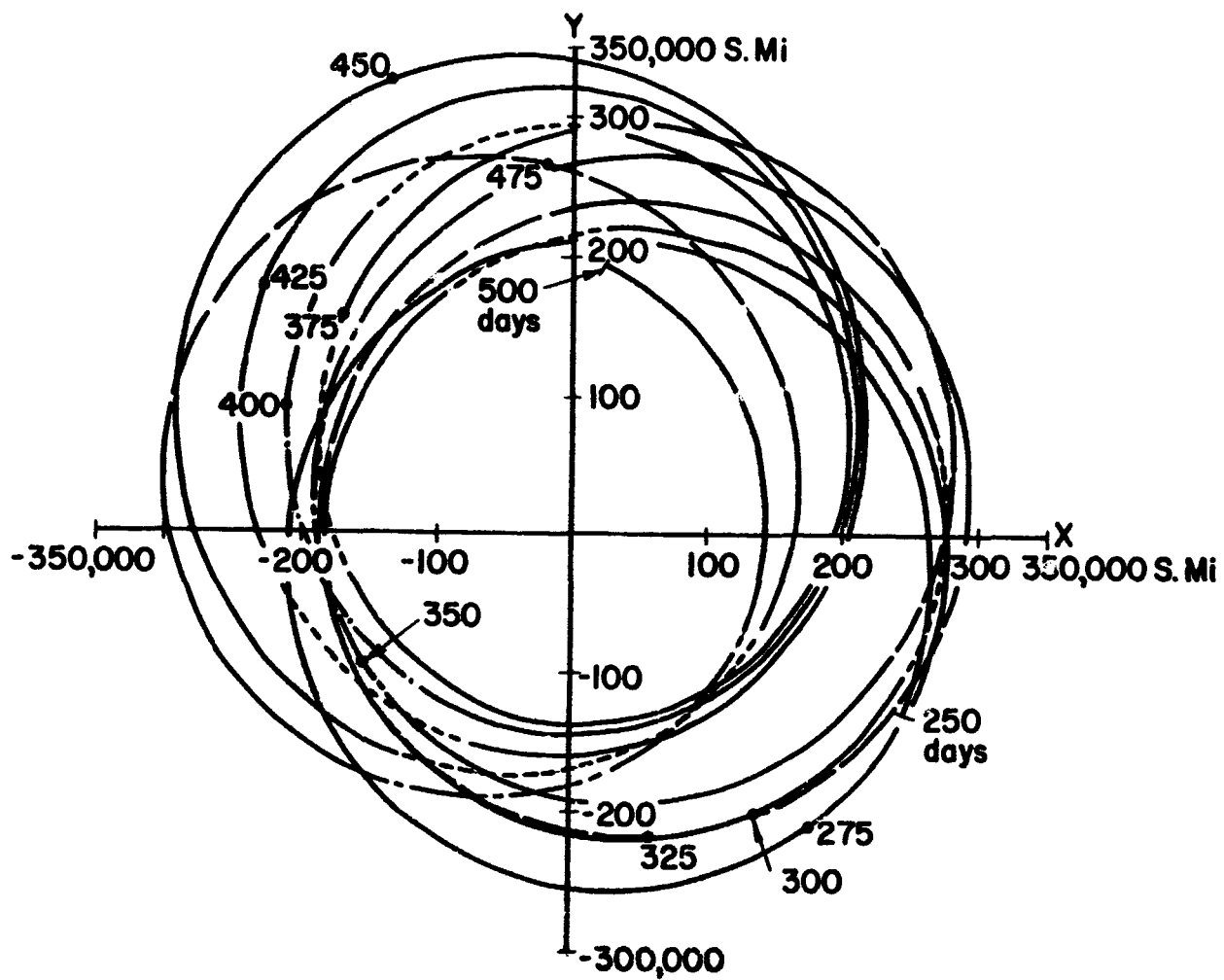


FIGURE 39c. L_4 NONROTATING (X, Y)-RESULTS FOR INITIAL
 JD 2439796.735 FROM 250 DAYS TO 500 DAYS

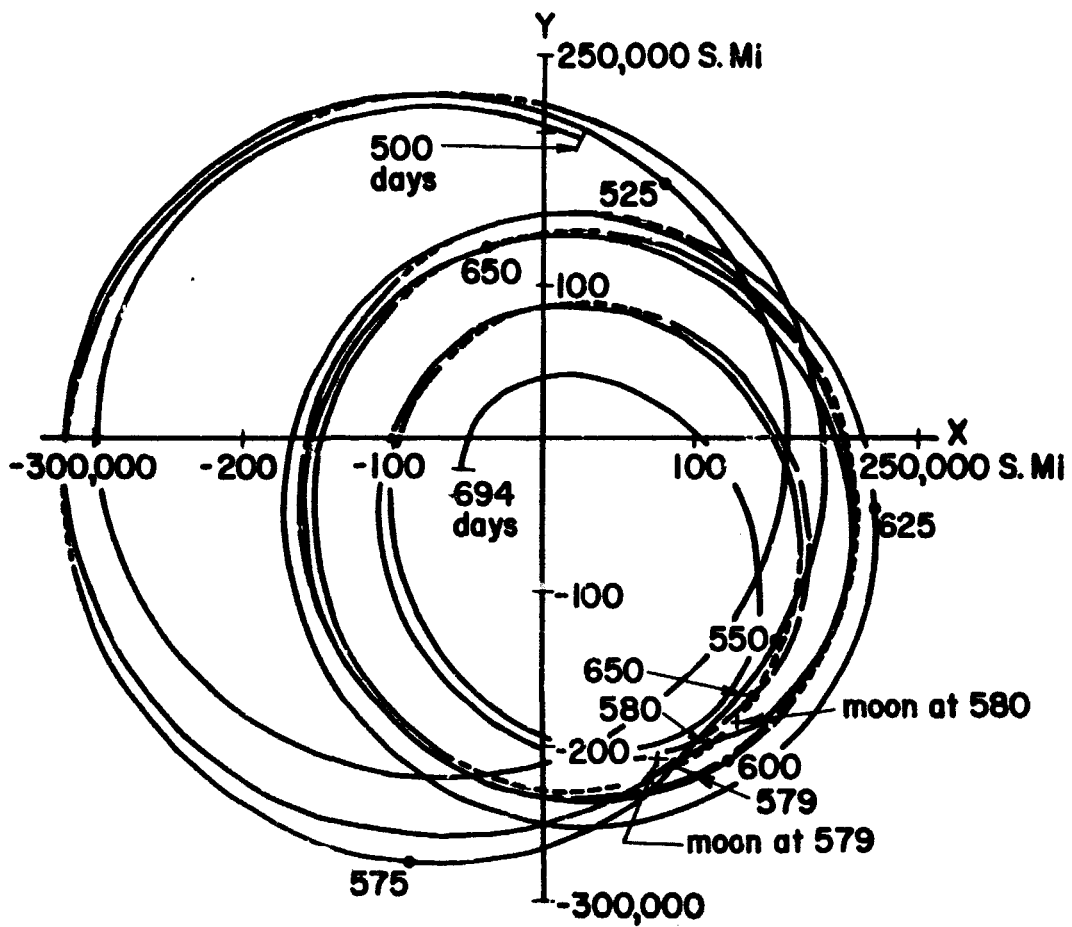


FIGURE 39d. L_4 NONROTATING (X, Y)-RESULTS FOR INITIAL JD 2439796.735 FROM 500 DAYS TO 694 DAYS

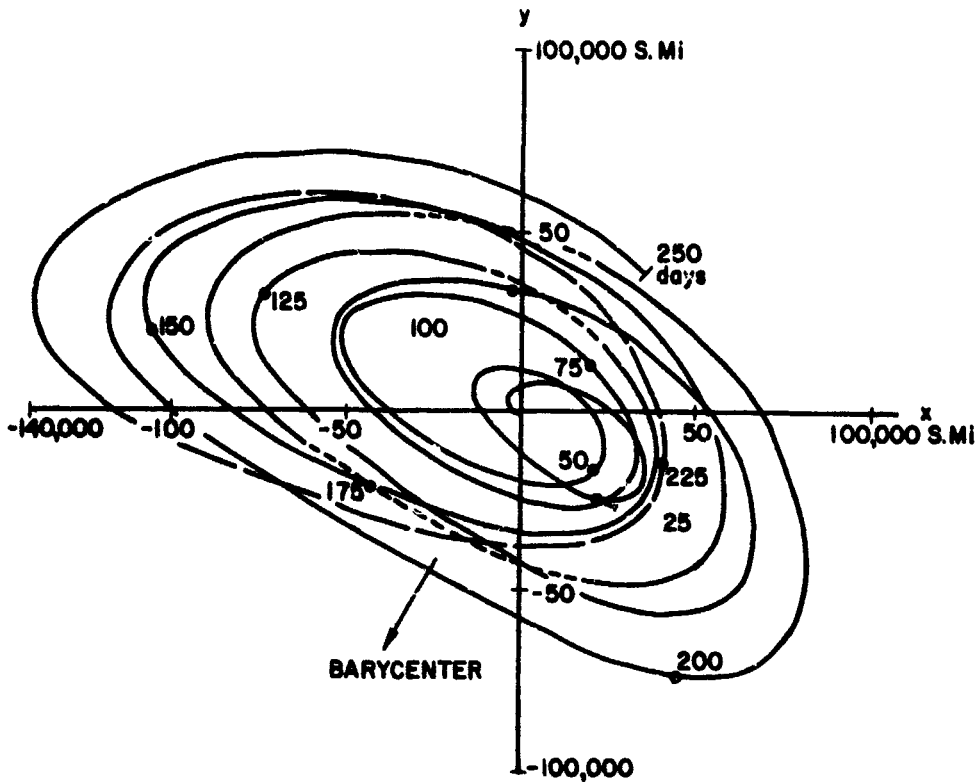


FIGURE 40a. L_4 ROTATING (x, y) -RESULTS FOR INITIAL JD 2439796.735 FROM 0 DAYS TO 250 DAYS

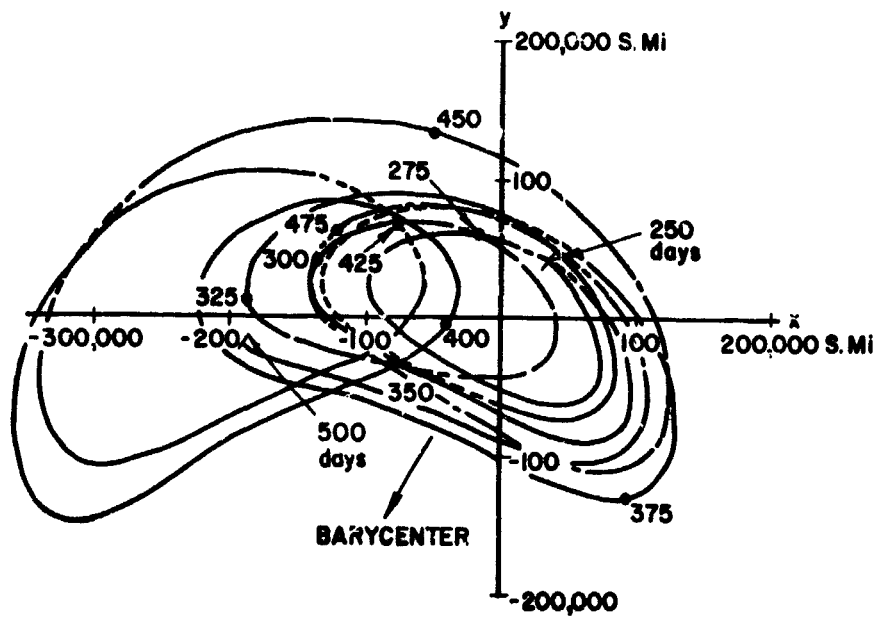


FIGURE 40b. L_4 ROTATING (x, y) -RESULTS FOR INITIAL JD 2439796.735 FROM 250 DAYS TO 500 DAYS

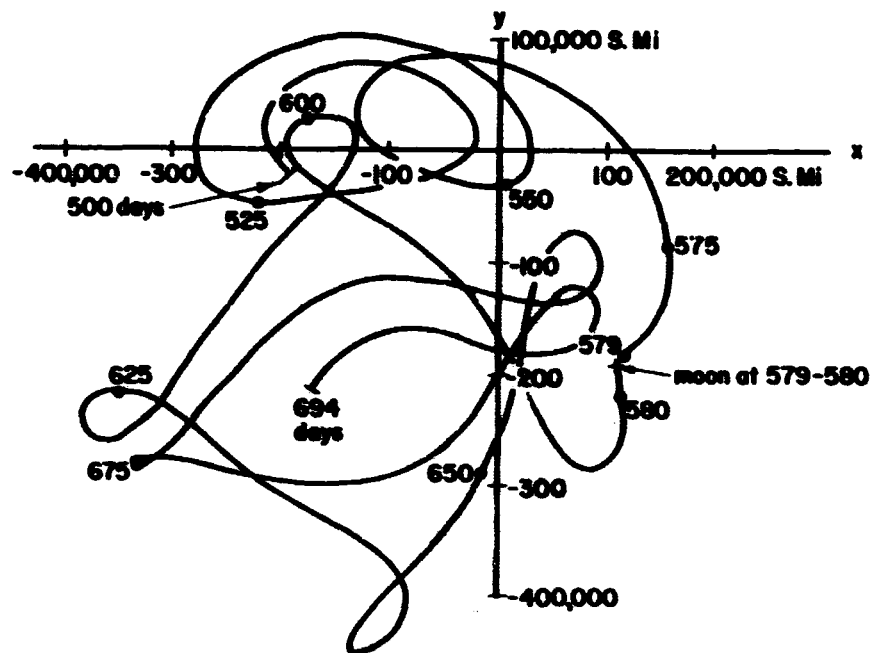


FIGURE 40c. L_4 ROTATING (x, y) -RESULTS FOR INITIAL JD 2439796.735 FROM 500 DAYS TO 694 DAYS

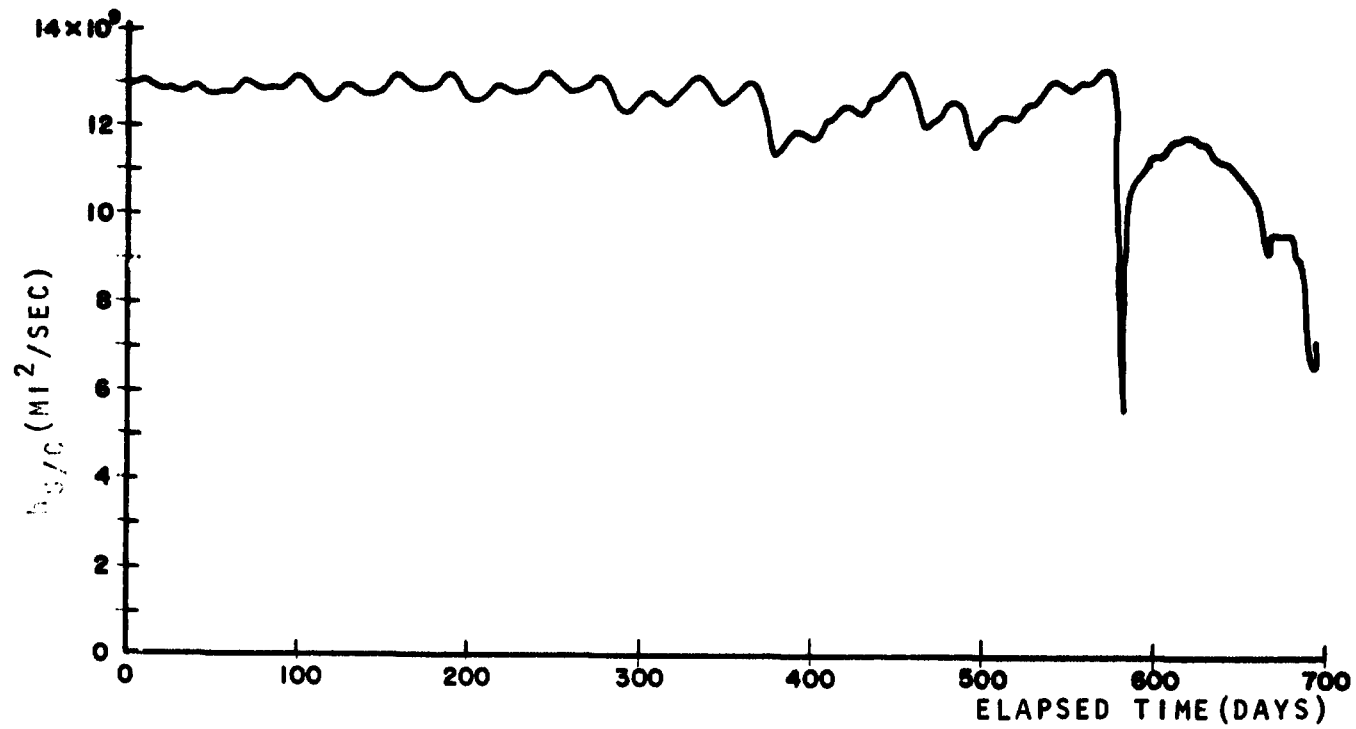


FIGURE 41. MAGNITUDE OF SPACECRAFT ANGULAR MOMENTUM VECTOR RELATIVE TO THE BARYCENTER VS. TIME FOR INITIAL JD 2439796.735

Initial conditions and results in nonrotating and rotating coordinate systems for spacecraft placement at L_5 . Using the same initial date of Julian Date 2,439,796.735, the spacecraft was assumed to be placed at L_5 with zero relative velocity. The radial velocity component \dot{r}_{BL} and the in-plane tangential velocity component, $r_{BL} \dot{\theta}^*$, is the same as for placement L_4 . The barycentered initial position and velocity are different. In this case the spacecraft is 60° behind the moon. The (X, Y, Z)-position and velocity for placement at L_5 are

$$\begin{array}{ll} X_S = -204,388 \text{ mi} & \dot{X}_S = 22,113 \text{ mi/day} \\ Y_S = 81,250 \text{ mi} & \dot{Y}_S = -54,418 \text{ mi/day} \\ Z_S = 15,445 \text{ mi} & \dot{Z}_S = -3,505 \text{ mi/day.} \end{array}$$

The initial step size used was .2 days. This was halved at 106 days and increased later. Throughout the computer run, the step size increased and again halved as required by the single step error bounds.

The results of the numerical integration are shown in Figs. 42. The computations were carried out to 2000 days, however, only the first 750 days are shown in the (X, Y)-plots. Figures 42a and 42b show the barycentered orbit for the first 250 days. For the 250 to 500 day period (Fig. 42c) the envelope of motion has expanded out considerably. It might be noted how the line joining the point of closest approach and farthest approach on each revolution rotates in a counterclockwise direction. In Fig. 42d, the orbit has contracted to a near elliptical orbit which is much the same with each revolution (period from 650 days to 750 days). After 750 days, the orbit again expands and contracts in the same manner as the 0 to 750 day period. The Z-component of displacement does not exceed 35,000 miles in the 2000-day period.

The rotating (x, y) -results are shown in Figs. 43. Note how the orbit expands to a maximum displacement from L_5 of approximately 240,000 miles (Fig. 43b) at slightly after 425 days. Note that the envelope of motion contracts in Fig. 43c and again begins to expand in Fig. 43d. The (x, y) -motion for the period from 1000 days to 2000 days is much the same. During this 2000 day period, the z-component of displacement does not exceed 10,000 miles. The expansion-contraction can be observed from Figs. 44a through 44b, the magnitude of the displacement vector from L_5 versus time. The expansion-contraction over almost three cycles is illustrated. The period of this pulsation is approximately 700 days. Thus, the motion is stable for a period of 2000 days and, in fact, one can extrapolate this to 2500 days by noting that the envelope of motion is beginning to contract at 2000 days. With a period of pulsation of 700 days, it thus appears that the motion will be stable through 2500 days.

The magnitude of the angular momentum vector relative to the barycenter is shown in Fig. 45. Note that the magnitude has only slight variations during the periods in which the spacecraft is near the L_5 point, e.g., the period from 750 days to 850 days. During periods of wide displacement from L_5 , the angular momentum varies quite noticeably.

Accuracy

It is extremely difficult to make a definite statement regarding the accuracy of the results. One can estimate the truncation error involved in the numerical integration process, however, estimation of the round-off error presents a formidable problem. As stated in the previous chapter, the Adams-Moulton-Runge-Kutta procedure was used to integrate the differential equations

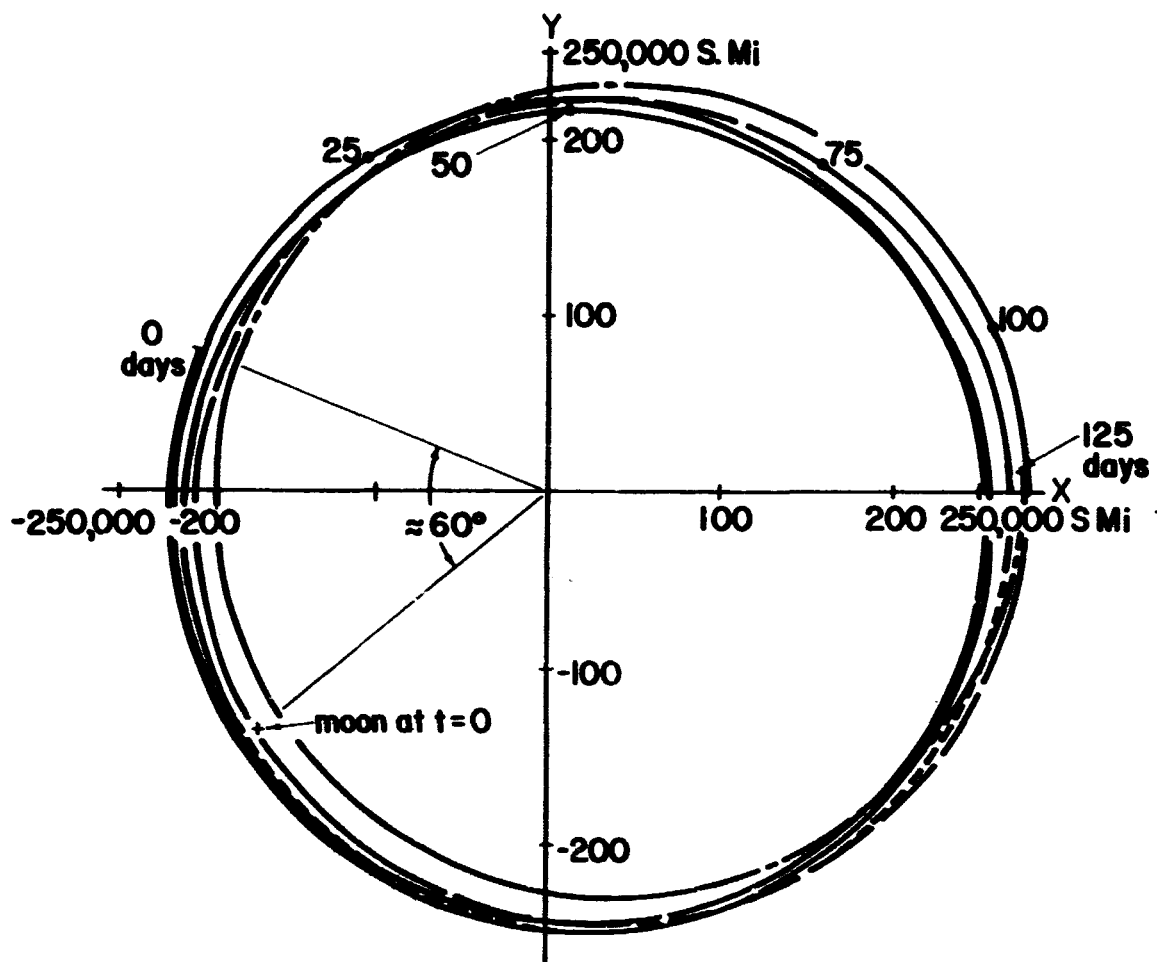


FIGURE 42a. L_5 NONROTATING (X, Y)-RESULTS FOR INITIAL JD 2439796.735 FROM 0 DAYS TO 125 DAYS

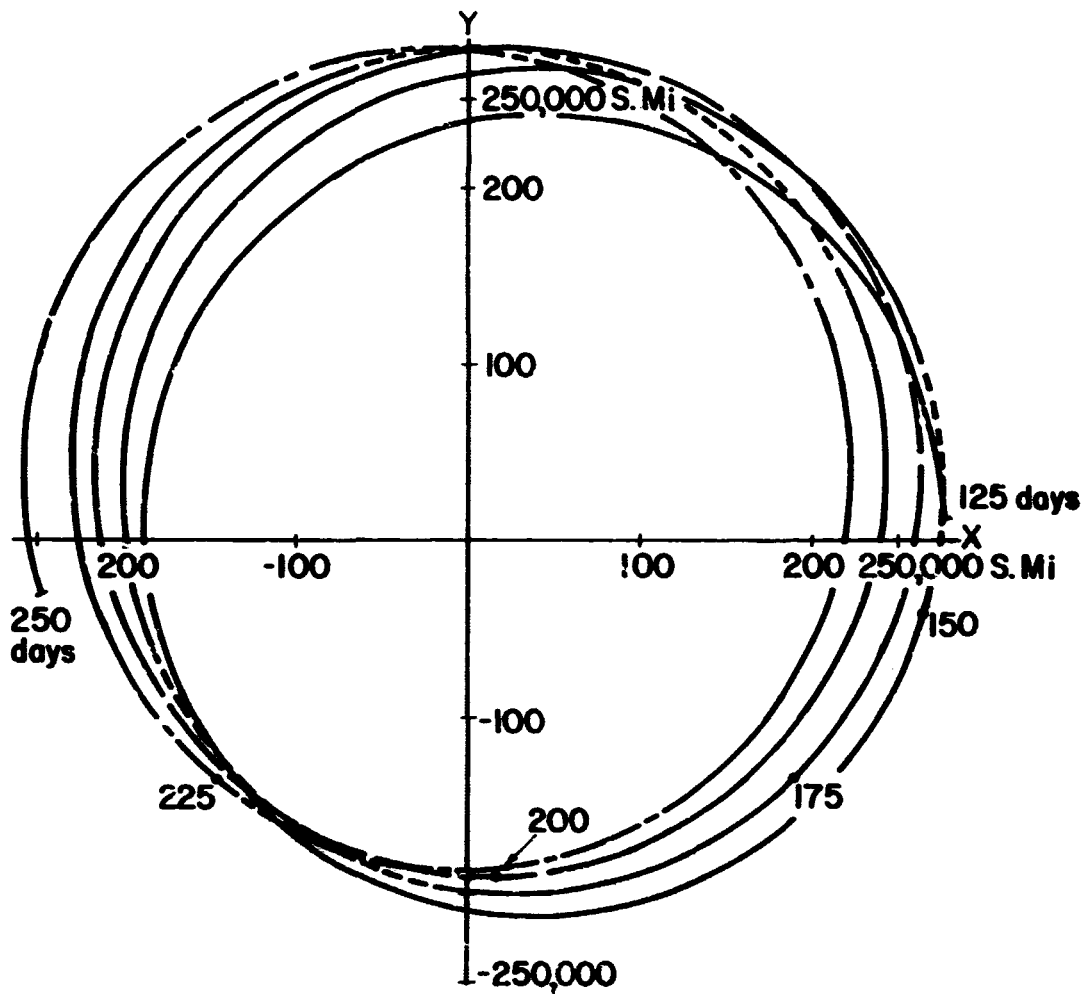


FIGURE 42b. L_5 NONROTATING (X,Y)-RESULTS FOR INITIAL JD 2439796.735 FROM 125 DAYS TO 250 DAYS

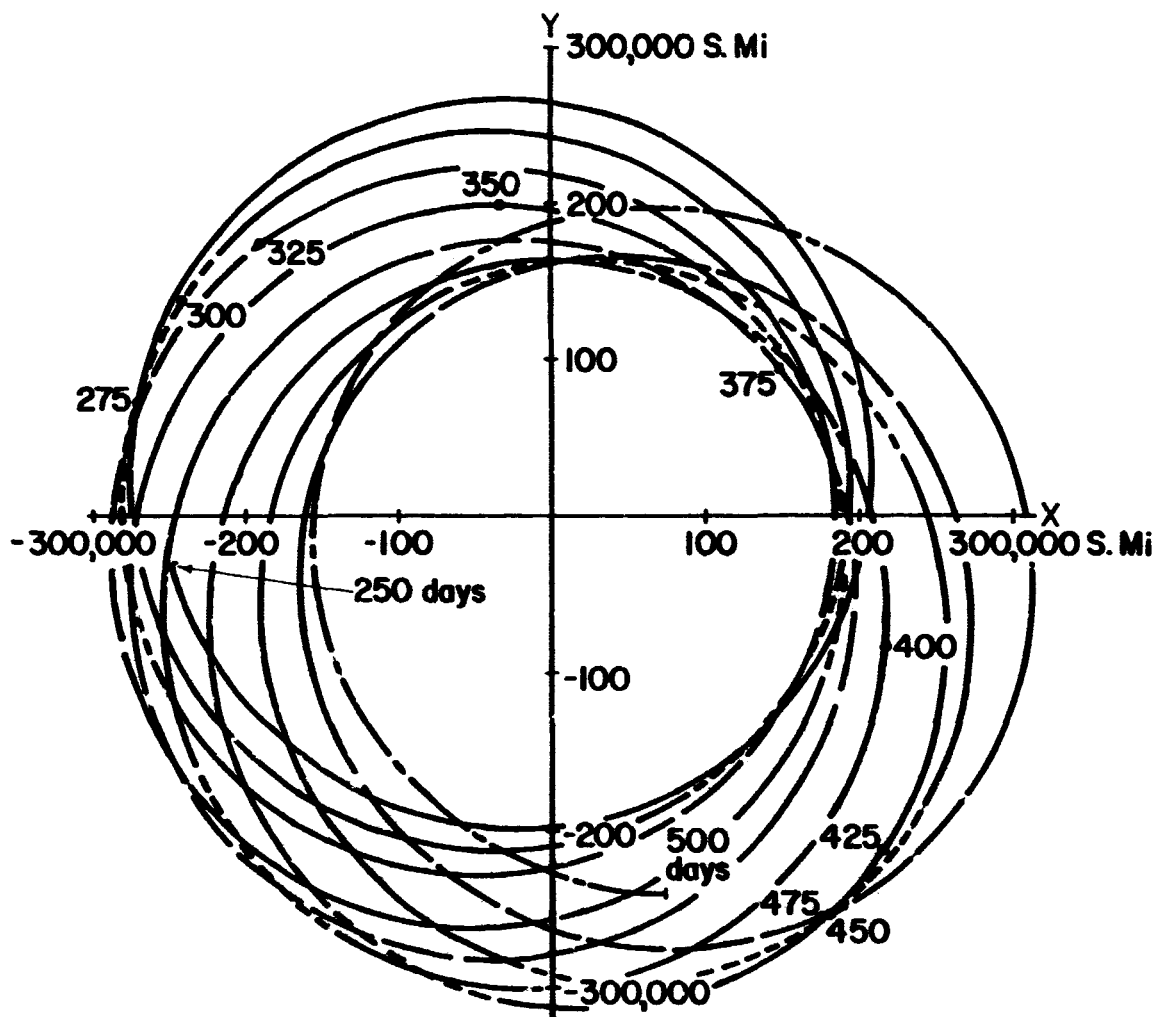


FIGURE 42c. L_5 NONROTATING (X,Y)-RESULTS FOR INITIAL
 JD 2439796.735 FROM 250 DAYS TO 500 DAYS

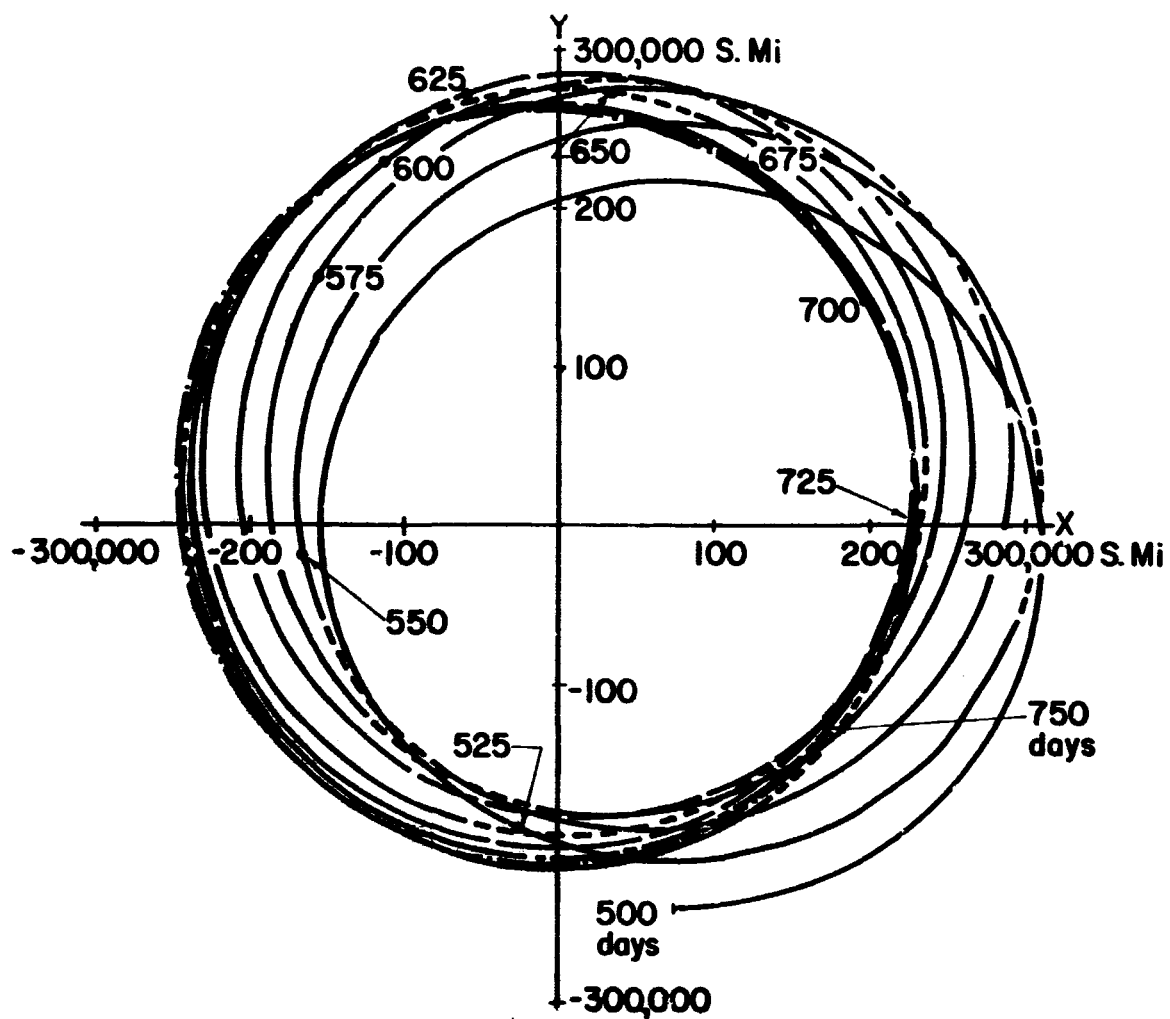


FIGURE 42d. L_5 NONROTATING (X, Y)-RESULTS FOR INITIAL JD 2439796.735 FROM 500 DAYS TO 750 DAYS

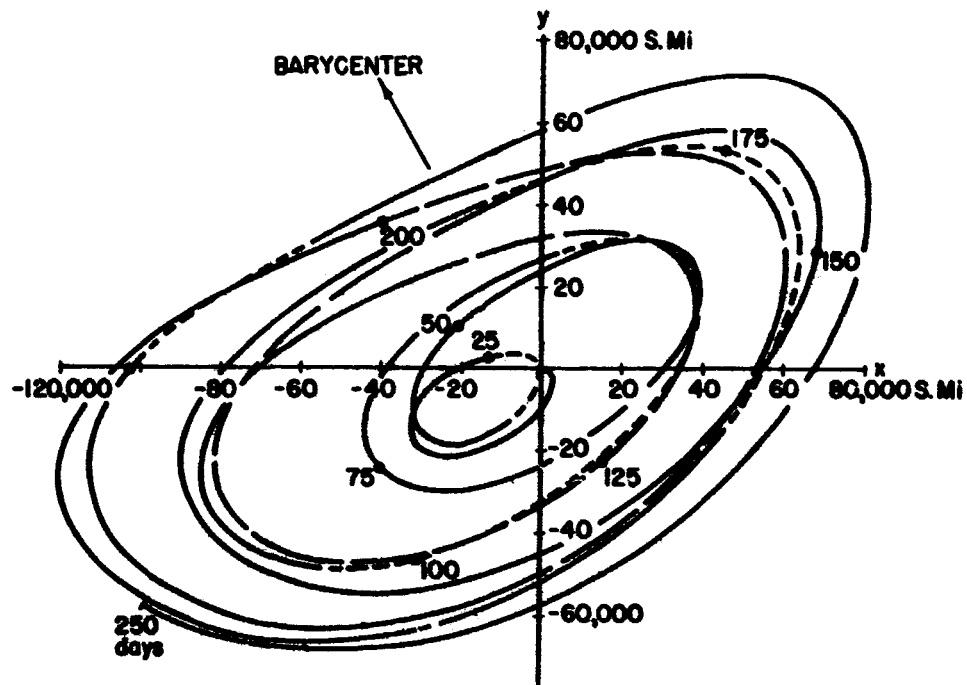


FIGURE 43a. L_5 ROTATING (x, y) -RESULTS FOR INITIAL JD 2439796.735 FROM 0 DAYS TO 250 DAYS

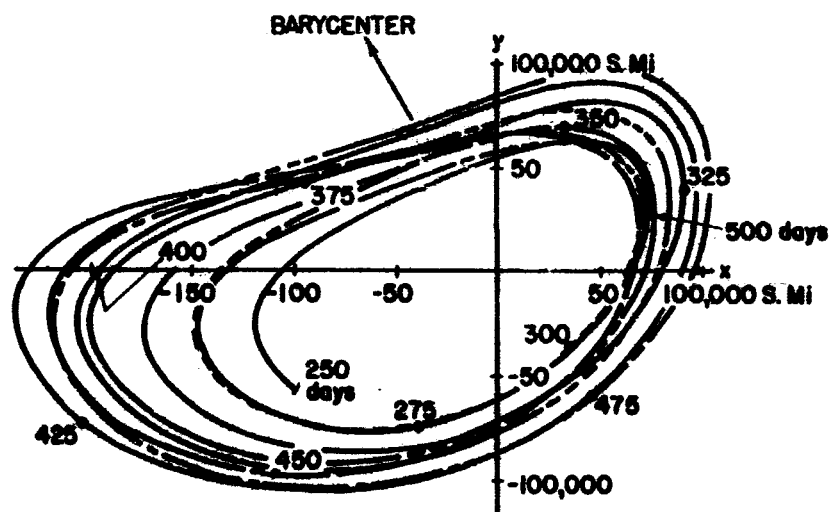


FIGURE 43b. L_5 ROTATING (x, y) -RESULTS FOR INITIAL JD 2439796.735 FROM 250 DAYS TO 500 DAYS

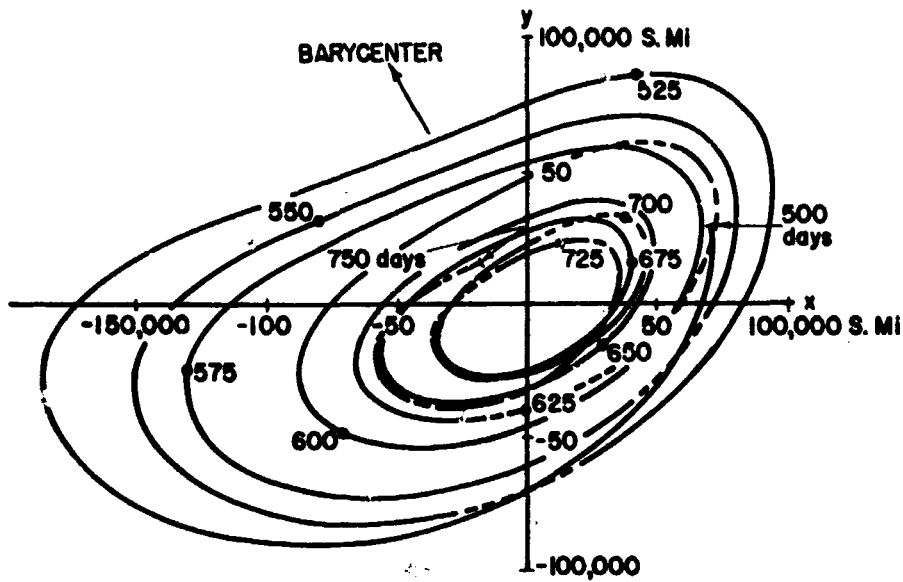


FIGURE 43c. L_5 ROTATING (x, y) -RESULTS FOR INITIAL JD 2439796.735 FROM 500 DAYS TO 750 DAYS

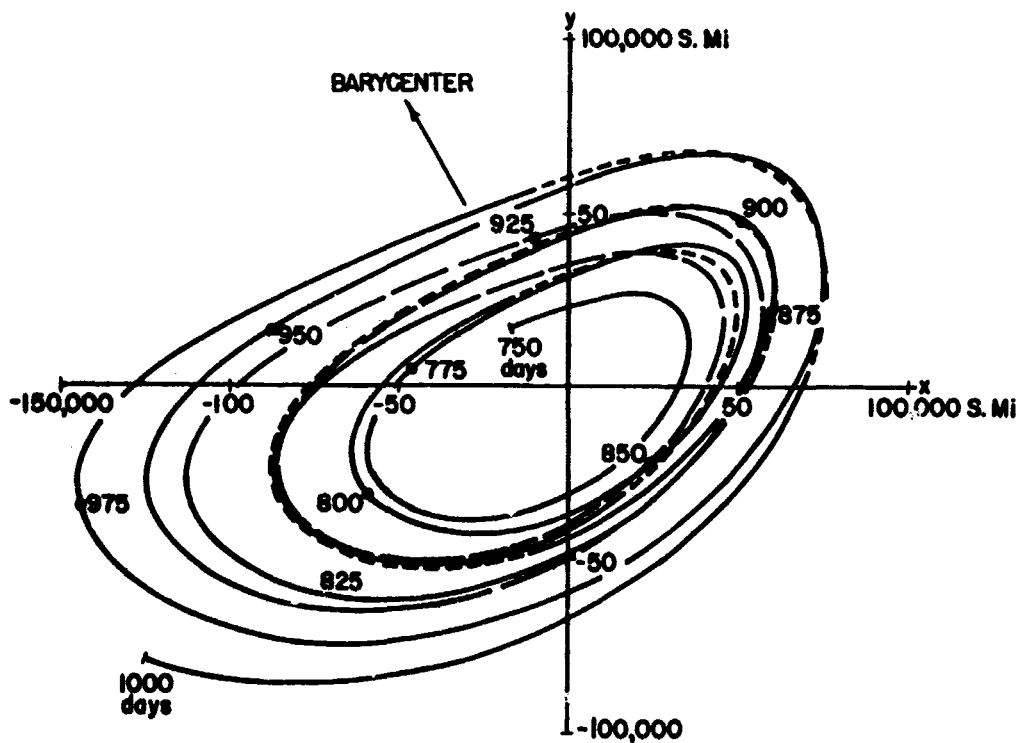


FIGURE 43d. L_5 ROTATING (x, y) -RESULTS FOR INITIAL JD 2439796.735 FROM 750 DAYS TO 1000 DAYS

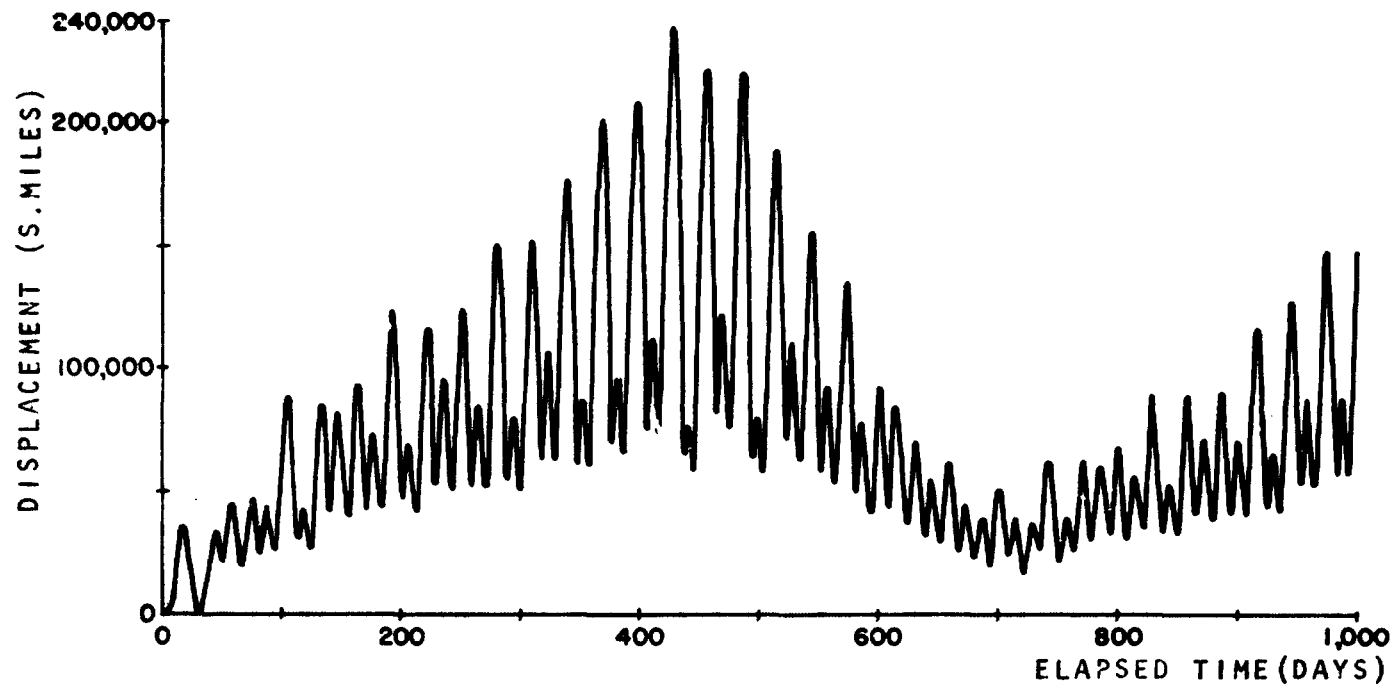


FIGURE 44a. MAGNITUDE OF DISPLACEMENT VECTOR FROM L_5 VS. TIME FOR INITIAL JD 2439796.735 FROM 0 DAYS TO 1000 DAYS

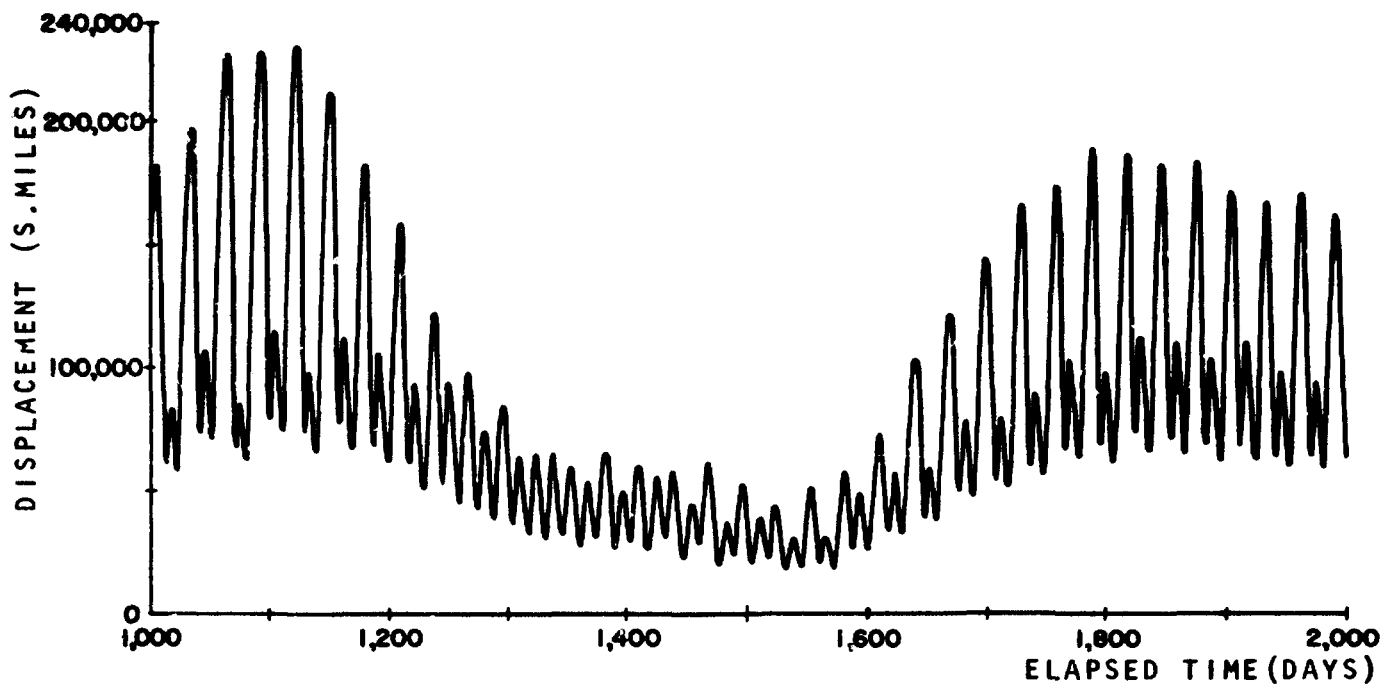


FIGURE 44b. MAGNITUDE OF DISPLACEMENT VECTOR FROM L₅ VS. TIME FOR INITIAL JD 2439796.735 FROM 1000 DAYS TO 2000 DAYS

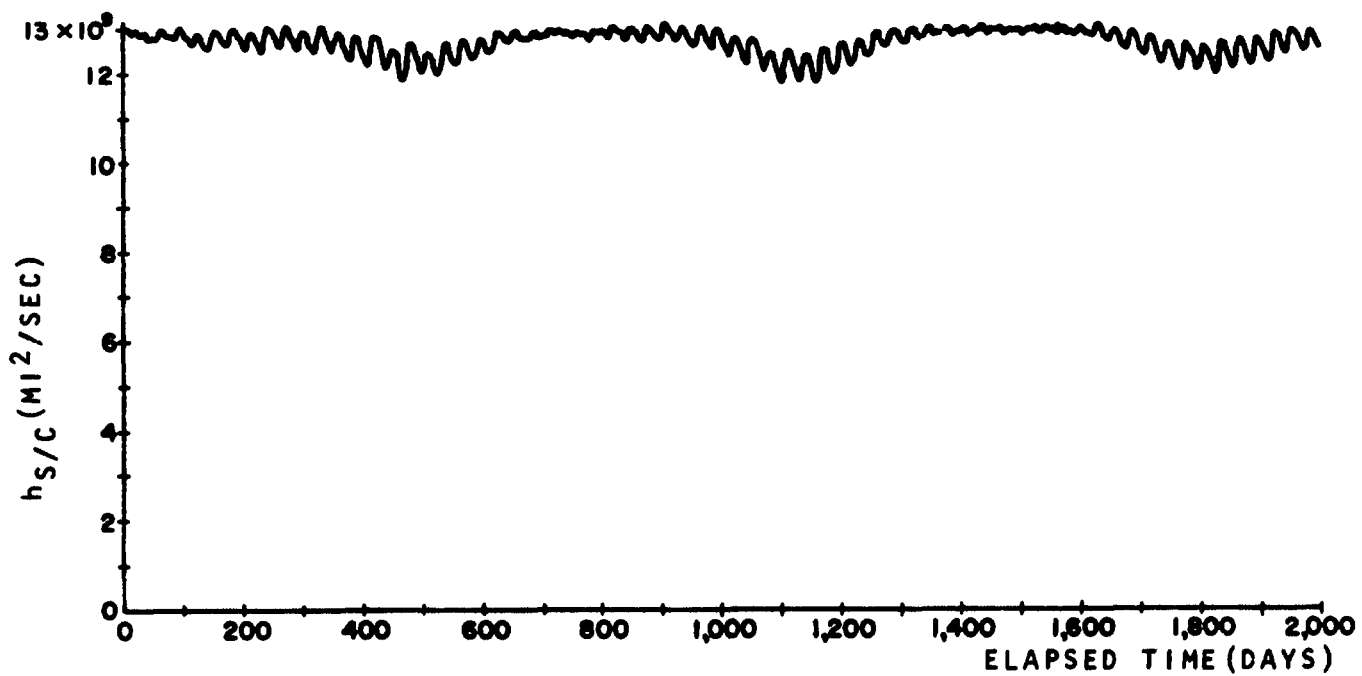


FIGURE 45. MAGNITUDE OF SPACECRAFT ANGULAR MOMENTUM VECTOR RELATIVE TO THE BARYCENTER VS. TIME FOR INITIAL JD 2439796.735

of the two-body case and then compared with the closed form solution. After 36,000 steps there was a difference of .1 mile in 4000 miles. This, obviously, does not inform one of the error involved in the "real world" model of this chapter. It does show that the procedure gives good results over a long time period. Since there is no closed form solution available for the "real world" model, no direct comparison of results can be made as was done in the two-body case. The method of Richardson (Ref. 29), sometimes called "Richardson's extrapolation," was applied to the Julian Date 2,439,796.735 case at L_4 . Two computer runs of 100 days elapsed time were made with fixed step sizes of .1 day and .05 days. Richardson's extrapolation was then used to obtain an improved value of the displacement and velocity in the barycentered system. The extrapolated values were compared with the data of the L_4 computer run with variable step size. It was found that there was a difference of no more than 2 miles in 200,000 miles. The velocity data agreed as well. It should be pointed out that the drawback in applying Richardson's extrapolation is that the formulas are derived assuming that there is no round-off error. Until better techniques are available for estimating error, it will remain difficult to say precisely what the error involved in the "real world" model integration is. One final point should be added. The single step error control is an effective device for controlling the error even though it is not an absolute error control.

Since the Adams-Moulton method is unconditionally stable, it appears that the data of the preceding sections represent to 4 or 5 decimal places the actual value. This opinion is derived from the considerations of the previous paragraph and the belief that round-off error, while existing, is not significant to affect the results in the first 4 or 5 decimal places.

CHAPTER V

CONCLUSIONS AND RECOMMENDATIONS

Certain very important conclusions can be drawn from the results of the two different mathematical models presented in Chapters III and IV.

These conclusions are as follows:

1. When the modified restricted four-body mathematical model with nodal regression has an orientation corresponding to the earth-moon-sun orientation on Julian Date 2,439,501.0, the results differ widely from the results of the "real world" model beginning at that Julian Date (compare Figs. 19 and 31). For insertion into the libration orbit on Julian Date 2,439,796.735 which simulates the case of $\psi_0 = 180^\circ$ of the simplified model discussed in Chapter III, the results of the "real world" model again differ widely from those of the modified restricted four-body model. For this latter insertion date, at L_4 , the spacecraft left a libration-point-centered motion at approximately 575 days in the "real world" model, whereas the motion was stable for 2500 days at L_4 in the modified restricted four-body model. Thus, it appears that the model assuming circular orbits and constant nodal regression does not represent the long term motion very well. Perhaps a model which includes a mean eccentricity for the moon would approximate more accurately the "real world" results.

2. The initial date has an important effect on the subsequent motion. This conclusion was made in Ref. 5 and can also be drawn from the data in Chapter III. From the results of these studies, it can be inferred that there will be an important effect due to the initial configuration in the "real world" model. However, as pointed out in Ref. 14, it is difficult to discern the initial configuration effects even though the qualitative effects are certainly present. Even so, from examination of the L_4 - and L_5 -results of the "real world" model for the initial Julian Date 2,439,796.735, it appears that the marked difference between the two orbits can be attributed primarily to the initial position and subsequent motion of the sun relative to the L_4 - and L_5 -points.
3. Long term stability of greater than five years does exist in the "real world" model. For spacecraft placement at L_5 on Julian Date 2,439,796.735, the spacecraft remained on a libration-point-centered motion (stable motion) for 2000 days (5.48 years). One can confidently extrapolate this motion to 2500 days (6.85 years) as shown by Figs. 44. For the same initial date, the spacecraft leaves a libration-point-centered motion after approximately 575 days when placed at L_4 . Thus, while one triangular libration point exhibits a long term stability, the other triangular point does not for the same initial date. This does not imply that L_5 is stable and L_4 is unstable for all initial orientations. Initial orientations can probably be determined in which the situation will be reversed, possibly when the sun, the earth, and the moon are nearly colinear in that order (a lunar eclipse or full moon).

4. The initial velocity specification has an important effect on the subsequent motion. This is evidenced by the data for Julian Date 2,439,501.0 with $\dot{r}_{BL} = 0$ and with $\dot{r}_{BL} \neq 0$. It is certainly possible that initial velocities could be found for this date which would extend the period of stable motion. The great sensitivity of the model to the initial velocity is indicated also in Ref. 14.
5. Only for the L_5 -point on Julian Date 2,439,796.735 does one observe the expansion-contraction of the envelope of motion which has been observed in previous simplified models (Ref. 5 and Chapter III of this report). The period of this pulsation appears to be about 700 days in the "real world" model at L_5 .
6. Considering the angular momentum plots, Figs. 32, 35, 41, and 45, a tentative conclusion can be drawn that if the angular momentum is maintained at the initial level during the libration-point-centered motion, perhaps by using a series of thrusts on the spacecraft, a stable motion may possibly be maintained.

It should be pointed out that the "real world" model of this report is only an approximation to the physical world. There are still some unknowns which will affect the results, however, the extent of the effect is not known. For example, the earth-moon mass ratio used was 81.3015 which is accurate to $\pm .0033$. It is conceivable that refinements of constants such as mass ratios could be made from the orbit determination of a spacecraft placed at either L_4 or L_5 .

As is often the case, this investigation has either answered or given insight to some questions, but it has also raised many more questions. This

problem is by no means completely solved and there are several areas for further research. They are as follows:

1. Consideration of the motion at different times of the month and year in an extended study of the effects of the initial configuration. There may be certain periods in which very long term stability or stability with a small envelope of motion can be achieved. As pointed out previously, stability was found to be a function of the initial orientation of the earth-moon-sun system in the model with circular orbits and nodal regression as well as in the "real world" model.
2. Study the effects of initial position and velocity on the stability. It was found in Ref. 4 that the envelope of motion could be reduced by an initial velocity relative to the libration point. This is also indicated in Ref. 14. It would be of some interest to determine the initial position and velocity relative to the libration point which would yield a "more stable" motion in the "real world" model.
3. A thorough analysis of the effect that the planets and noncentral gravitational fields of the earth and moon have on the long term motion should be made. If the planets neglected in the "real world" model (viz., Uranus, Neptune, and Pluto) are included in addition to the noncentral fields of the earth and moon, the model would be quite complex and would probably require that most calculations be made in double precision. This would increase the necessary computer time considerably. It should also be noted that the effects of the planets on the motion of a spacecraft relative to the barycenter (X, Y, Z)-system is somewhat reduced by the effects of the planets on the acceleration of the barycenter. This can

be seen from the differential equations of motion for the "real world" model, Eqs. (67).

4. A study should be made of means for "station-keeping," i. e., applying a thrust to the spacecraft at intervals or using a constant low-thrust device to keep the spacecraft near the libration point of interest. It is possible that solar sails could be used in combination with the low-thrust propulsion for this purpose.
5. The equations of motion for the spacecraft should be expressed in terms of the rates of change of the orbit elements in a barycentered system. This would provide a comparison with the results obtained by integrating the acceleration components in a rectangular coordinate system. It is quite possible that computer time could be reduced by using the orbit elements.
6. Analytical approaches should be pursued, even though they are extremely difficult to obtain for sophisticated models. In fact, as stated earlier, a closed form solution to the "real world" model of this report would require a solution to a nine-body problem. However, it may be possible to obtain certain characteristics of the long term motion in the "real world" model using an analytical approach.

APPENDIX A

ORDER OF MAGNITUDE OF GRAVITATIONAL FORCES

The gravitational attraction of the earth and the moon on a spacecraft in the earth-moon system is very much larger than the attraction due to the sun and planets. However, it is very useful to determine the order of magnitude of the attraction due to the sun and planets on the aforementioned spacecraft. This was done by making the assumption that all the planets move in circular orbits around the sun, the radii of which are the semimajor axes of the Epoch 1900. A quantity, F/m_S , is computed from Newton's Law of Gravitation

$$F = \frac{Gm_S m_{\text{body}}}{r^2} \quad , \quad \frac{F}{m_S} = \frac{Gm_{\text{body}}}{r^2}$$

for a body in the earth-moon system. For the inferior planets, viz., Mercury and Venus, the computation is made at inferior conjunction and superior conjunction. The computation is made at conjunction and opposition for the superior planets, the planets outside the earth's orbit. The aspects of the inferior and superior planets are illustrated in Fig. A-1 (Ref. 30). The results of the computation are shown in Table A-1. It should be pointed out that these results do not by any means show exact values for F/m_S . The reason for this lies in the fact that the distance between the earth and some specific planet will vary from opposition to opposition or from conjunction to conjunction.

The results are, therefore, representative values and should be considered on an order of magnitude basis.

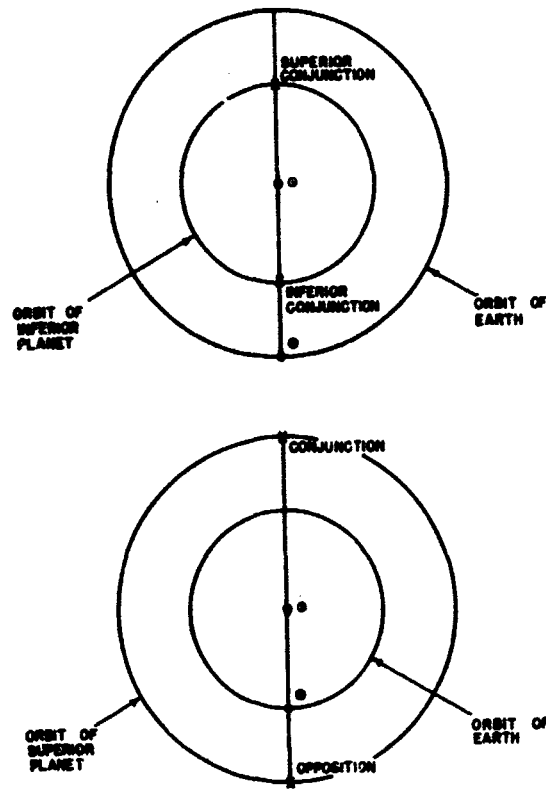


FIGURE A-1. ASPECTS OF THE INFERIOR AND THE SUPERIOR PLANETS

Body	Semimajor Axis of Orbit in A. U. (Ref. 2)	F/m_S in km/sec ²		F/m_S in A. U. /day ²	
		Inferior Conjunction or Opposition	Superior Conjunction or Conjunction	Inferior Conjunction or Opposition	Superior Conjunction or Conjunction
Sun	---	5.92×10^{-6}	5.92×10^{-6}	2.96×10^{-4}	2.96×10^{-4}
Mercury	0.387098	2.58×10^{-12}	5.04×10^{-13}	1.29×10^{-10}	2.51×10^{-11}
Venus	0.723331	1.90×10^{-10}	4.89×10^{-12}	9.46×10^{-9}	2.44×10^{-10}
Mars	1.523679	7.00×10^{-12}	3.02×10^{-13}	3.49×10^{-10}	1.51×10^{-11}
Jupiter	5.2027	3.21×10^{-10}	1.47×10^{-10}	1.60×10^{-8}	7.34×10^{-9}
Saturn	9.546	2.32×10^{-11}	1.53×10^{-11}	1.16×10^{-9}	7.61×10^{-10}
Uranus	19.20	7.84×10^{-13}	6.37×10^{-13}	3.91×10^{-11}	3.18×10^{-11}
Neptune	30.09	3.72×10^{-13}	3.26×10^{-13}	1.86×10^{-11}	1.62×10^{-11}
Pluto	39.5	9.99×10^{-15}	9.03×10^{-15}	4.99×10^{-13}	4.51×10^{-13}

Table A-1. Order of Magnitude of Gravitational Attraction on Spacecraft 1 A. U. from the Sun

APPENDIX B

DERIVATIONS OF EQUATIONS FOR DETERMINING THE ORIENTATION OF THE EARTH-MOON SYSTEM

By definition, the earth-moon orbital plane is a plane perpendicular to the angular momentum vector which includes both the earth and the moon. The angular momentum vector of the earth-moon system is determined from

$$\begin{aligned}\bar{H} &= m_{\oplus} \bar{r}_{B\oplus} \times \dot{\bar{r}}_{B\oplus} + m_{\lrcorner} \bar{r}_{B\lrcorner} \times \dot{\bar{r}}_{B\lrcorner} \\ &= H_X \bar{i} + H_Y \bar{j} + H_Z \bar{k}\end{aligned}\tag{B-1}$$

where

$$\begin{aligned}H_X &= m_{\oplus} (Y_{\oplus} \dot{Z}_{\oplus} - Z_{\oplus} \dot{Y}_{\oplus}) + m_{\lrcorner} (Y_{\lrcorner} \dot{Z}_{\lrcorner} - Z_{\lrcorner} \dot{Y}_{\lrcorner}) \\ &= H_{X_{\oplus}} + H_{X_{\lrcorner}} \\ H_Y &= m_{\oplus} (Z_{\oplus} \dot{X}_{\oplus} - X_{\oplus} \dot{Z}_{\oplus}) + m_{\lrcorner} (Z_{\lrcorner} \dot{X}_{\lrcorner} - X_{\lrcorner} \dot{Z}_{\lrcorner}) \\ &= H_{Y_{\oplus}} + H_{Y_{\lrcorner}} \\ H_Z &= m_{\oplus} (X_{\oplus} \dot{Y}_{\oplus} - Y_{\oplus} \dot{X}_{\oplus}) + m_{\lrcorner} (X_{\lrcorner} \dot{Y}_{\lrcorner} - Y_{\lrcorner} \dot{X}_{\lrcorner}) \\ &= H_{Z_{\oplus}} + H_{Z_{\lrcorner}}\end{aligned}\tag{B-2}$$

The angular momentum is determined with respect to the (X, Y, Z)-barycentered coordinate system. The earth-moon orbital plane and the angles

defining its orientation are illustrated in Fig. B-1. The angle Ω^* is the angle measured in the (X, Y)-plane between the X-axis and the ascending node; the angle i^* is the angle between the (X, Y)-plane and the earth-moon orbital plane. Since the angular momentum vector \bar{H} is perpendicular to the line of nodes, its projection on the (X, Y)-plane is perpendicular also to the line of nodes. Therefore, from Fig. B-2,

$$\begin{aligned} \sin i^* &= \frac{(H_X^2 + H_Y^2)^{1/2}}{H} , \quad \cos i^* = \frac{H_Z}{H} , \\ \tan i^* &= \frac{(H_X^2 + H_Y^2)^{1/2}}{H_Z} , \end{aligned} \quad (\text{B-3})$$

$$\begin{aligned} \sin \Omega^* &= \frac{H_X}{(H_X^2 + H_Y^2)^{1/2}} , \quad \cos \Omega^* = -\frac{H_Y}{(H_X^2 + H_Y^2)^{1/2}} \\ \tan \Omega^* &= -\frac{H_X}{H_Y} , \end{aligned} \quad (\text{B-4})$$

where H is the magnitude of \bar{H} .

The following expressions are determined from Fig. B-1:

$$r_{B\text{D}} \sin \theta^* = R ,$$

$$\sin i^* = \frac{Z_{\text{D}}}{R} ,$$

then

$$\sin \theta^* = \frac{Z_{\text{D}}}{r_{B\text{D}} \sin i^*}$$

and

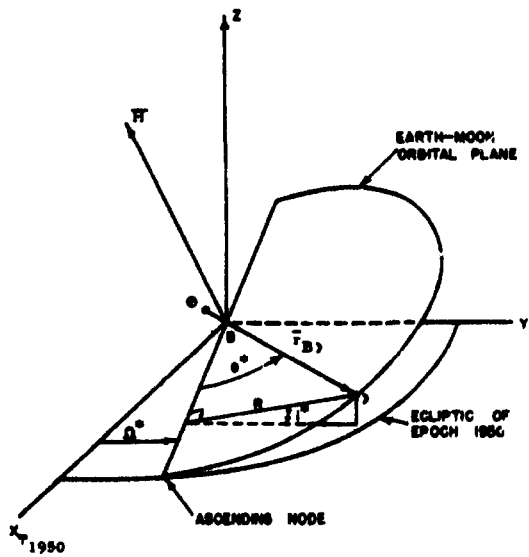


FIGURE B-1. DEFINITION OF ANGLES

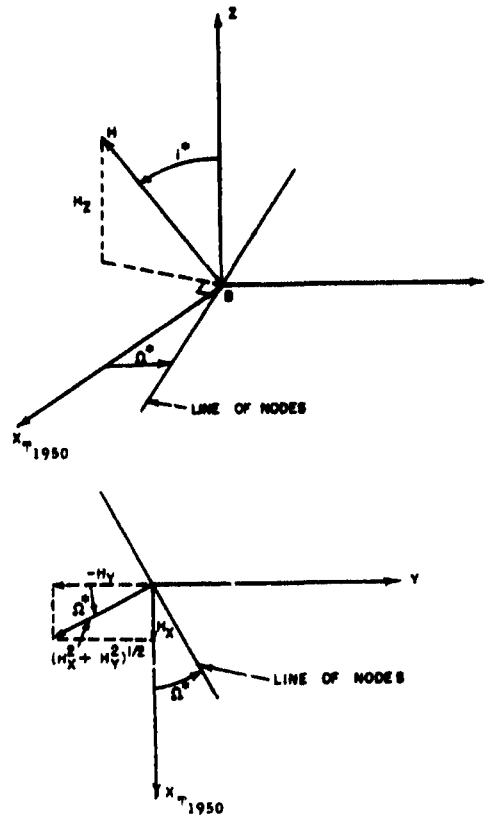


FIGURE B-2. DETERMINATION OF i° AND Ω°

$$r_{B\downarrow} \cos \theta^* = X_{\downarrow} \cos \Omega^* + Y_{\downarrow} \sin \Omega^* ,$$

$$\tan \theta^* = \frac{Z_{\downarrow}}{\sin i (X_{\downarrow} \cos \Omega^* + Y_{\downarrow} \sin \Omega^*)} , \quad (\text{B-5})$$

where R is the component of $\bar{r}_{B\downarrow}$ which is perpendicular to the line of nodes and which lies in the earth-moon orbital plane. Note that the calculation of the total angular momentum \bar{H} requires position and velocity of both the earth and the moon. The computation may be simplified by showing that the angular momentum due to the earth may be determined from the angular momentum due to the moon. The barycenter is, by definition,

$$\bar{r}_{\odot B} = \frac{m_{\oplus} \bar{r}_{\oplus \odot} + m_{\downarrow} \bar{r}_{\downarrow \odot}}{m_{\oplus} + m_{\downarrow}} \quad (\text{B-6})$$

also,

$$\bar{r}_{\downarrow \odot} = \bar{r}_{\downarrow \oplus} + \bar{r}_{\oplus \odot} ,$$

therefore,

$$\bar{r}_{\downarrow \odot} = \frac{m_{\oplus} \bar{r}_{\oplus \odot} + m_{\downarrow} (\bar{r}_{\downarrow \oplus} + \bar{r}_{\oplus \odot})}{m_{\oplus} + m_{\downarrow}}$$

$$\bar{r}_{\downarrow \odot} = \bar{r}_{\downarrow \oplus} + \frac{m_{\downarrow}}{m_{\downarrow} + m_{\oplus}} \bar{r}_{\oplus \odot} \quad (\text{B-7})$$

and

$$\bar{r}_{\oplus \odot} = \bar{r}_{\downarrow \odot} - \frac{m_{\downarrow}}{m_{\downarrow} + m_{\oplus}} \bar{r}_{\oplus \odot} + \bar{r}_{\oplus \odot}$$

$$\bar{r}_{\oplus \odot} = \bar{r}_{\downarrow \odot} + \frac{m_{\oplus}}{m_{\downarrow} + m_{\oplus}} \bar{r}_{\oplus \odot} \quad (\text{B-8})$$

Also

$$\bar{r}_{\odot\oplus} = \bar{r}_{\odot B} + \bar{r}_{B\oplus}$$

$$\bar{r}_{\odot\oplus} = \bar{r}_{\odot B} + \bar{r}_{B\oplus}$$

Therefore,

$$\bar{r}_{B\oplus} = \bar{r}_{\odot\oplus} - \bar{r}_{\odot B}$$

$$\bar{r}_{B\oplus} = -\frac{m_{\odot}}{m_{\odot} + m_{\oplus}} \bar{r}_{\oplus} \quad (\text{B-9})$$

or

$$\bar{r}_{B\oplus} = -M_M \bar{r}_{\oplus} \quad ,$$

and

$$\dot{\bar{r}}_{B\oplus} = -M_M \dot{\bar{r}}_{\oplus}$$

Similarly,

$$\bar{r}_{B\odot} = \bar{r}_{\odot\oplus} - \bar{r}_{\odot B}$$

$$\bar{r}_{B\odot} = \frac{m_{\oplus}}{m_{\odot} + m_{\oplus}} \bar{r}_{\oplus} \quad (\text{B-10})$$

or

$$\bar{r}_{B\odot} = M_E \bar{r}_{\oplus}$$

and

$$\bar{r}_{\oplus} = \frac{1}{M_E} \bar{r}_{B\odot}$$

Therefore, by Eq. (B-9),

$$\bar{r}_{B\oplus} = -\frac{M_M}{M_E} \bar{r}_{B\odot}$$

$$\bar{r}_{B\oplus} = -\frac{m_{\odot}}{m_{\oplus}} \bar{r}_{B\odot} \quad (\text{B-11})$$

and

$$\dot{\vec{r}}_{B\oplus} = -\frac{m_J}{m_\oplus} \dot{\vec{r}}_B$$

But, using Eqs. (B-9), (B-1), and (B-2),

$$\begin{aligned} H_{X_\oplus} &= m_\oplus \left(-\frac{m_J}{m_\oplus} Y_J \right) \left(-\frac{m_J}{m_\oplus} \dot{Z}_J \right) - \left(-\frac{m_J}{m_\oplus} Z_J \right) \left(-\frac{m_J}{m_\oplus} \dot{Y}_J \right) \\ &= m_\oplus \left(\frac{m_J^2}{m_\oplus^2} \right) \left[Y_J \dot{Z}_J - Z_J \dot{Y}_J \right] \end{aligned}$$

$$H_{X_\oplus} = \frac{m_J}{m_\oplus} H_{X_J}$$

Similarly,

$$H_{Y_\oplus} = \frac{m_J}{m_\oplus} H_{Y_J}$$

$$H_{Z_\oplus} = \frac{m_J}{m_\oplus} H_{Z_J}$$

(B-12)

Therefore, since

$$H_X = H_{X_J} + H_{X_\oplus}$$

then

$$H_X = \left(1 + \frac{m_J}{m_\oplus} \right) H_{X_J}$$

Similarly,

$$H_Y = \left(1 + \frac{m_J}{m_\oplus} \right) H_{Y_J}$$

(B-13)

$$H_Z = \left(1 + \frac{m_J}{m_\oplus} \right) H_{Z_J}$$

Then

$$\begin{aligned}
 H &= |\mathbf{H}| = H_X^2 + H_Y^2 + H_Z^2 \\
 &= \left(1 + \frac{m_J}{m_\oplus}\right) \left[H_{X,J}^2 + H_{Y,J}^2 + H_{Z,J}^2 \right]^{1/2}
 \end{aligned} \tag{B-14}$$

and

$$\begin{aligned}
 \sin i^* &= \frac{\left(1 + \frac{m_J}{m_\oplus}\right) \left[H_{X,J}^2 + H_{Y,J}^2 \right]^{1/2}}{\left(1 + \frac{m_J}{m_\oplus}\right) \left[H_{X,J}^2 + H_{Y,J}^2 + H_{Z,J}^2 \right]^{1/2}} \\
 \sin i^* &= \frac{\left[h_{X,J}^2 + h_{Y,J}^2 \right]^{1/2}}{\left[h_{X,J}^2 + h_{Y,J}^2 + h_{Z,J}^2 \right]^{1/2}}
 \end{aligned}$$

Similarly

$$\cos i^* = \frac{h_{Z,J}}{\left[h_{X,J}^2 + h_{Y,J}^2 + h_{Z,J}^2 \right]^{1/2}} \tag{B-15}$$

and

$$\tan i^* = \frac{\left[h_{X,J}^2 + h_{Y,J}^2 \right]^{1/2}}{h_{Z,J}}$$

Also,

$$\sin \Omega^* = \frac{h_{X_D}}{\left[h_{X_D}^2 + h_{Y_D}^2 \right]^{1/2}}$$

$$\cos \Omega^* = - \frac{h_{Y_D}}{\left[h_{X_D}^2 + h_{Y_D}^2 \right]^{1/2}} \quad (\text{B-16})$$

and

$$\tan \Omega^* = - \frac{h_{X_D}}{h_{Y_D}}$$

Therefore, the inclination i^* and the longitude of the ascending node Ω^* can be computed using only the angular momentum per unit mass of the moon (or earth).

APPENDIX C

DETERMINATION OF INITIAL CONDITIONS USING THE EARTH-MOON ORBITAL PLANE

In order to determine the initial position and velocity of a spacecraft relative to the (X, Y, Z) -barycentered coordinate system, it is necessary to determine the position and velocity of the triangular libration point under investigation. Assuming that the triangular libration points lie in the earth-moon orbital plane, i. e., the plane defined by the angular momentum vector \bar{H} of the earth-moon system, the location of L_4 is as shown in Fig. C-1. The (ξ, η, ζ) -coordinate system is also shown in Fig. C-1 and is oriented such that the ξ -axis lies along the earth-moon line in the direction of the moon, the η -axis lies in the earth-moon orbital plane, and the ζ -axis is perpendicular to the orbital plane and is, therefore, in the same direction as the angular momentum vector. The (x, y, z) - L_4 -centered coordinate system is oriented such that the x -axis is parallel to the ξ -axis, the y -axis is in the orbital plane, and the z -axis is perpendicular to the earth-moon orbital plane.

The triangular libration points lie at the vertices of equilateral triangles as shown in Fig. C-1. The libration point L_4 is shown in Fig. C-2, the in-plane orientation. The ξ -coordinate of L_4 , ξ_p , is determined from

$$\xi_p = \frac{r_{\oplus}}{2} - r_{B\oplus} \quad (C-1)$$

where $r_{B\oplus}$ is the magnitude of the barycenter-earth distance. The η -coordinate of L_4 is given by

$$\eta_p = r_{\oplus} \sin 60^\circ \quad (C-2)$$

where r_{\oplus} is the instantaneous earth-moon distance. Then the initial position of the spacecraft in the (X, Y, Z)-coordinate system is

$$\begin{bmatrix} X_S \\ Y_S \\ Z_S \end{bmatrix} = A \begin{bmatrix} x_S + \xi_p \\ y_S + \eta_p \\ z_S \end{bmatrix} \quad (C-3)$$

where x_S , y_S , and z_S are the coordinates of the spacecraft expressed in the (x, y, z)- L_4 -centered coordinate system. Furthermore, the matrix A is given by Eq. (13) in which Ω , θ , and i are replaced by Ω^* , θ^* , and i^* , respectively. The quantities Ω^* , θ^* , and i^* are determined from Eqs. (B-15), (B-16), and (B-5) and are illustrated in Fig. C-1.

The initial conditions for the velocities present a somewhat more difficult problem. Since the actual motion of the moon is not circular, the lunar velocity vector will not, in general, be perpendicular to the earth-moon vector \bar{r}_{\oplus} . The problem is then to determine the velocity of the libration point L_4 which would maintain the equilateral configuration in the restricted three-body sense. For example, if the earth-moon-spacecraft system were considered as a three-body problem in which the earth and the moon move in elliptical orbits around the barycenter, then the libration point L_4 will also move in an elliptical orbit (Ref. 31). Therefore, if a spacecraft is placed at L_4 , it must be

given a velocity, relative to the (X, Y, Z)-coordinate system, equal to that of the libration point in order to maintain the equilateral configuration. It appears that there is some relation between the radial velocity of the moon and the radial velocity of the libration point which would be necessary to maintain the equilateral configuration in the restricted three-body sense. The velocity of the moon is

$$\bar{V}_D = \dot{r}_{B_D} \bar{\epsilon}_\xi + r_{B_D} \dot{\theta}^* \bar{\epsilon}_\eta + \dot{\zeta}_D \bar{\epsilon}_\zeta \quad (C-4)$$

where \bar{V}_D is known in the (X, Y, Z)-system and $\dot{\zeta}_D$ is zero because of the manner in which the earth-moon orbital plane is defined (see Appendix D for proof). Therefore, \dot{r}_{B_D} and $r_{B_D} \dot{\theta}^*$ can be determined from

$$\begin{bmatrix} \dot{X}_D \\ \dot{Y}_D \\ \dot{Z}_D \end{bmatrix} = A \begin{bmatrix} \dot{r}_{B_D} \\ r_{B_D} \dot{\theta}^* \\ 0 \end{bmatrix} \quad (C-5)$$

or

$$\begin{bmatrix} \dot{r}_{B_D} \\ r_{B_D} \dot{\theta}^* \\ 0 \end{bmatrix} = A^T \begin{bmatrix} \dot{X}_D \\ \dot{Y}_D \\ \dot{Z}_D \end{bmatrix} \quad (C-6)$$

Using the absolute magnitudes of the vectors involved (no signs)

$$r_{\oplus D} = r_{B_D} + r_{B\oplus} \quad ,$$

but, by the definition of the barycenter,

$$m_D r_{B_D} = m_{\oplus} r_{B\oplus}$$

then

$$r_{\oplus} = r_{B\oplus} \left(\frac{m_{\oplus}}{m_{\oplus}} \right) + r_{B\oplus}$$

or

$$r_{B\oplus} = r_{\oplus} \left[\frac{m_{\oplus}}{m_{\oplus} + m_{\oplus}} \right]$$

Now,

$$\tan \phi = \frac{\eta_p}{\xi_p} \quad (7)$$

and from Eqs. (C-1) and (C-2)

$$\begin{aligned} \tan \phi &= \frac{r_{\oplus} \sin 60^\circ}{\frac{r_{\oplus}}{2} - r_{B\oplus}} \\ &= \frac{\sin 60^\circ}{\frac{1}{2} - \frac{m_{\oplus}}{m_{\oplus} + m_{\oplus}}} \\ &= \text{constant.} \end{aligned}$$

Therefore

$$\phi = \text{constant.}$$

From the law of sines

$$\frac{r_{B\oplus}}{\sin(120^\circ - \phi)} = \frac{r_{BL}}{\sin 60^\circ}$$

as can be seen from Fig. C-2. Taking the first derivative with respect to time yields

$$\dot{r}_{BL} = \dot{r}_{B\oplus} \frac{\sin 60^\circ}{\sin(120^\circ - \phi)} \quad (C-8)$$

That is, considering the triangular configuration as a body which always maintains the same configuration, the relation between the lunar radial velocity and the L_4 radial velocity is given by Eq. (C-8). Furthermore, L_4 will have the same angular velocity as the moon. The angular velocity $\dot{\theta}^*$ and \dot{r}_B can be determined from Eq. (C-6). Also,

$$r_{BL} = \left(\xi_p^2 + \eta_p^2 \right)^{1/2} \quad (C-9)$$

The velocity of L_4 can be written as

$$\bar{V}_L = \frac{\sin 60^\circ}{\sin(120^\circ - \phi)} \dot{r}_B \bar{\epsilon}_r + r_{BL} \dot{\theta}^* \bar{\epsilon}_\theta$$

where $\bar{\epsilon}_r$ is a unit vector along \bar{r}_{BL} and $\bar{\epsilon}_\theta$ is a unit vector perpendicular to $\bar{\epsilon}_r$ as shown in Fig. C-2. Assuming that the spacecraft can have a velocity relative to the (x, y, z) -coordinate system (see Fig. C-2) at L_4 , the velocity of the spacecraft at insertion is

$$\begin{aligned} \bar{V}_S = & \left[\frac{\sin 60^\circ}{\sin(120^\circ - \phi)} \dot{r}_B + \dot{x}_S \cos \phi + \dot{y}_S \sin \phi \right] \bar{\epsilon}_r \\ & + \left[\dot{r}_{BL} \dot{\theta}^* - x_S \sin \phi + \dot{y}_S \cos \phi \right] \bar{\epsilon}_\theta + \dot{z}_S \bar{\epsilon}_z \end{aligned}$$

Therefore,

$$\begin{bmatrix} \dot{x}_S \\ \dot{y}_S \\ \dot{z}_S \end{bmatrix} = A^* \begin{bmatrix} \frac{\sin 60^\circ}{\sin(120^\circ - \phi)} \dot{r}_B + \dot{x}_S \cos \phi + \dot{y}_S \sin \phi \\ \dot{r}_{BL} \dot{\theta}^* - x_S \sin \phi + \dot{y}_S \cos \phi \\ \dot{z}_S \end{bmatrix} \quad (C-10)$$

where A^* is the same matrix as used in Eq. (C-3) except that it must be evaluated at $\theta^* + \phi$ instead of θ^* .

Equations (C-3) and (C-10) represent the initial position and velocity for spacecraft placement at L_4 . For placement of the spacecraft at L_5 , the initial position equations are obtained by replacing η_p by $-\eta_p$ in Eq. (C-3). The orientation of the (x, y)-coordinate system located at L_5 is shown in Fig. C-3. Furthermore, the initial velocity can be obtained by substituting $-\phi$ for ϕ in Eqs. (C-10) in all terms involving ϕ (including the matrix A) except

$$\dot{r}_B \frac{\sin 60^\circ}{\sin(120^\circ - \phi)}$$

Substituting $-\phi$ in the above term yields an incorrect result.

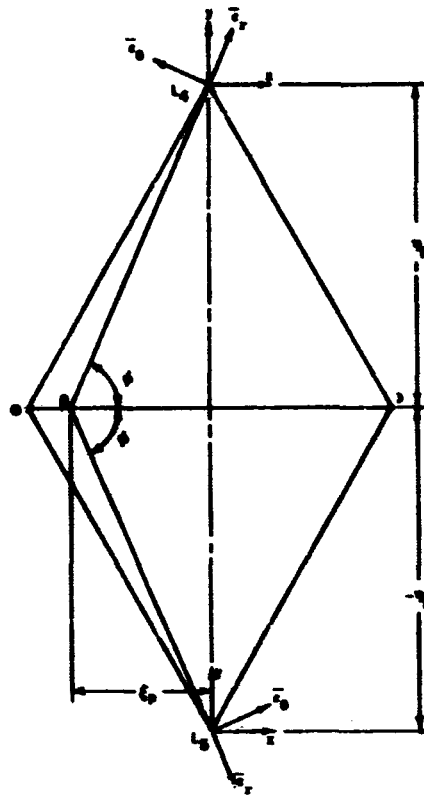


FIGURE C-3. IN-PLANE ORIENTATION OF THE L_4
AND L_5 COORDINATE SYSTEMS

APPENDIX D

PROOF OF $\dot{\zeta}_y = 0$

From Eq. (C-6), one has

$$\dot{\zeta}_y = \sin \Omega^* \sin i^* \dot{X}_y - \cos \Omega^* \sin i^* \dot{Y}_y + \cos i^* \dot{Z}_y. \quad (D-1)$$

Combining Eqs. (B-3), (B-4), (B-5), with Eq. (D-1) gives

$$\dot{\zeta}_y = \frac{H_X}{H} \dot{X}_y + \frac{H_Y}{H} \dot{Y}_y + \frac{H_Z}{H} \dot{Z}_y, \quad (D-2)$$

where H_X , H_Y , and H_Z represent the total angular momentum components of the earth-moon system and H is the magnitude of the total angular momentum.

Rewriting

$$\dot{\zeta}_y = \frac{1}{H} (H_X \dot{X}_y + H_Y \dot{Y}_y + H_Z \dot{Z}_y) \quad (D-3)$$

Using the relations between the total angular momentum and that of the moon alone, i. e., Eq. (B-13) yields

$$\dot{\zeta}_y = \frac{\left(1 + \frac{m_y}{m_\oplus}\right)}{H} (H_X \dot{X}_y + h_Y \dot{Y}_y + H_Z \dot{Z}_y) \quad (D-4)$$

Combining Eqs. (D-3), (B-1), and (B-2) gives

$$\begin{aligned} \dot{\zeta}_y = \frac{\left(1 + \frac{m_y}{m_\oplus}\right)}{H} m_y & \left[\dot{X}_y (Y_y \dot{Z}_y - Z_y \dot{Y}_y) \right. \\ & + \dot{Y}_y (Z_y \dot{X}_y - X_y \dot{Z}_y) \\ & \left. + \dot{Z}_y (X_y \dot{Y}_y - Y_y \dot{X}_y) \right] \end{aligned} \quad (\text{D-5})$$

Combining like terms of Eqs. (D-5),

$$\zeta_y = \frac{\left(1 + \frac{m_y}{m_\oplus}\right)}{H} m_y [0] = 0 \quad , \quad (\text{D-6})$$

i. e. , the moon has no component of velocity perpendicular to the earth-moon orbital plane (the plane defined by the angular momentum). This could also be shown by consideration of the $\bar{\mathbf{r}} \times \dot{\bar{\mathbf{r}}}$ vector.

REFERENCES

1. Moulton, F. R., An Introduction to Celestial Mechanics (The MacMillan Co., New York, 1962), Chapter VIII.
2. Danby, J. M. A., Fundamentals of Celestial Mechanics (The MacMillan Co., New York, 1962), Chapter 8 and 9, Appendix C.
3. Flammarion, C., The Flammarion Book of Astronomy (Simon and Schuster, New York, 1964), pp. 156 and 300.
4. Tapley, B. D., and J. M. Lewallen, "Solar influence on satellite motion near the stable earth-moon libration points," AIAA Journal, Vol. 2, No. 4, April, 1964, pp. 728-732.
5. Tapley, B. D., and B. E. Schutz, "Some additional results on solar influenced libration point motion," Second Aerospace Sciences Meeting, AIAA Paper No. 65-88, January, 1965.
6. Schechter, H. B., and W. C. Hollis, "Stability of the Trojan Points in the four-body problem," The Rand Corporation, Memorandum RM-3992-PR, September, 1964.
7. de Vries, J. P., and W. M. Pauson, "A study of motion near libration points in the earth-moon system," General Electric Company, TIS R62SD5, January, 1962.
8. de Vries, J. P., and W. M. Pauson, "Motion of a particle in the vicinity of a triangular libration point in the earth-moon system," General Electric Company, TIS R63SD99, November, 1963.
9. Guffey, H. F., and H. L. McKinley, "Libration point studies by numerical techniques," M. S. thesis, USAF Institute of Technology, Wright-Patterson Air Force Base, Ohio, March, 1962.
10. Pohl, F. V., "The least density of a spherical swarm of particles with an application to astronomical observations of K. Kordylewski," AIAA Astrodynamics Conference, Preprint No. 63-425, August, 1963.

11. Deprit, A., "Routh's critical mass ratio at the triangular libration centers," *Astrodynamics Specialist Conference*, AIAA Paper No. 65-681, September, 1965.
12. Dusek, H., "Motion in the vicinity of libration points in a generalized restricted three-body model," *Astrodynamics Specialist Conference*, AIAA Paper No. 65-682, September, 1965.
13. Breakwell, J., and R. Pringle, "Resonances affecting motion near the earth-moon equilateral libration points," *Astrodynamics Specialist Conference*, AIAA Paper No. 65-683, September, 1965.
14. Wolaver, L. E., "Effect of initial configurations on libration point motion," *Astrodynamics Specialist Conference*, AIAA Paper No. 65-684, September, 1965.
15. Bennett, A., "Analytical determination of characteristic exponents," *Astrodynamics Specialist Conference*, AIAA Paper No. 65-685, September, 1965.
16. Steg, L., and E. Shoemaker, "Libration point satellites," A Review of Space Research, Space Science Summer Study, University of Iowa, 1962, sponsored by the Space Science Board of the National Academy of Sciences, pp. 4-34 to 4-35.
17. Rechtin, E., "Lunar communications," Chapter 9, Lunar Missions and Exploration, edited by Leondes, C. T., and R. W. Vance (John Wiley and Sons, Inc., New York, 1964), pp. 431-433.
18. Anonymous, "New natural satellites of the earth," Sky and Telescope (News Note) XXII, 16, July, 1961.
19. Anonymous, "More about the earth's cloud satellites," Sky and Telescope, XXII, 63, August, 1961.
20. Michael, W. H., Jr., "Considerations of the motion of a small body in the vicinity of the stable libration points of the earth-moon system," NASA TR-160.
21. Lastman, G. J., "Solution of n simultaneous first order differential equations by the Adams-Moulton method using a Runge-Kutta starter and partial double precision arithmetic," UTD-2-03-046 (D2 UTEX RKAM) The University of Texas Computation Center, January, 1964.
22. Bellman, R. E., Dynamic Programming (Princeton University Press, Princeton, 1957), p. x.
23. Clarke, V. C., Jr., "Constants and related data for use in trajectory calculations as adopted by the ad hoc NASA Standard Constants Committee," JPL TN No. 32-604, March 6, 1964.

24. Housner, G. W., and D. E. Hudson, Applied Mechanics: Dynamics (D. Van Nostrand Company, Inc., Princeton, 1959), pp. 38-40.
25. Goldstein, H., Classical Mechanics (Addison-Wesley, Reading, Massachusetts, 1959), pp. 97-100 and 107-109.
26. The American Ephemeris and Nautical Almanac for the Year 1965, (United States Government Printing Office, Washington, D. C., 1963), p. 493.
27. Clark, J. R., "A solar system ephemeris for 1950 to 2000," M. S. thesis, The University of Texas, Austin, Texas, May, 1965.
28. Peabody, P. R., J. F. Scott, and E. G. Orozco, "Users' Description of JPL Ephemeris Tapes," JPL TR No. 32-580, March 2, 1964.
29. Henrici, P., Discrete Variable Methods in Ordinary Differential Equations (John Wiley and Sons, Inc., New York, 1962), pp. 34-35.
30. Baker, R. H., Astronomy (D. Van Nostrand Company, Inc., Princeton, 1961), pp. 172-173.
31. McCuskey, S. W., Introduction to Celestial Mechanics (Addison-Wesley, Reading, Massachusetts, 1963), pp. 107-108.

VITA

Bob E. Schutz, the son of Lola and Ernest Schutz, was born in Brownfield, Texas, on September 6, 1940. He graduated from Brackenridge High School in San Antonio in 1958 and enrolled in San Antonio College. In 1960 he transferred to The University of Texas and received the Bachelor of Science Degree in Aerospace Engineering in 1963 and began working toward the Master of Science Degree in the same year. He has been employed for the summer at the U. S. Naval Ordnance Laboratory in Silver Spring, Maryland, as an engineering aid in the supersonic wind tunnel; at the N. A. S. A. Manned Spacecraft Center in Houston, Texas, in the Rendezvous Analysis Branch of Mission Planning, and was engaged in preliminary mission planning for GT-3; and at the Launch Systems Branch of The Boeing Company in New Orleans, Louisiana, in the Program Planning and Reporting Branch concerned with S-1C management. He has been on a Teaching Assistantship in the Aerospace Engineering Department since January, 1964. He is a member of Sigma Gamma Tau, Tau Beta Pi, and an associate member of Sigma Xi and plans to continue his education at The University of Texas.

Permanent address: 128 Dunning
San Antonio, Texas

This thesis was typed by Mrs. Patricia J. McIlvain.